Living on the edge of stability, the limits of the nuclear landscape

Morten Hjorth-Jensen

Michigan State University, USA and University of Oslo, Norway

International Conference on Nuclear Theory in the Supercomputing Era, Ames, May 13-17 2013: And many happy returns JAMES!

Outline

People

Michigan State University

Scott Bogner, Alex B. Brown, and Nicolas Michel

University of Oslo

Gustav Bårdsen, Sigve Bøe Skattum, Andreas Ekström, Jørgen Høgberget, Maxim Kartamychev, Karl Leikanger and Sarah Reimann

Oak Ridge National Laboratory and University of Tennessee, Knoxville

David J. Dean, Gaute Hagen, Gustav Jansen, Witek Nazarewicz, and Thomas Papenbrock

University of Idaho

Ruprecht Machleidt

Argonne National Laboratory

Stefan Wild and Jason Sarich

Chalmers, Gothenburg

Christian Forssen, Boris Karlsson and Jimmy Rotureau

The first three take away messages for understanding physics towards driplines

- Three-body and more complicated forces are expected to play an important role and should be included in first principle calculations.
- Continuum (resonances and non-resonant contributions) needs to be included in theory analyses.
- Correlations are strong towards the dripline, mean field is not a useful picture.

But, there is more to the picture than meets the eye....

INT workshop 2004, Bruce Barrett, David Dean, MHJ and James Vary

See Bruce Barrett *et al* J. Phys. G **31** (2005)

- It should be fully microscopic and start with present two- and three-body interactions derived from *e.g.*, effective field theory;
- It can be improved upon systematically, e.g., by inclusion of three-body interactions and more complicated correlations;
- It allows for description of both closed-shell systems and valence systems;
- For nuclear systems where shell-model studies are the only feasible ones, viz., a small model space requiring an effective interaction, one should be able to derive effective two and three-body equations and interactions for the shell model;

INT workshop 2004, Bruce Barrett, David Dean, MHJ and James Vary

See Bruce Barrett *et al* J. Phys. G **31** (2005)

- It is amenable to parallel computing;
- It can be used to generate excited spectra for nuclei like where many shells are involved (It is hard for the traditional shell model to go beyond one major shell. The inclusion of several shells may imply the need of complex effective interactions needed in studies of weakly bound systems); and
- Finally, nuclear structure results should be used in marrying microscopic many-body results with reaction studies. This will be another hot topic of future *ab initio* research.

Scales in Nuclear Physics

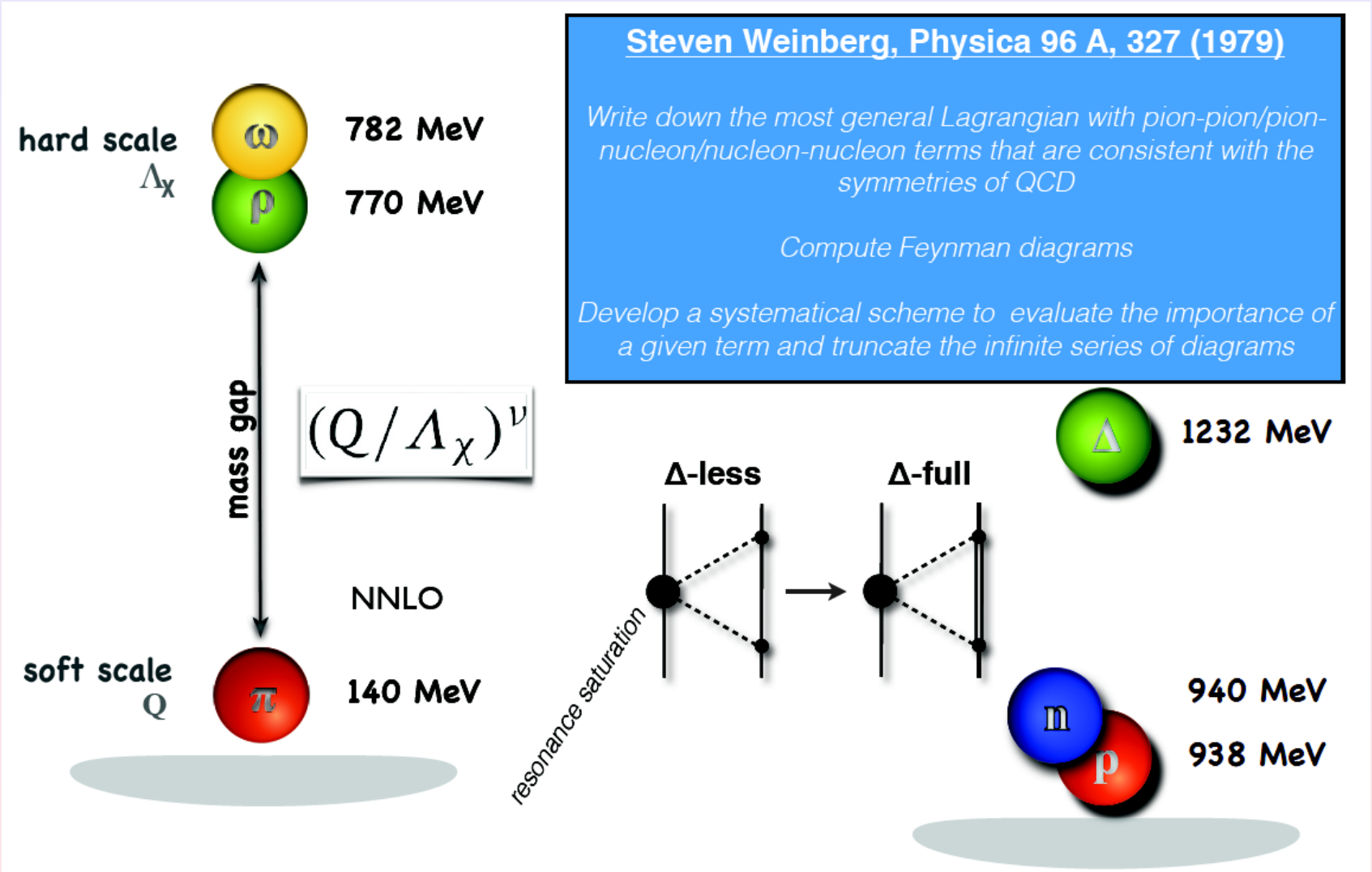

Forces in Nuclear Physics (without isobars)

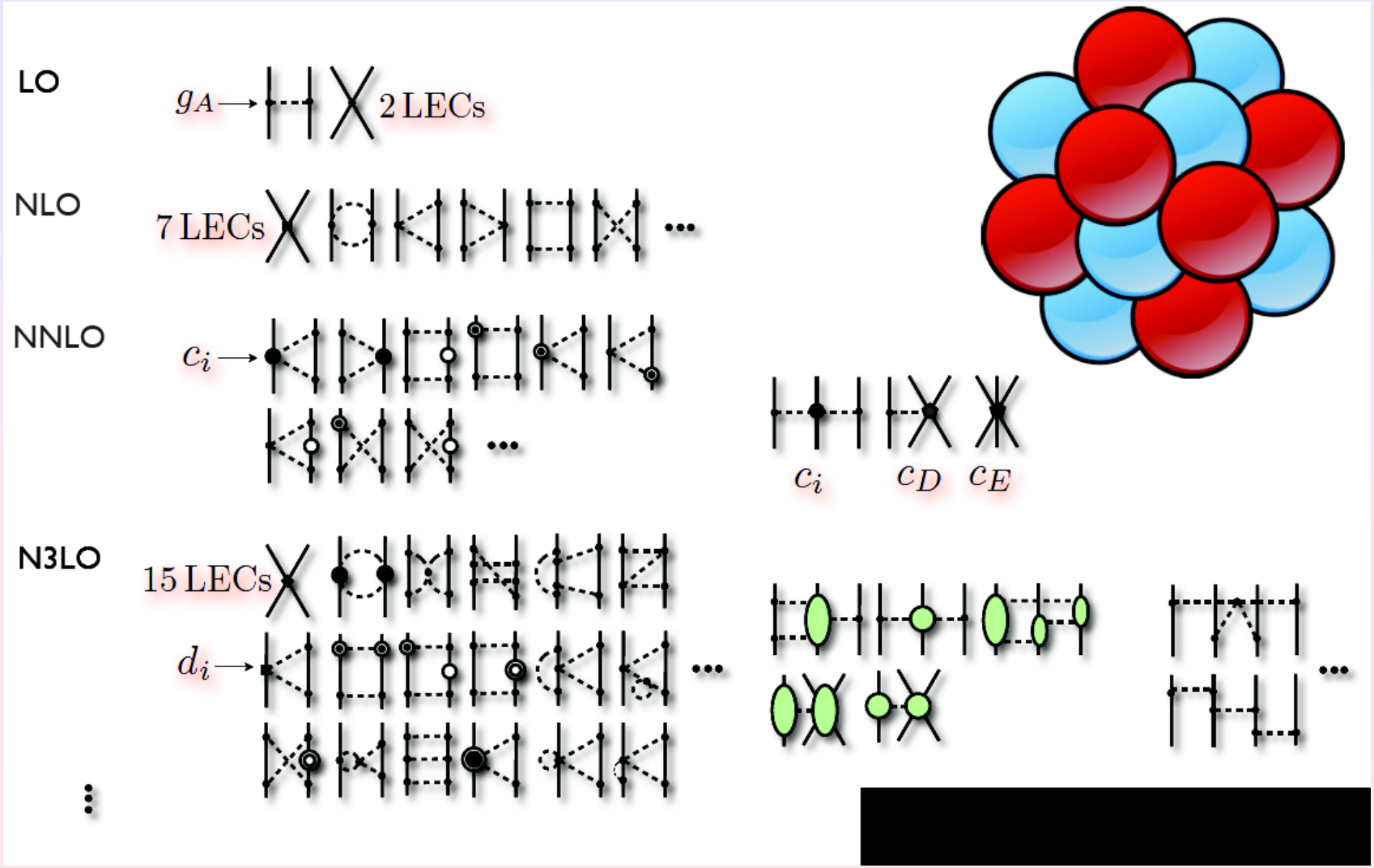

Key intellectual issues

How well do you understand your favourite theory?

- Can we understand the link between QCD (Lattice) and Effective field theories?
- Can we link the cutoff of the interaction with a specific model-space size? That is, can we link many-body theories with effective field theories? All interactions have a cutoff Λ ($\Lambda \sim 500 - 700$ MeV). A cutoff produces always missing many-body physics (intruder states etc).
- Can we provide proper error estimates (single-particle basis truncation and truncations in number of excitations)?

Key intellectual issues

How well do you understand your favourite theory?

- Do we understand how many-body forces evolve as we add more and more particles?
- Can we link ab initio methods with density functional theories? Possible road to multiscale physics.
- Can we develop proper error estimates for chiral forces in a nuclear medium?
- A proper many-body approach to reactions.

Our research

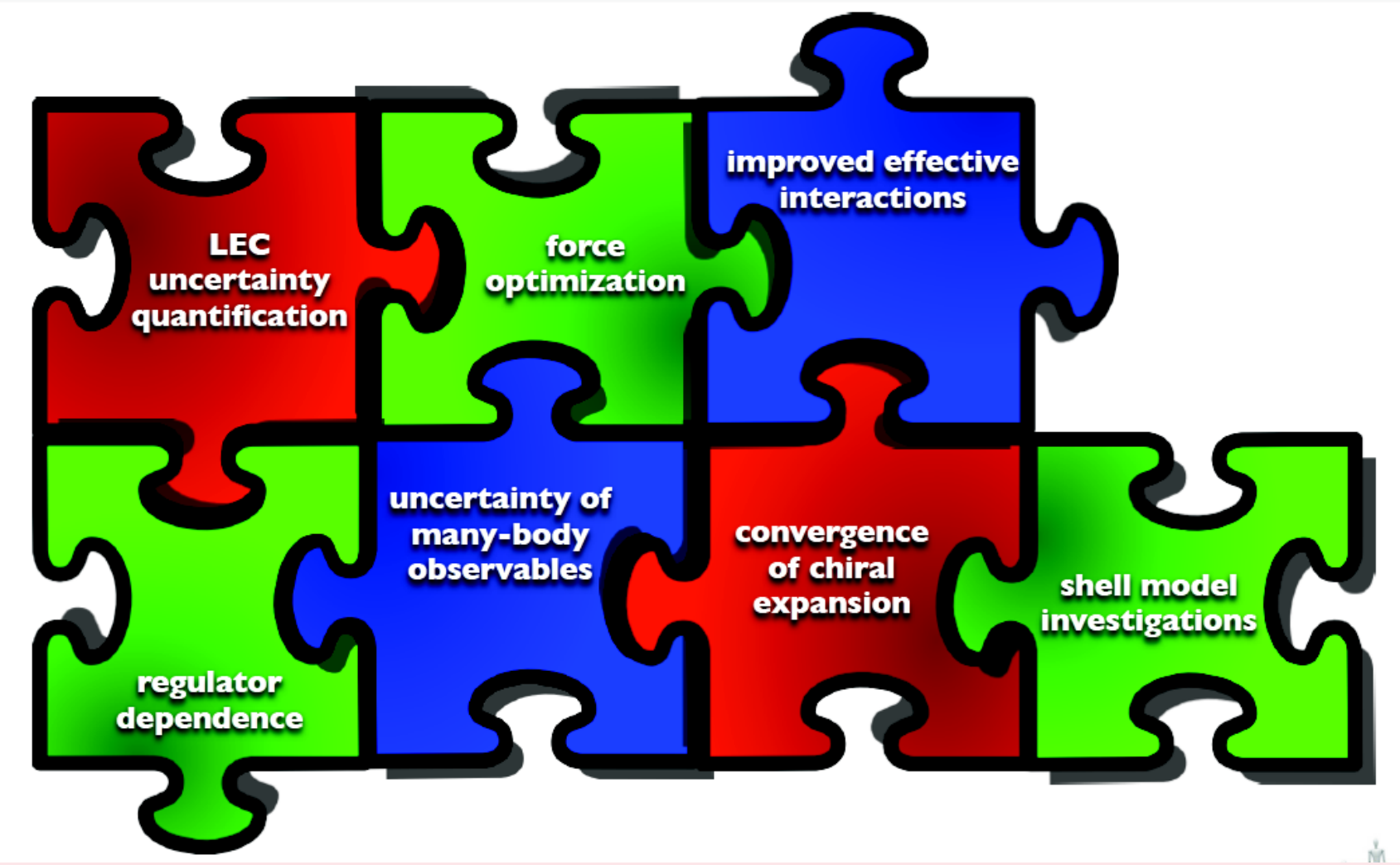

Why do we stress these requirements? Can we extract something simple?

Otsuka *et al*, PRL **104**, 012501 (2010)

The monopole term is defined as

$$v_{\mathrm{m};j,j'} = \frac{\sum_{k,k'} \langle jkj'k'|V|jkj'k'\rangle}{\sum_{k,k'} 1}$$

where j denotes a single-particle orbit with k being its magnetic substate and $\langle \cdot\cdot|V|\cdot\cdot\rangle$ is the antisymmetrized two-body matrix element.
It can be parameterized in terms of simple central part (gaussian) plus a tensor part (important for understanding shell evolution).

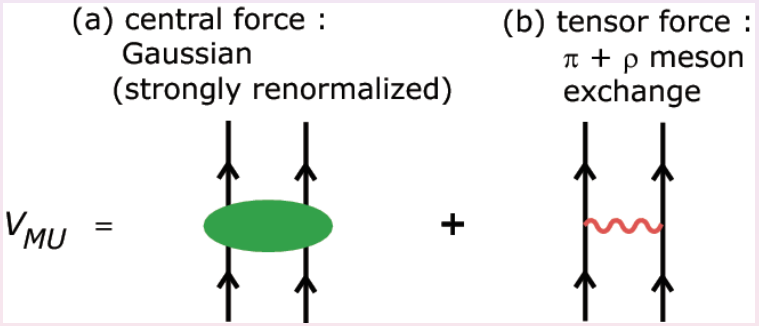

Evolution of quasiparticle states in terms of the monopole part

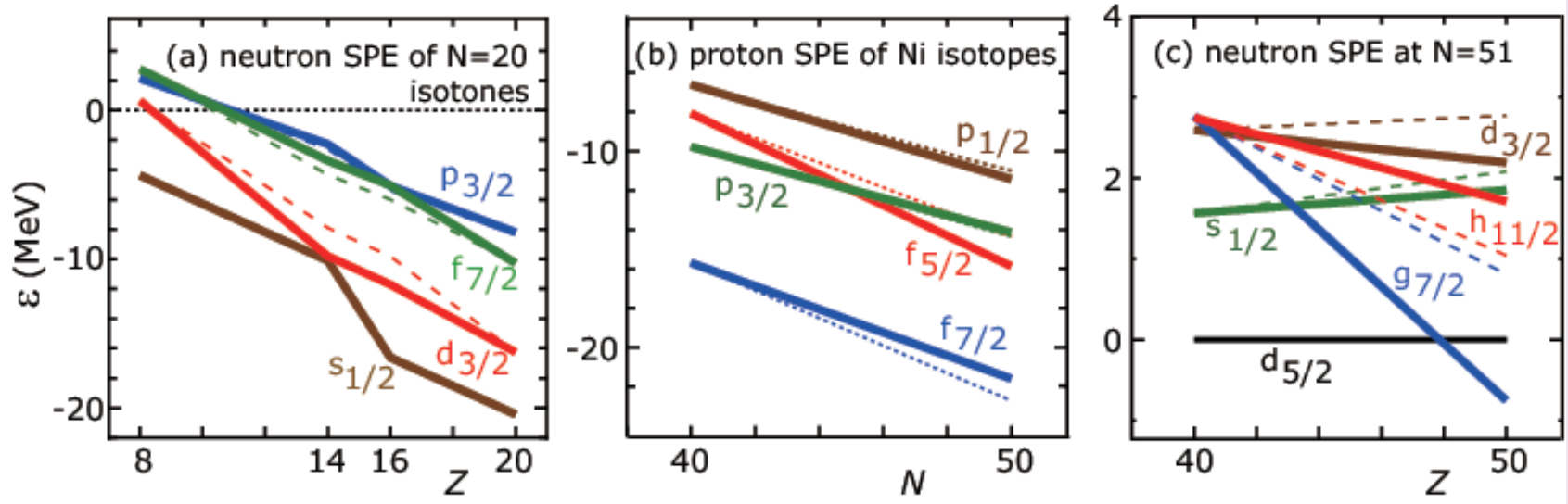

Ground state of ^{101}Sn, Darby *et al*, PRL105, 2010

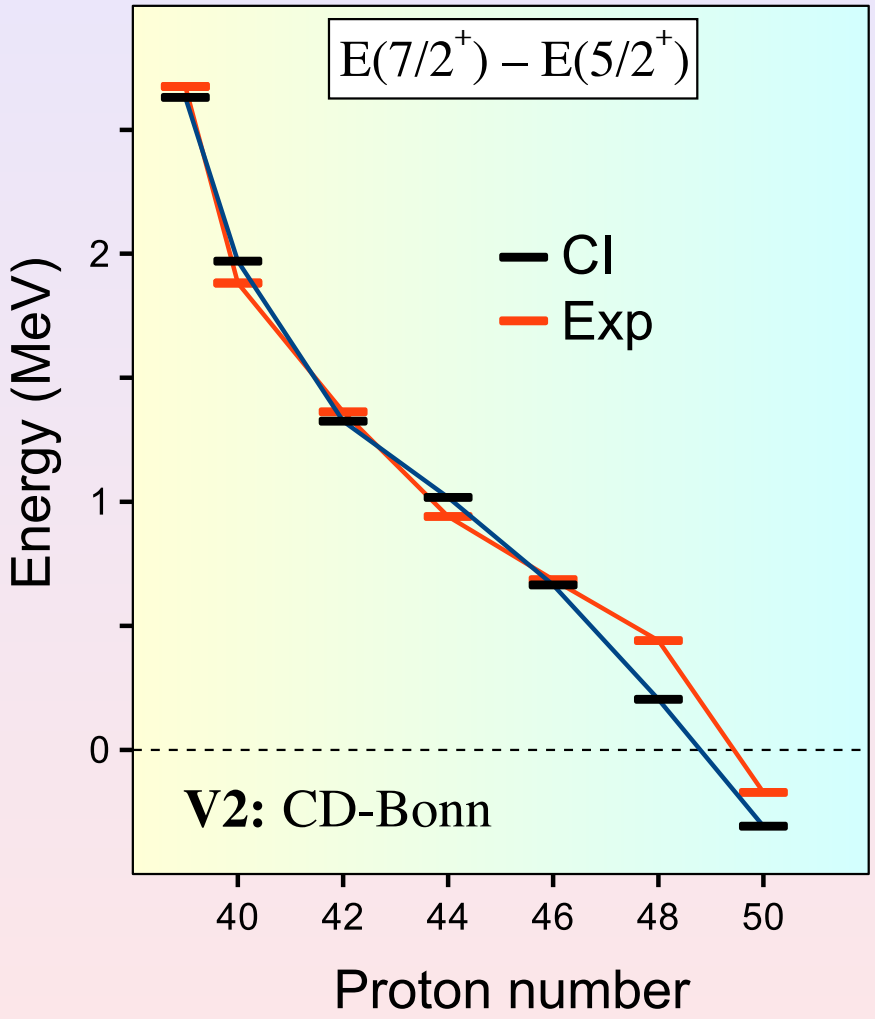

- Shell-model calculation with ^{88}Sr as core. MBPT to third order.
- Ground state of ^{101}Sn is $7/2^+$
- Core-polarization and tensor force crucial
- One crucial matrix element $\langle (0g_{7/2})^2 J = 0 | V | (0g_{7/2})^2 J = 0 \rangle$

Intermezzo: Many-body methods and quantum dots

Application to quantum dots

Circular quantum dots, comparison between different many-body methods.

1. Simple Hamiltonian, negligible three-body or more complicated many-body forces, hope is that missing many-body physics is negligible
2. Harmonic oscillator basis, two dimensions
3. Can provide exact error estimate on truncation in terms of single-particle basis, S. Kvaal, Phys. Rev. B **80**, 045321 (2009).
4. Truncation in terms of many-body excitations such as 1p-1h, 2p-2h, 3p-3h can only be justified *a posteriori*. Work in progress however, see Thorsten Rohwedder and Reinhold Schneider, Math. Modelling and Numerical Analysis, in press.

Many-body methods and quantum dots

The Hamiltonian for quantum dots

The one-body part of our Hamiltonian becomes

$$\hat{H}_0 = \sum_{i=1}^{N} (-\frac{1}{2}\nabla_i^2 + \frac{\omega^2}{2} r^2),$$

whereas the interacting part is (in our work as a renormalized one)

$$\hat{V} = \sum_{i<j}^{N} \frac{1}{|\mathbf{r}_i - \mathbf{r}_j|}.$$

The unperturbed part of the Hamiltonian yields the single-particle energies

$$\epsilon = \omega \left(2n + |m| + 1\right).$$

Gives rise to magic numbers 2, 6, 12, 20, 30, 42 . . .

The Hamiltonian for quantum dots

Define R as the number of shells.
The error in the energy made in truncating at a given shell is (S. Kvaal, Phys. Rev. B **80**, 045321 (2009))

$$\Delta E \sim O(R_{ho}^{-k+\delta-1}).$$

Here, k is the number of times a given wave function Ψ may be differentiated weakly, $\delta \in [0, 1)$ is a constant and R_{ho} is the last oscillator shell.

Many-body methods and quantum dots, Reimann, Høgberget, MHJ and Bogner, to be published

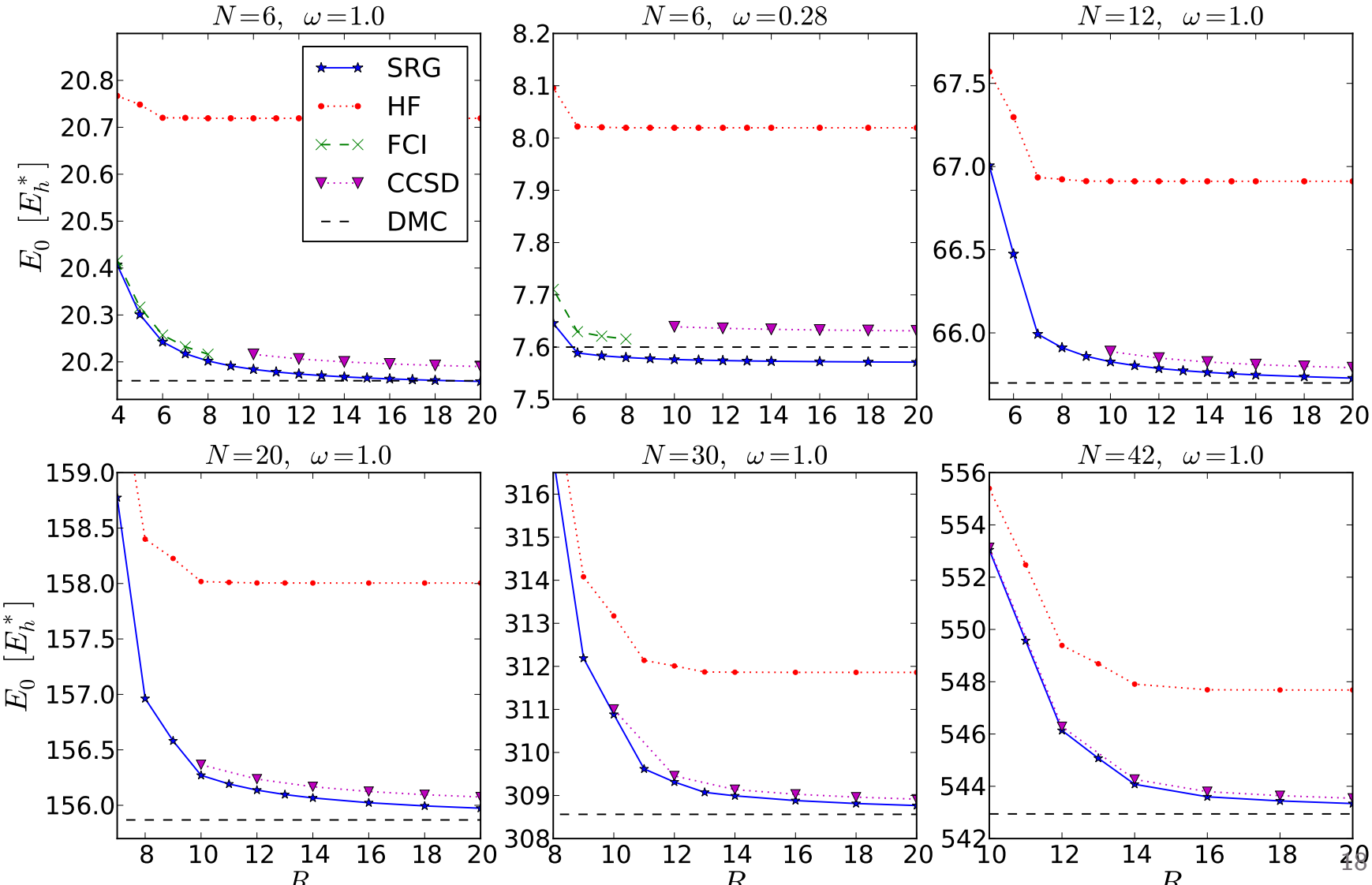

Petit quantum dot summary

- Essentially no missing many-body physics, in nuclear physics this is a problem. But keep in mind that the QED coupling constant depends weakly on energy.
- Even for small ω excellent agreements. Need to test for even smaller values where correlations become increasingly important
- Correlations beyond Hartree-Fock level become small for larger systems (ground state properties). Mean-field a good starting point, as in heavier nuclei.

Do we understand the physics of dripline systems?

- The oxygen isotopes are the heaviest isotopes for which the drip line is well established.
- Two out of four stable even-even isotopes exhibit a doubly magic nature, namely ^{22}O ($Z = 8$, $N = 14$) and ^{24}O ($Z = 8$, $N = 16$).
- The structure of ^{22}O and ^{24}O is assumed to be governed by the evolution of the $1s_{1/2}$ and $0d_{5/2}$ one-quasiparticle states.
- The isotopes ^{25}O ^{26}O, ^{27}O and ^{28}O are outside the drip line, since the $0d_{3/2}$ orbit is not bound.

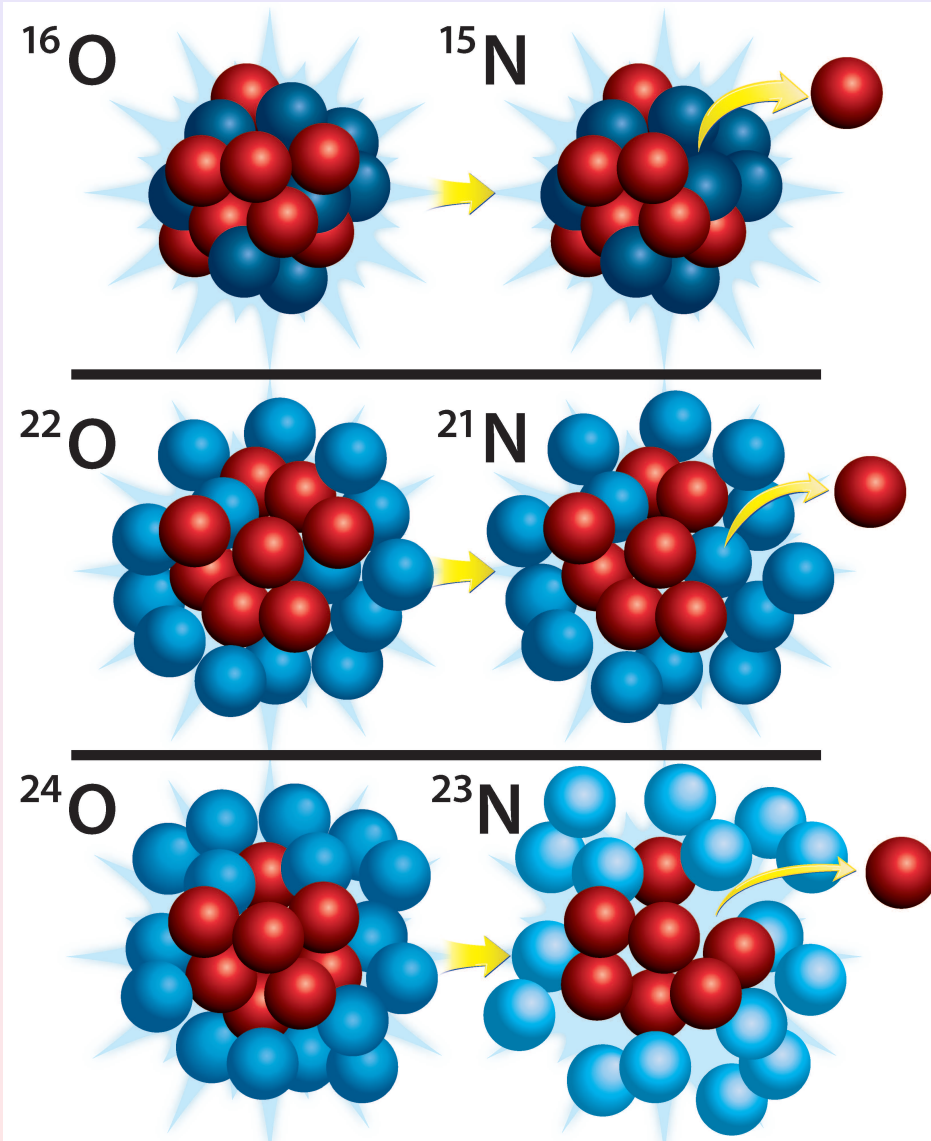

Recent Articles on Oxygen Isotopes

Many experiments worldwide!

- ^{24}O and lighter: C. R. Hoffman *et al.*, Phys. Lett. B **672**, 17 (2009); R. Kanungo *et al.*, Phys. Rev. Lett. **102**, 152501 (2009);C. R. Hoffman *et al.*, Phys. Rev. C **83**, 031303(R) (2011); Stanoiu *et al.*, Phys. Rev. C **69**, 034312 (2004)
- ^{25}O: C. R. Hoffman *et al.*, Phys. Rev. Lett. **102**,152501 (2009).
- ^{26}O: E. Lunderberg *et al.*, Phys. Rev. Lett., **108**, 142503 (2012).
- S. Tshoo *et al*, N=16 Spherical Shell Closure in ^{24}O, Phys. Rev. Lett. **109**, 022501 (2012)
- ^{26}O: Z. Kohley *et al.*, Study of two-neutron radioactivity in the decay of 26O, arXiv:1303.2617
- Theory: Oxygen isotopes with three-body forces, Otsuka *et al.*, Phys. Rev. Lett., **105**, 032501 (2010). Hagen *et al.*, Phys. Rev. Lett., **108**, 242501 (2012).

Calcium isotopes and FRIB plans and capabilities

- The Ca isotope exhibit several possible closed-shell nuclei ^{40}Ca, ^{48}Ca, ^{52}Ca, ^{54}Ca, and ^{60}Ca.
- Magic neutron numbers are then $N = 20, 28, 32, 34, 40$.
- Published masses available up to ^{52}Ca, Gallant *et al.*,Phys. Rev. Lett. **109**, 032506 (2012).
- Heaviest observed ^{57,58}Ca. NSCL experiment, O. B. Tarasov *et al.*, Phys. Rev. Lett. **102**, 142501 (2009). Cross sections for ^{59,60}Ca assumed small ($< 10^{-12}$mb).
- Which degrees of freedom prevail close to ^{60}Ca and beyond?

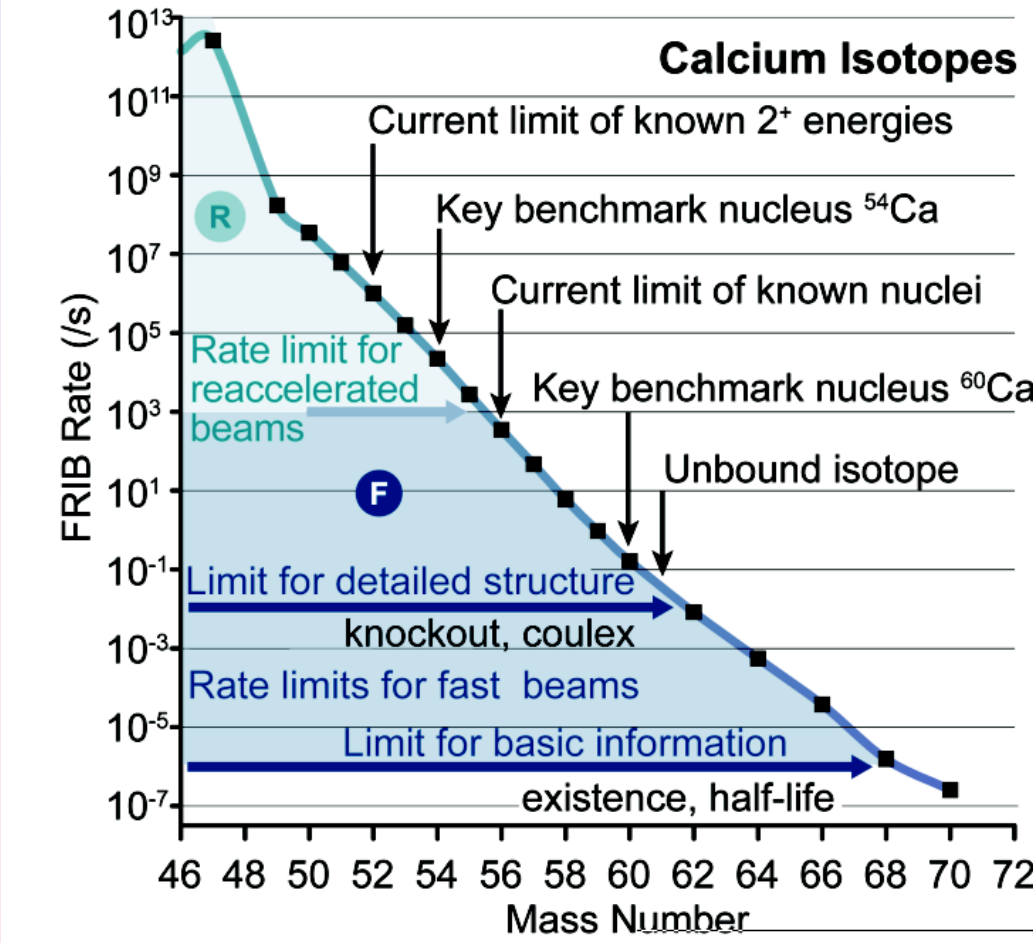

More on Calcium Isotopes

- **Mass models and mean field models predict the dripline at $A \sim 70$!** Important consequences for modeling of nucleosynthesis related processes.
- Can we predict reliably which is the last stable calcium isotope?
- And how does this compare with popular mass models on the market? See Nature 486, 509 (2012).
- And which parts of the underlying forces are driving the physics towards the dripline?

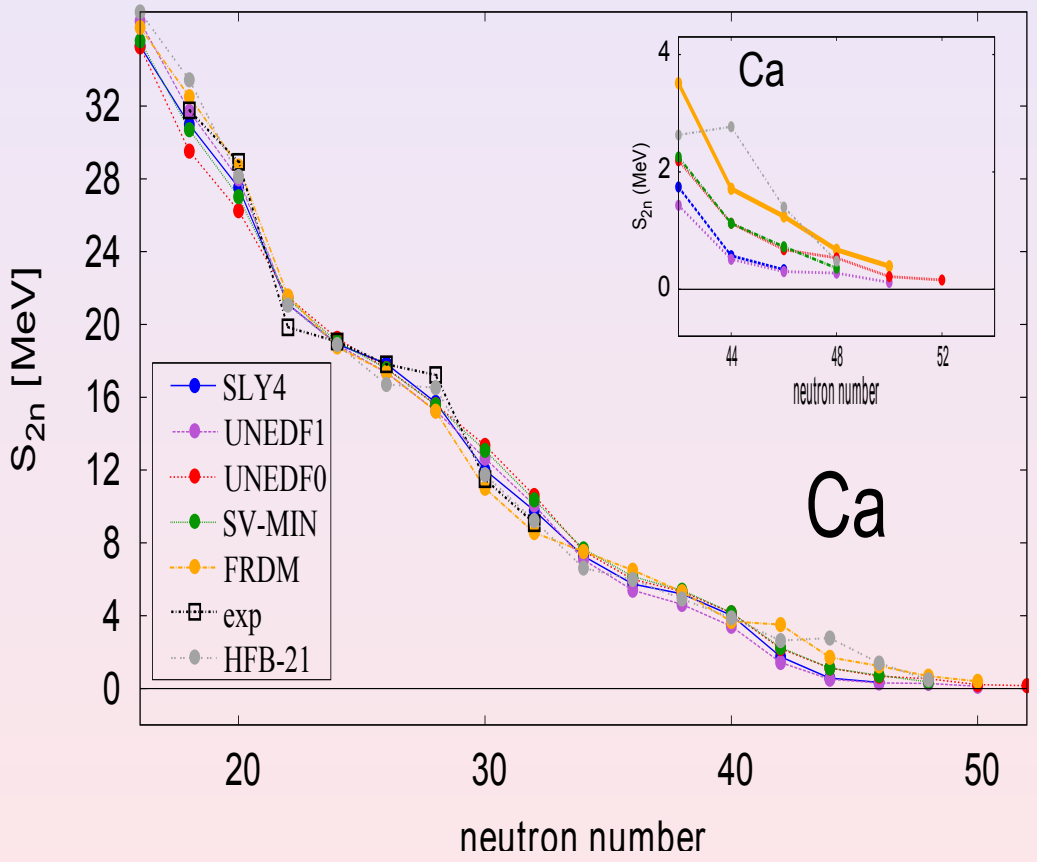

Other chains of isotopes of crucial interest for FRIB like physics: nickel isotopes

- This chain of isotopes exhibits four possible closed-shell nuclei ^{48}Ni, ^{56}Ni, ^{68}Ni and ^{78}Ni. **FRIB plans systematic studies from ^{48}Ni to ^{88}Ni.**
- Compute several of these nuclei and the corresponding $A \pm 1$ and $A \pm 2$ systems like ^{79}Cu soon. Need for experiments in the vicinity of say ^{78}Ni.
- Neutron skin possible for ^{84}Ni at FRIB.
- Which is the best closed-shell nucleus? And again, which part of the nuclear forces drives it? Is it the strong spin-orbit force, the tensor force, or ..?

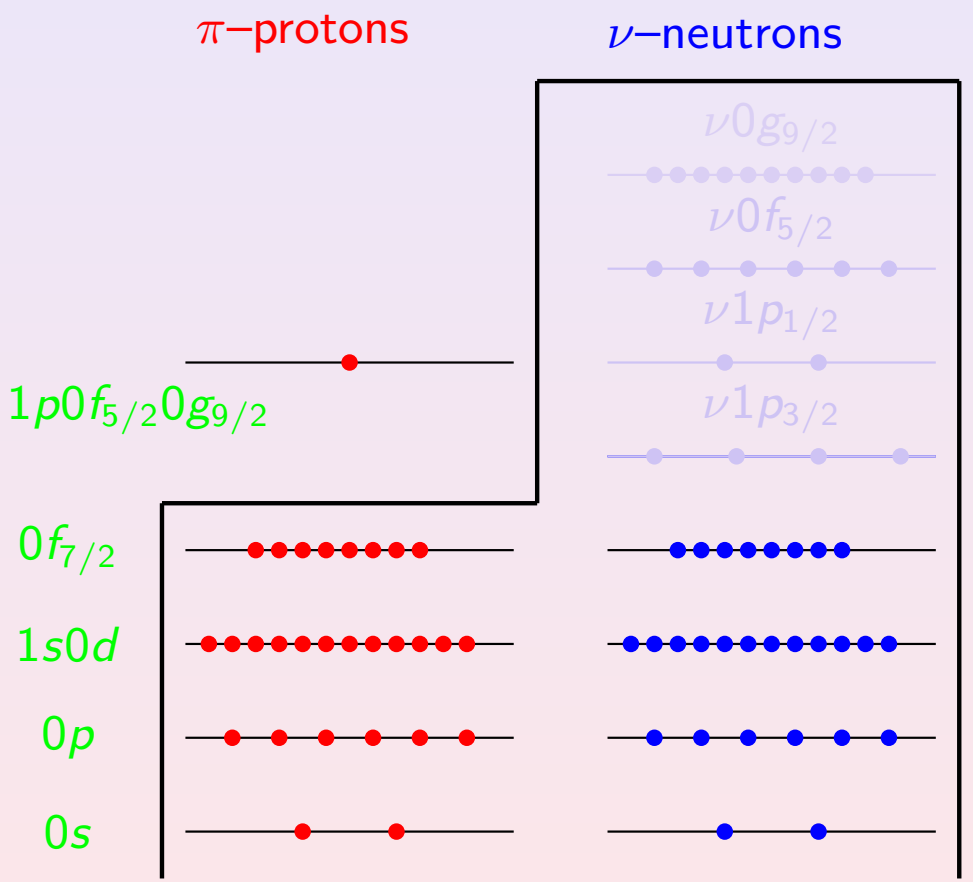

Other chains of isotopes of crucial interest for FRIB like physics: nickel isotopes

- This chain of isotopes exhibits four possible closed-shell nuclei ^{48}Ni, ^{56}Ni, ^{68}Ni and ^{78}Ni. **FRIB plans systematic studies from ^{48}Ni to ^{88}Ni.**
- Compute several of these nuclei and the corresponding $A \pm 1$ and $A \pm 2$ systems like ^{79}Cu soon. Need for experiments in the vicinity of say ^{78}Ni.
- Neutron skin possible for ^{84}Ni at FRIB.
- Which is the best closed-shell nucleus? And again, which part of the nuclear forces drives it? Is it the strong spin-orbit force, the tensor force, or ..?

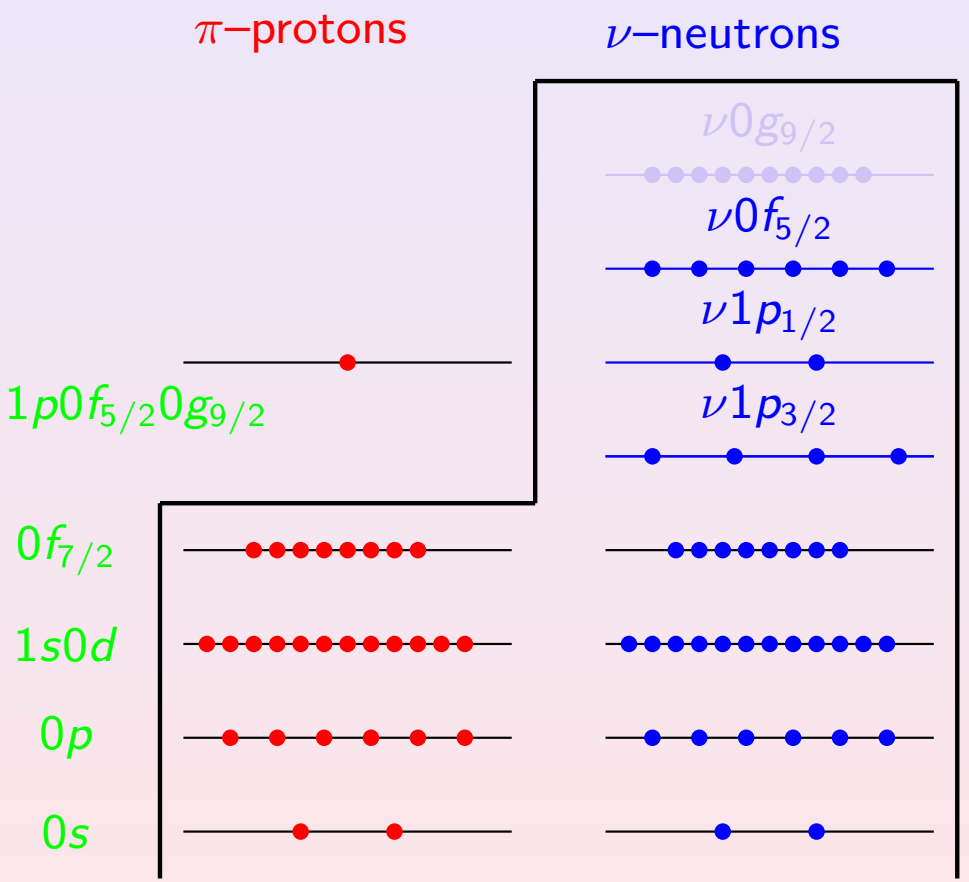

Other chains of isotopes of crucial interest for FRIB like physics: nickel isotopes

- This chain of isotopes exhibits four possible closed-shell nuclei ^{48}Ni, ^{56}Ni, ^{68}Ni and ^{78}Ni. **FRIB plans systematic studies from ^{48}Ni to ^{88}Ni.**
- Compute several of these nuclei and the corresponding $A \pm 1$ and $A \pm 2$ systems like ^{79}Cu soon. Need for experiments in the vicinity of say ^{78}Ni.
- Neutron skin possible for ^{84}Ni at FRIB.
- Which is the best closed-shell nucleus? And again, which part of the nuclear forces drives it? Is it the strong spin-orbit force, the tensor force, or ..?

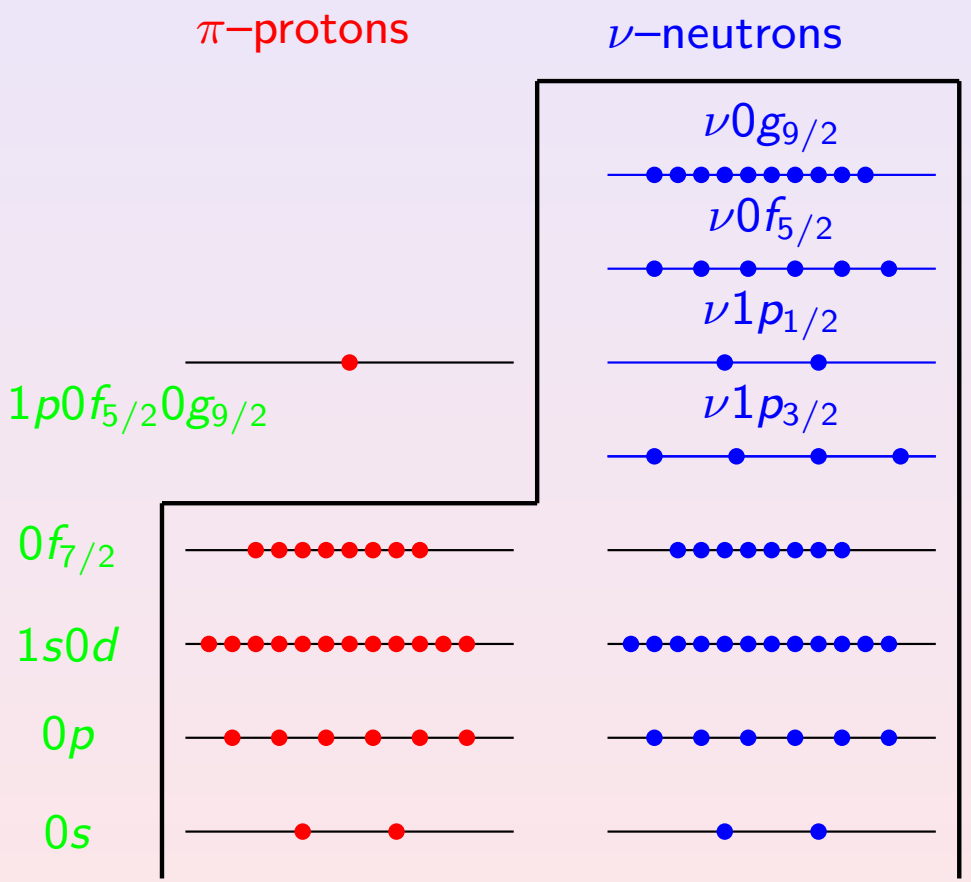

Tin isotopes

From ^{100}Sn to nuclei beyond ^{132}Sn

1. We will most likely be able to run coupled-cluster calculations for nuclei like ^{100}Sn, ^{114}Sn, ^{116}Sn, ^{132}Sn, ^{140}Sn and $A \pm 1$ and $A \pm 2$ nuclei within the next one to two years. FRIB can reach to ^{140}Sn. Interest also for EOS studies.
2. Can then test the development of many-body forces for an even larger chain of isotopes.
3. ^{137}Sn is the last reported neutron-rich isotope (with half-life).
4. To understand which parts of the nuclear Hamiltonian that drives the properties of such nuclei will be crucial for our understanding of the stability of matter.
5. Zr isotopes form also long chains of neutron-rich isotopes. **FRIB plans from ^{80}Zr to ^{120}Zr.**
6. And why neutron rich isotopes? **Here the possibility to constrain nuclear forces from in-medium results.**

Oxygen isotopes with three-body forces, Hagen *et al*, Phys. Rev. Lett. **108**, 242501 (2012).

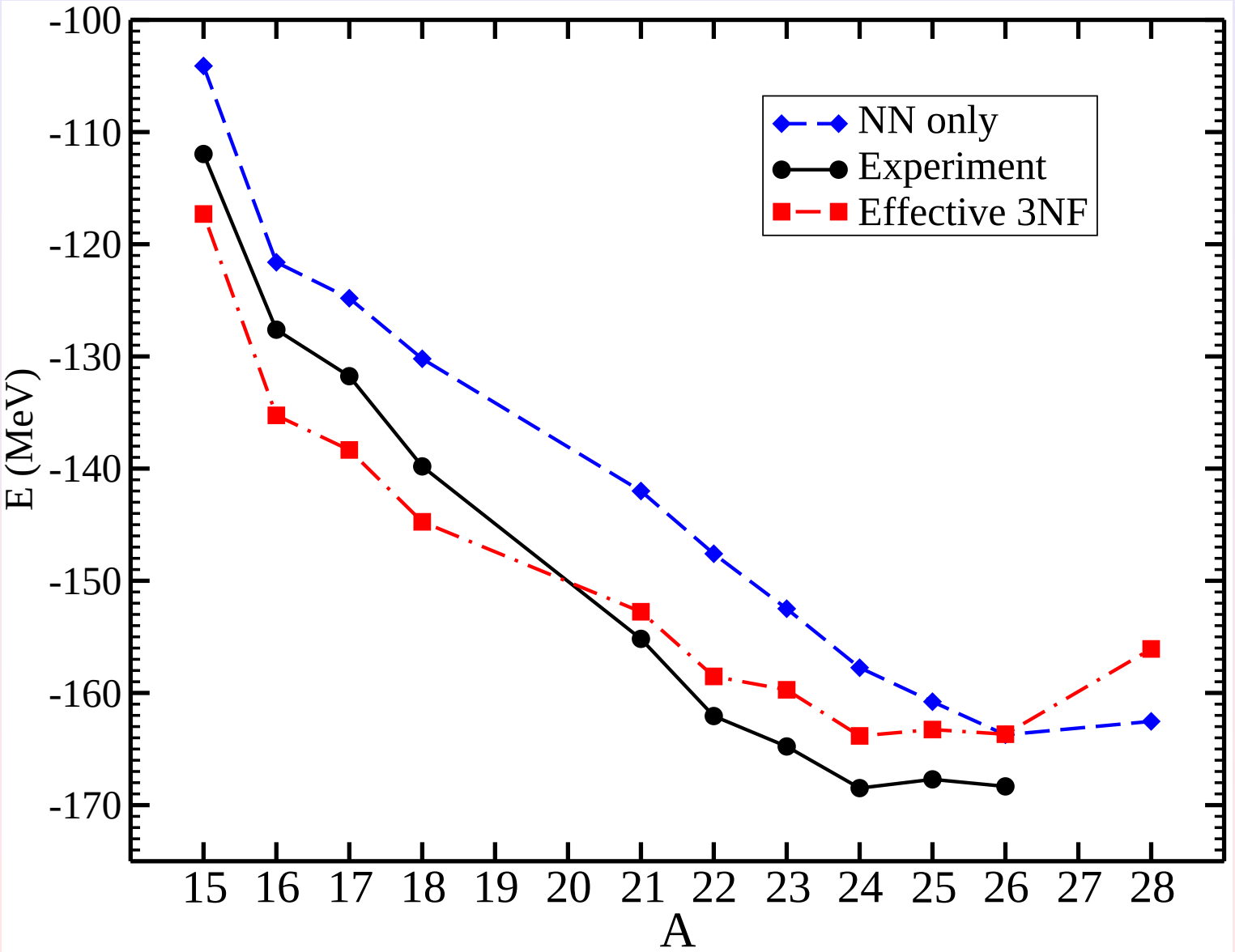

Calcium isotopes with three-body forces, Hagen *et al*, Phys. Rev. Lett. **109**, 032502 (2012)

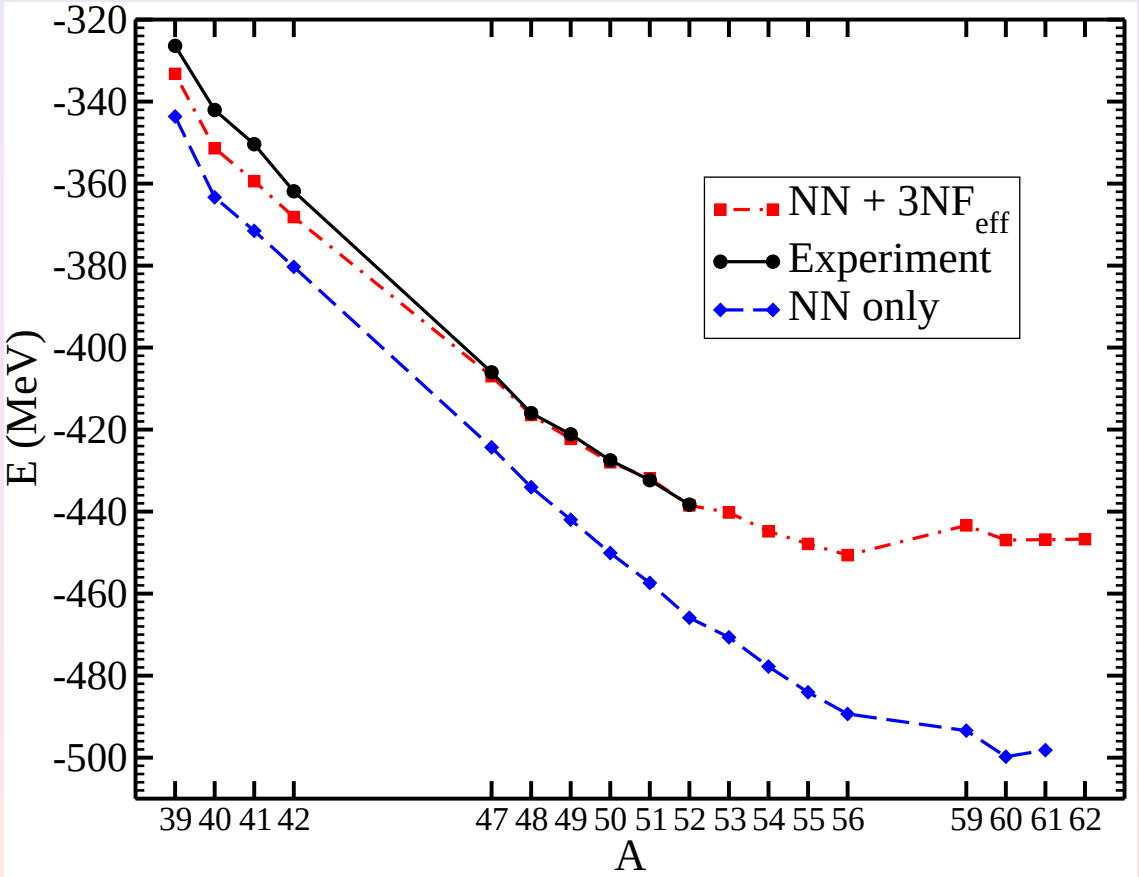

- Same Hamiltonian model as for the oxygen isotopes
- Only change is C_E from 0.71 to $c_E = 0.735$. $k_F = 1.0$ fm^{-1}.
- Most mass models predict dripline at $A = 70$
- We predict it at $A \sim 60$?

What about the fluorine isotopes

- The dripline is predicted at ^{31}F. But not all are bound. The ground state of ^{28}F is an unbound resonance of 220 keV above the ground state of ^{27}F.
- ^{26}F is bound by only 0.80(12) MeV
- ^{26}F can be interpreted as a closed ^{24}O core plus a *deeply bound* proton in the $\pi 0d_{5/2}$ orbit and an unbound neutron in the $\nu 0d_{3/2}$ orbit.

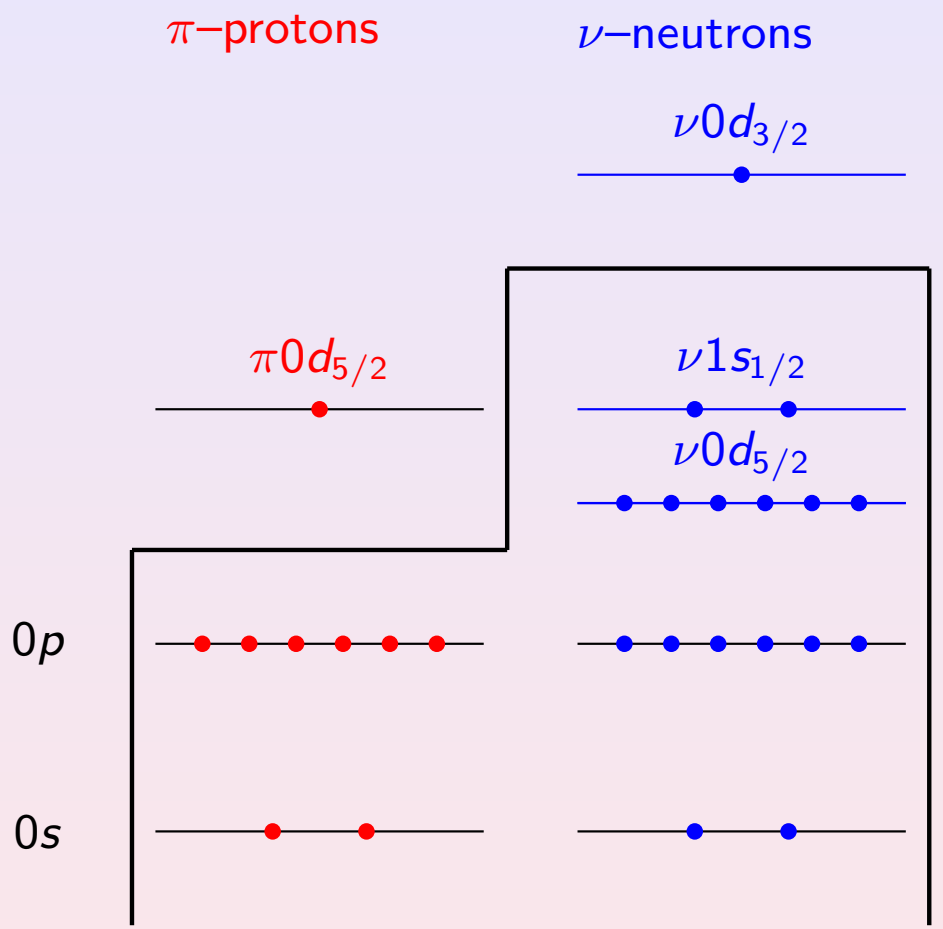

Results for ^{26}F, Lepailleur *et al*, Phys. Rev. Lett. **110**, 082502 (2013)

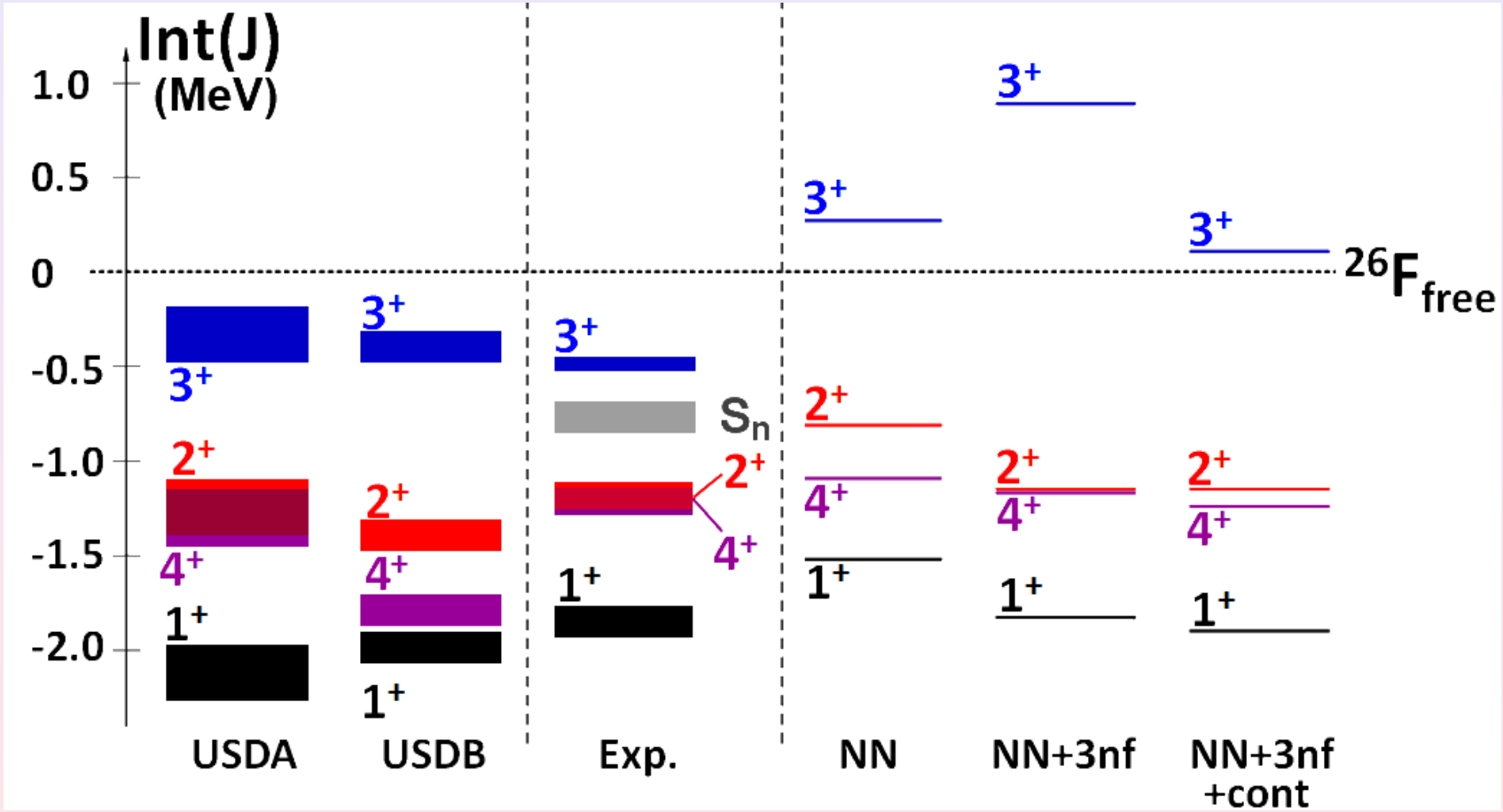

What about refitting the force? Ekström *et al*, Phys. Rev. Lett. **110**, 192502 (2013)

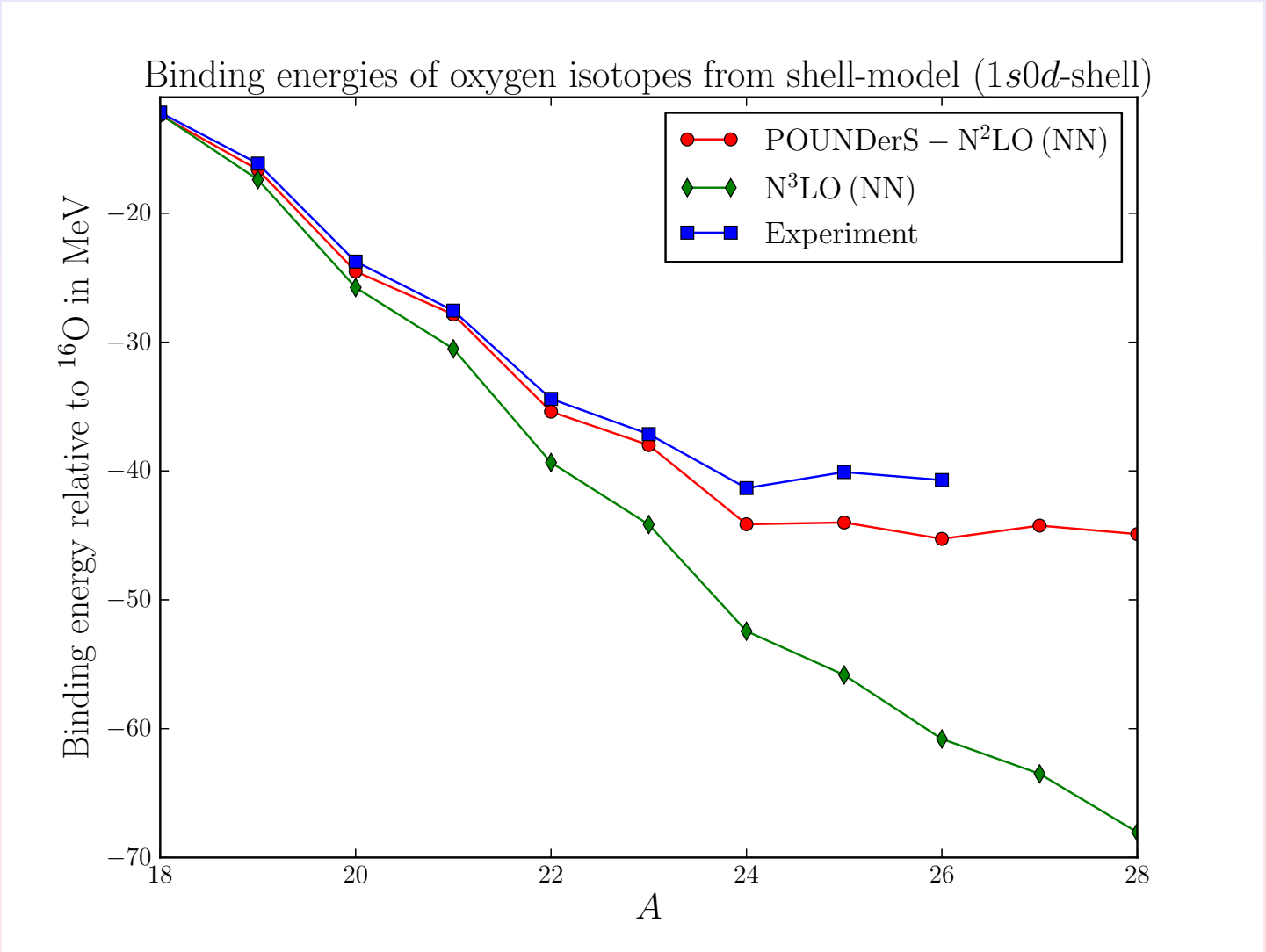

What is done here? Chiral interactions at order NNLO

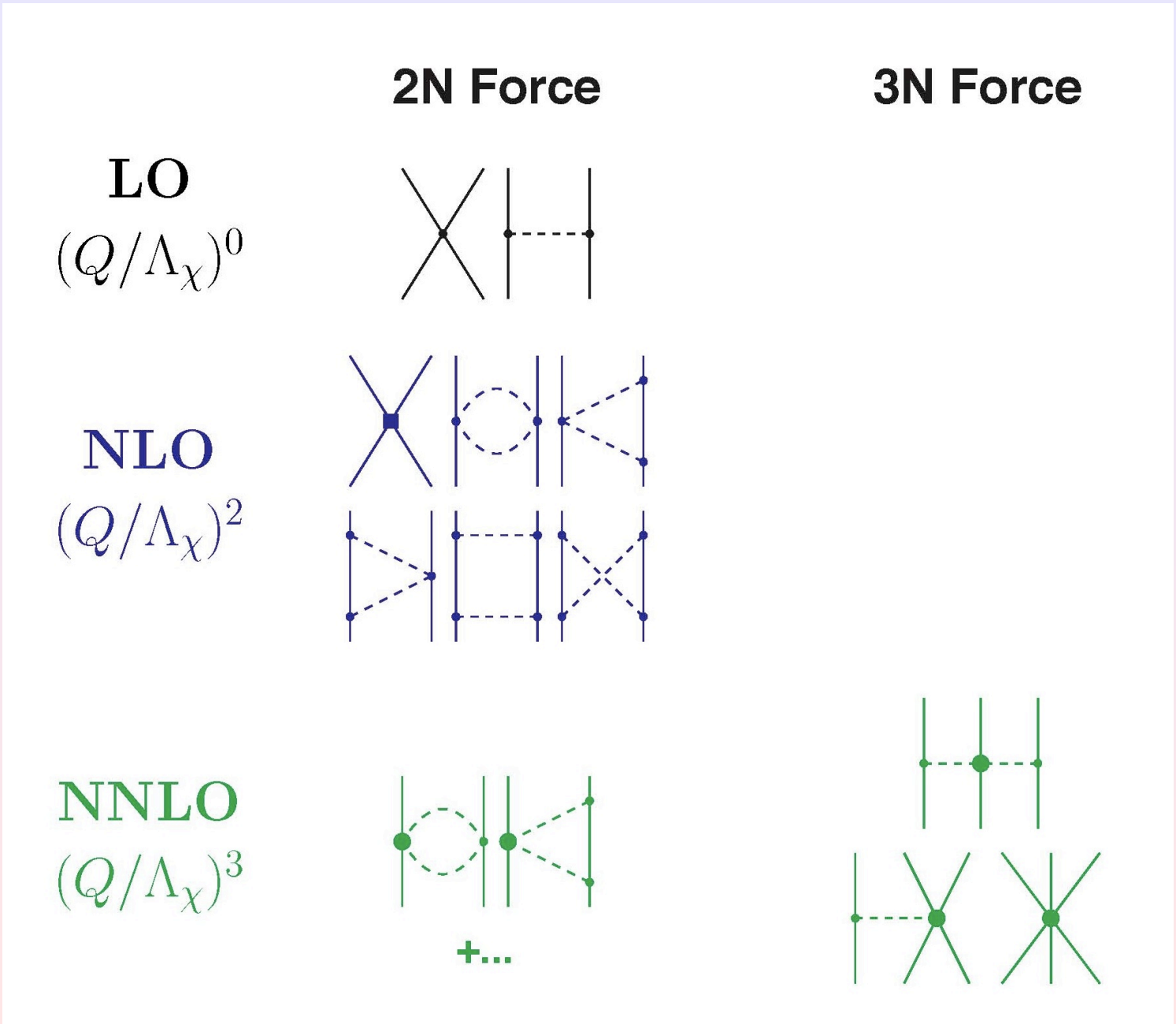

The parameters

[5+2+2] reagarded as constants

$m_{\pi^+}, m_{\pi^-}, m_{\pi^0}, m_n, m_p,\ g_A, f_\pi,\ \Lambda_{LS}, \Lambda_\chi$

[14+2] Optimization parameters up to NNLO

$\tilde{C}^{pp}_{^1S_0}, \tilde{C}^{nn}_{^1S_0}, \tilde{C}^{np}_{^1S_0}, \tilde{C}_{^3S_1}$

$C_{^1S_0}, C_{^3P_0}, C_{^1P_1}, C_{^3P_1}, C_{^3S_1}, C_{^3S_1-{}^3D_1}, C_{^3P_2}$

$c_1, c_3, c_4, (c_D, c_E)$

[21] Additional parameters at N3LO

$c_2, \bar{d}_1, \bar{d}_2, \bar{d}_3, \bar{d}_5, \bar{d}_{14} - \bar{d}_{15}$

$D_{^1S_0}, \hat{D}_{^1S_0}, D_{^3P_0}, D_{^1P_1}, D_{^3P_1}, \hat{D}_{^3S_1}, D_{^3S_1}, D_{^3D_1}, \hat{D}_{^3S_1-{}^3D_1}$

$D_{^3S_1-{}^3D_1}, D_{^1D_2}, D_{^3D_2}, D_{^3P_2}, D_{^3P_2-{}^3F_2}, D_{^3D_3}$

The parameters

[5+2+2] reagarded as constants

$m_{\pi^+}, m_{\pi^-}, m_{\pi^0}, m_n, m_p,\ g_A, f_\pi,\ \Lambda_{LS}, \Lambda_\chi$

[14+2] Optimization parameters up to NNLO

$\tilde{C}^{pp}_{^1S_0}, \tilde{C}^{nn}_{^1S_0}, \tilde{C}^{np}_{^1S_0}, \tilde{C}_{^3S_1}$

$C_{^1S_0}, C_{^3P_0}, C_{^1P_1}, C_{^3P_1}, C_{^3S_1}, C_{^3S_1-{}^3D_1}, C_{^3P_2}$

$c_1, c_3, c_4, (c_D, c_E)$

[21] Additional parameters at N3LO

$c_2, \bar{d}_1, \bar{d}_2, \bar{d}_3, \bar{d}_5, \bar{d}_{14} - \bar{d}_{15}$

$D_{^1S_0}, \hat{D}_{^1S_0}, D_{^3P_0}, D_{^1P_1}, D_{^3P_1}, \hat{D}_{^3S_1}, D_{^3S_1}, D_{^3D_1}, \hat{D}_{^3S_1-{}^3D_1}$

$D_{^3S_1-{}^3D_1}, D_{^1D_2}, D_{^3D_2}, D_{^3P_2}, D_{^3P_2-{}^3F_2}, D_{^3D_3}$

POUNDerS

Practical Optimization Using No Derivatives (Square/Structure)

function evaluation

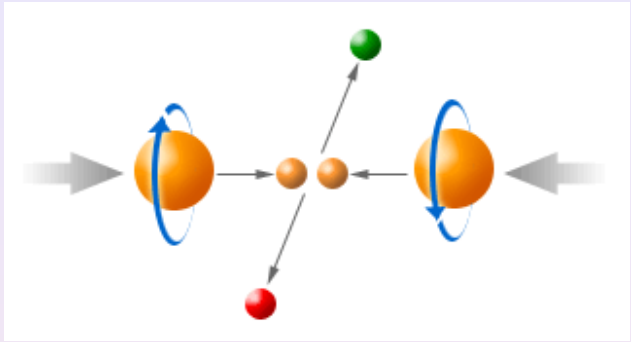

POUNDerS step

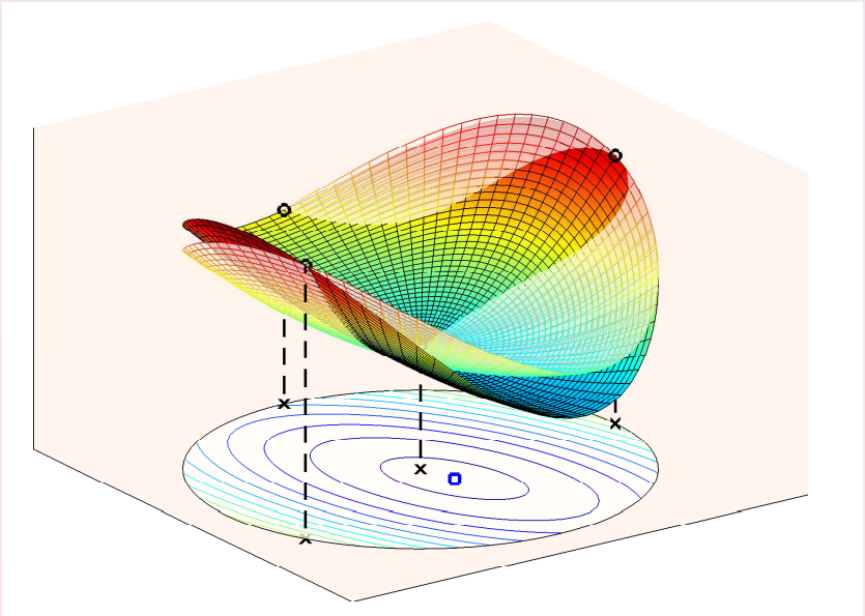

- Optimize over computationally expensive, nonlinear functions arising in science and engineering
- Function values all you have, and derivatives are computationally expensive

Optimization strategy wrt phase shifts from the Nijmegen multienergy PWA.

Initial study (this)

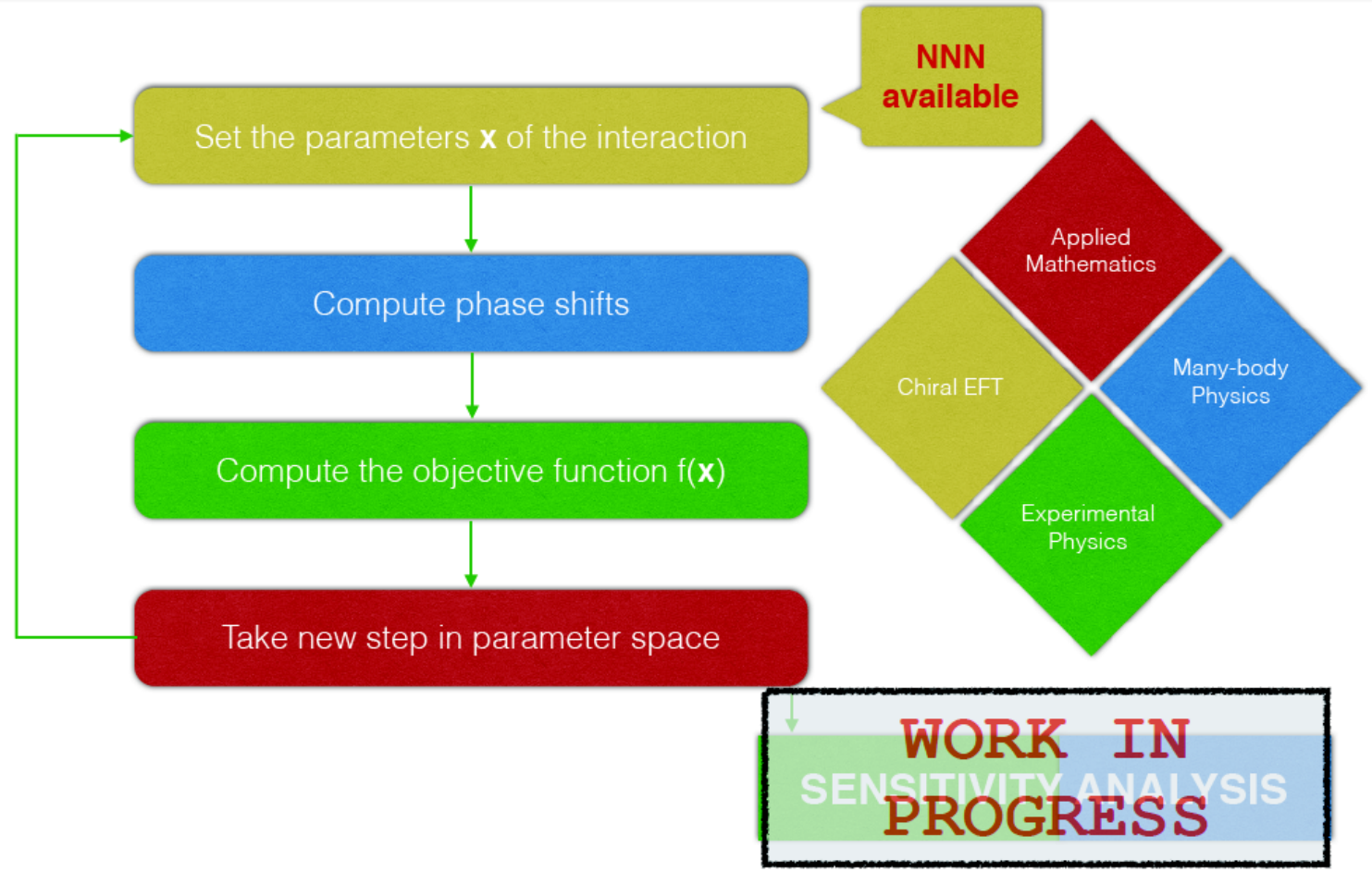

Coupled-cluster calculations, Ekström *et al*, Phys. Rev. Lett. **110**, 192502 (2013)

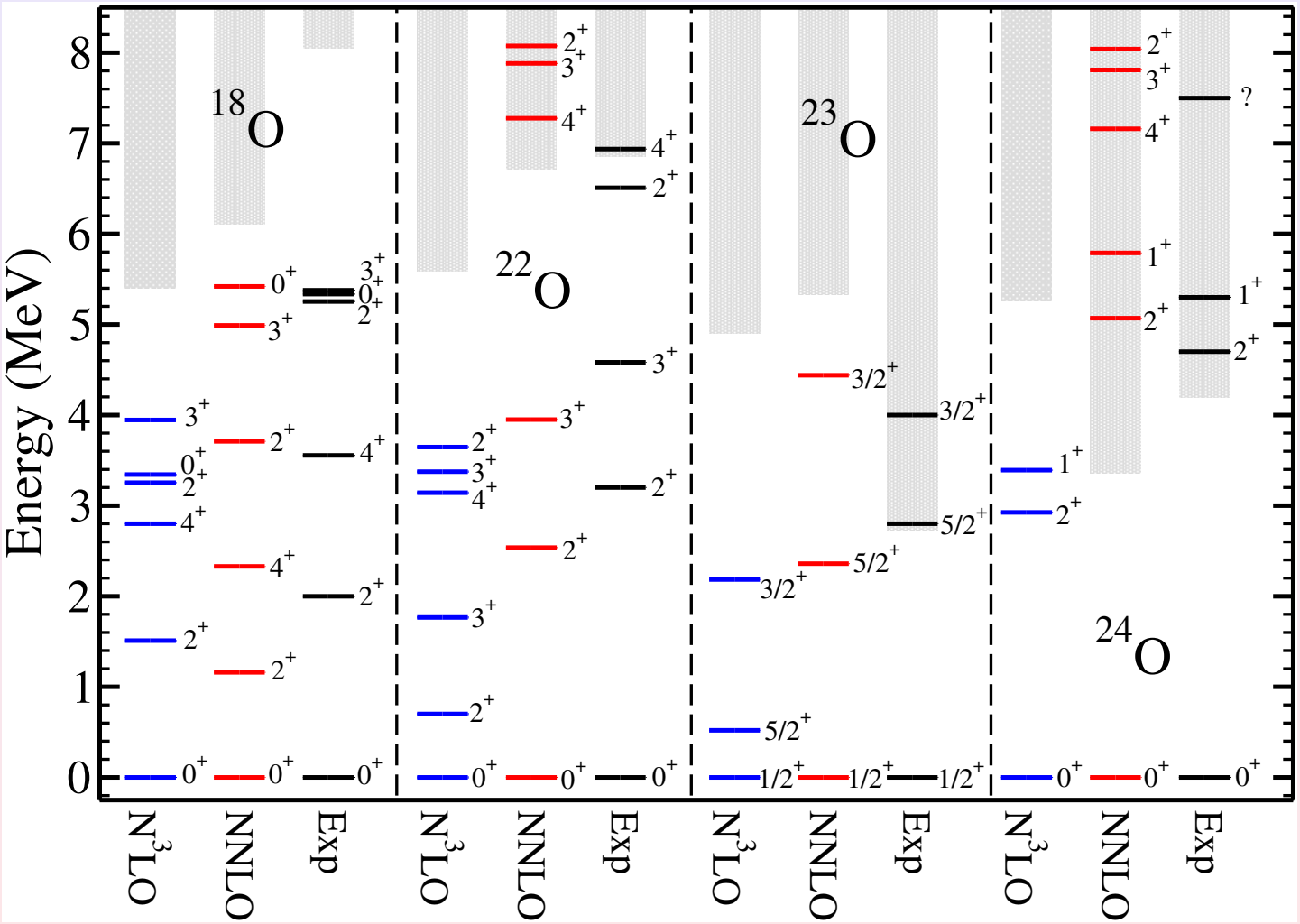

Ekström *et al*, Phys. Rev. Lett. **110**, 192502 (2013).
Excited states in calcium

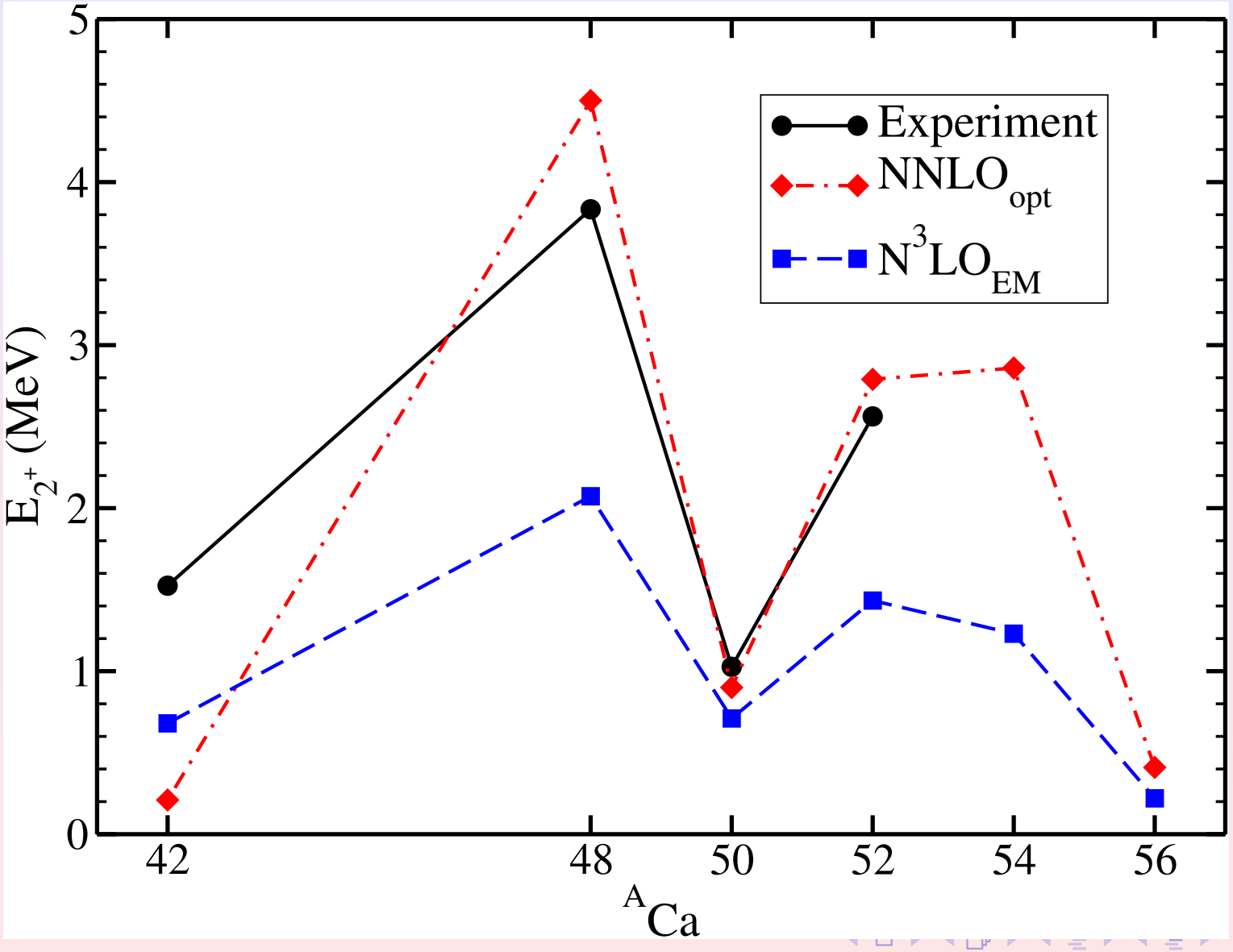

Ekström *et al*, Phys. Rev. Lett. **110**, 192502 (2013).
Neutron star matter

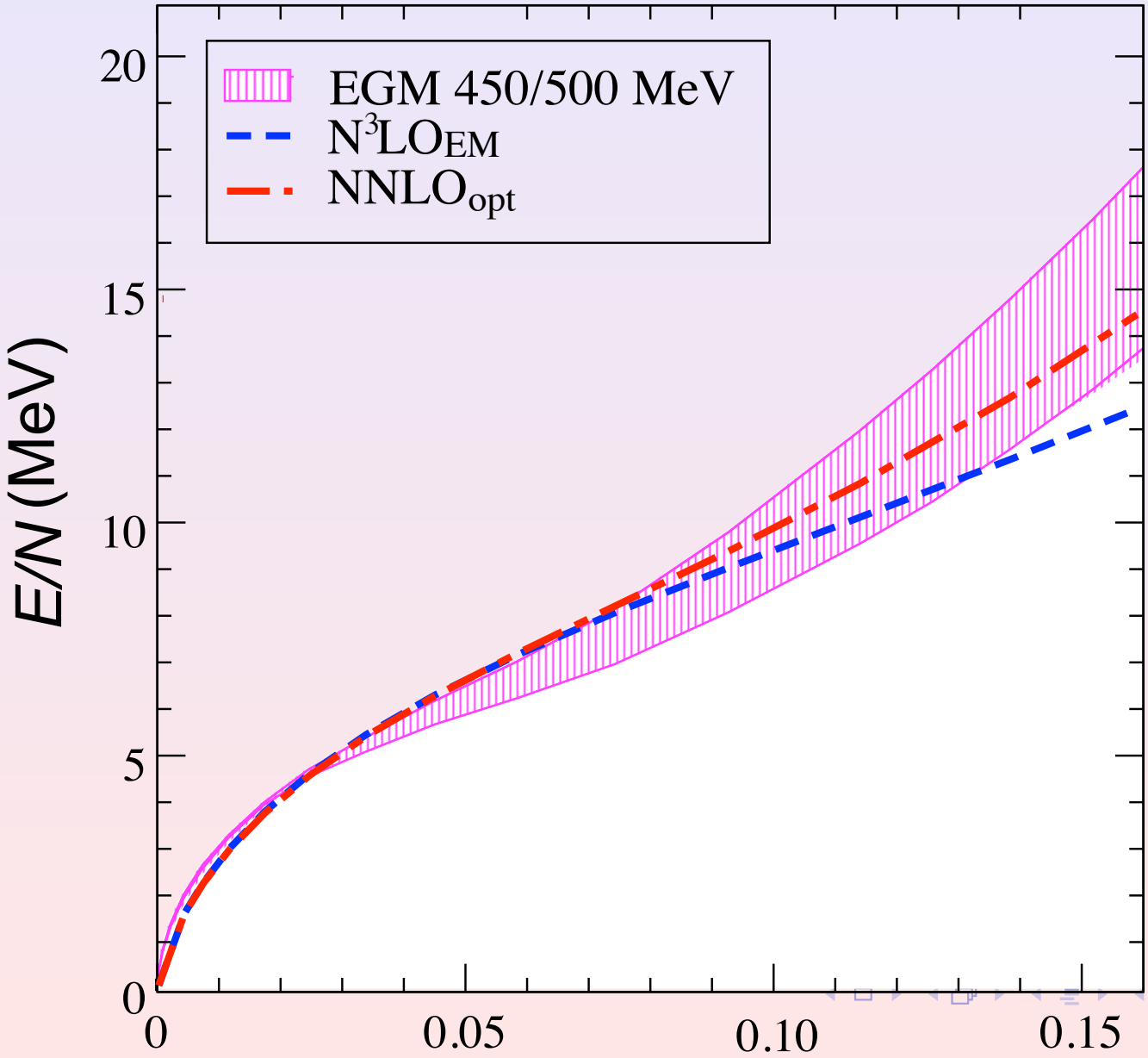

Summary and perspectives. Where are we now?

- **Better optmized nuclear forces improve agreement with data at two-nucleon force level. Smaller three-body forces**. This will this apply to the next order as well?
- **Correlations due to three-body forces and continuum effects are important when we move towards the driplines.**
- **Correlations are strong towards the dripline, mean field is not a useful picture**
- We have just started studying better optimized forces. Till now we have studied mainly neutron-rich systems. Are now fitting to cross sections.
- With proper error estimates at the two- and three-body level, we can provide better error estimates in many-body calculations

Our final aim is to provide a reliable theory with proper error estimates

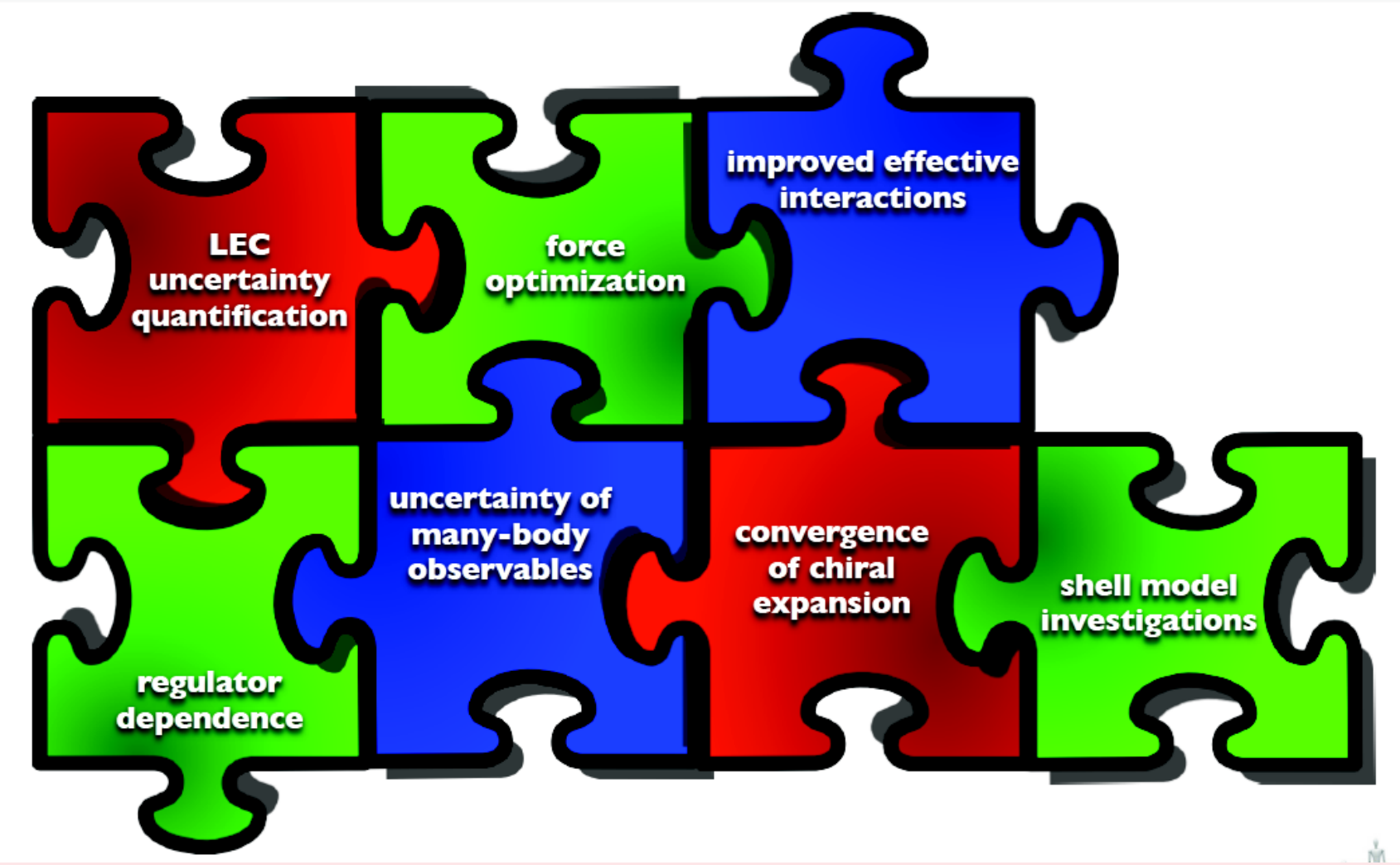

Optimization strategy, in figure form

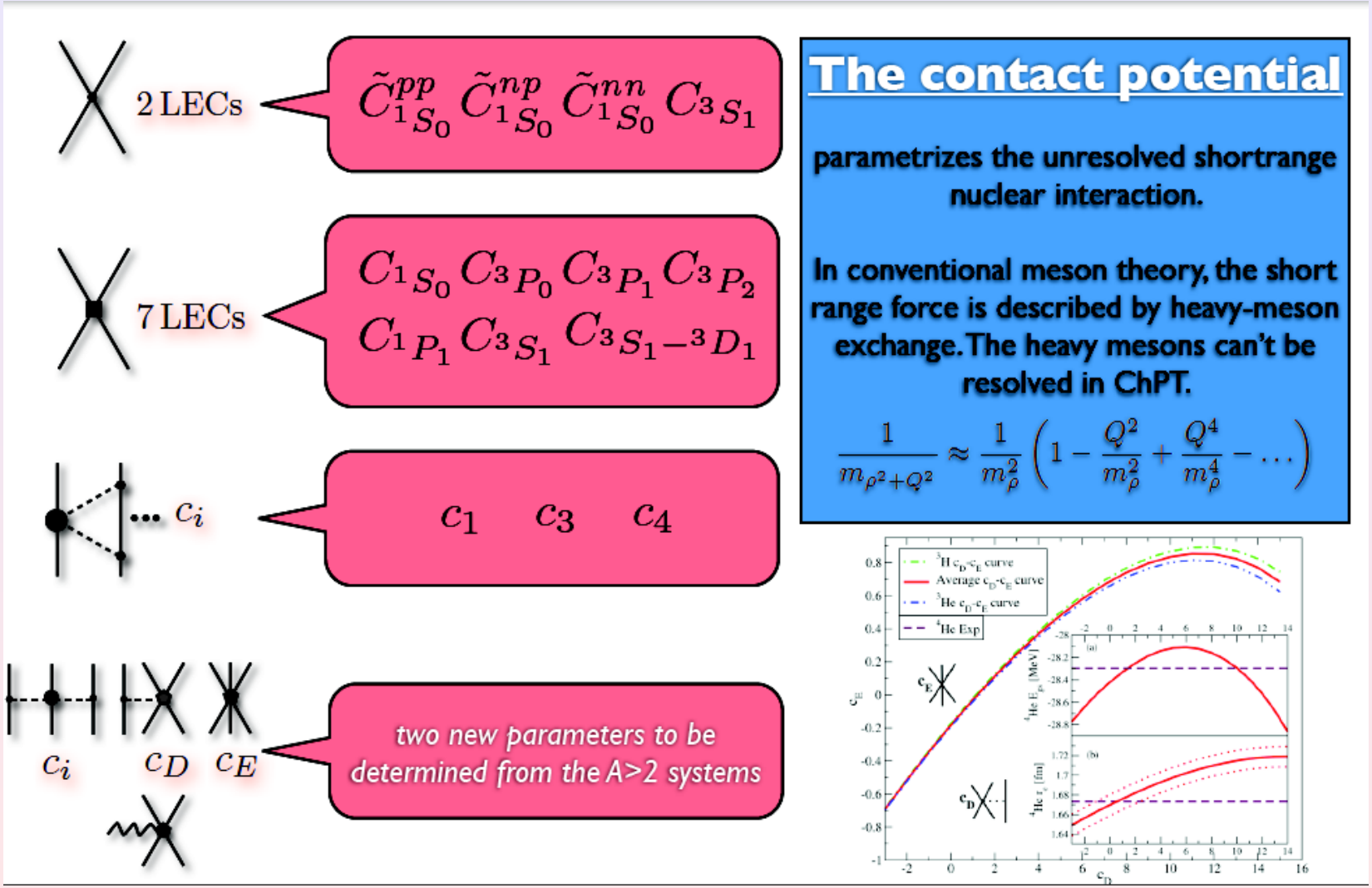

Optimization strategy, level 0 or version 0

πN

The πN contacts c_1, c_3, c_4 were optimized simultaneously using the peripheral ($L \geq 2$) waves ${}^1D_2, {}^3D_2, {}^3F_2, E_2, {}^3F_3, {}^1G_4$, and ${}^3F_4$

NN-contacts

The NN contacts $\tilde{C}^{pp}_{{}^1S_0}$ $\tilde{C}^{nn}_{{}^1S_0}$ $\tilde{C}^{np}_{{}^1S_0}$ $C_{{}^3P_0}$ $C_{{}^1P_1}$ $C_{{}^1S_0}$ $\tilde{C}_{{}^3S_1}$ $C_{{}^3S_1}$ $C_{{}^3S_1-{}^3D_1}$ $C_{{}^3P_2}$ were optimized in the respective partial wave.

Two remarks

- When computing the χ^2/datum, it turns out that this is lowered when the ${}^1P_1$-wave is weighted with experimental uncertainties
- The ${}^3S_1 - {}^3D_1$ coupled-channel is optimized with the additional constraint of reproducing the deuteron binding energy.

Everything else is a prediction

Optimization strategy, level 0 or version 0

πN

The πN contacts c_1, c_3, c_4 were optimized simultaneously using the peripheral ($L \geq 2$) waves ${}^1D_2, {}^3D_2, {}^3F_2, E_2, {}^3F_3, {}^1G_4$, and ${}^3F_4$

NN-contacts

The NN contacts $\tilde{C}_{^1S_0}^{pp}$ $\tilde{C}_{^1S_0}^{nn}$ $\tilde{C}_{^1S_0}^{np}$ $C_{^3P_0}$ $C_{^1P_1}$ $C_{^1S_0}$ $\tilde{C}_{^3S_1}$ $C_{^3S_1}$ $C_{^3S_1-{}^3D_1}$ $C_{^3P_2}$ were optimized in the respective partial wave.

Two remarks

- When computing the χ^2/datum, it turns out that this is lowered when the ${}^1P_1$-wave is weighted with experimental uncertainties
- The ${}^3S_1 - {}^3D_1$ coupled-channel is optimized with the additional constraint of reproducing the deuteron binding energy.

Everything else is a prediction

Optimization strategy, level 0 or version 0

πN

The πN contacts c_1, c_3, c_4 were optimized simultaneously using the peripheral ($L \geq 2$) waves ${}^1D_2, {}^3D_2, {}^3F_2, E_2, {}^3F_3, {}^1G_4$, and ${}^3F_4$

NN-contacts

The NN contacts $\tilde{C}^{pp}_{{}^1S_0}$ $\tilde{C}^{nn}_{{}^1S_0}$ $\tilde{C}^{np}_{{}^1S_0}$ $C_{{}^3P_0}$ $C_{{}^1P_1}$ $C_{{}^1S_0}$ $\tilde{C}_{{}^3S_1}$ $C_{{}^3S_1}$ $C_{{}^3S_1-{}^3D_1}$ $C_{{}^3P_2}$ were optimized in the respective partial wave.

Two remarks

- When computing the χ^2/datum, it turns out that this is lowered when the ${}^1P_1$-wave is weighted with experimental uncertainties
- The ${}^3S_1 - {}^3D_1$ coupled-channel is optimized with the additional constraint of reproducing the deuteron binding energy.

Everything else is a prediction

Optimization strategy, level 0 or version 0

πN

The πN contacts c_1, c_3, c_4 were optimized simultaneously using the peripheral ($L \geq 2$) waves ${}^1D_2, {}^3D_2, {}^3F_2, E_2, {}^3F_3, {}^1G_4$, and ${}^3F_4$

NN-contacts

The NN contacts $\tilde{C}^{pp}_{{}^1S_0}$ $\tilde{C}^{nn}_{{}^1S_0}$ $\tilde{C}^{np}_{{}^1S_0}$ $C_{{}^3P_0}$ $C_{{}^1P_1}$ $C_{{}^1S_0}$ $\tilde{C}_{{}^3S_1}$ $C_{{}^3S_1}$ $C_{{}^3S_1-{}^3D_1}$ $C_{{}^3P_2}$ were optimized in the respective partial wave.

Two remarks

- When computing the χ^2/datum, it turns out that this is lowered when the ${}^1P_1$-wave is weighted with experimental uncertainties
- The ${}^3S_1 - {}^3D_1$ coupled-channel is optimized with the additional constraint of reproducing the deuteron binding energy.

Everything else is a prediction

χ^2/datum, *np* scattering data (1999 database)

The previous picture...

T_{lab} bin (MeV)	N3LO	NNLO[1]	NLO[1]	AV18
0-100	1.06	1.71	5.20	0.95
100-190	1.08	12.9	49.3	1.10
190-290	1.15	19.2	68.3	1.11
0-290	**1.10**	**10.1**	**36.2**	**1.04**

[1] E. Epelbaum et al., Eur. Phys. J. A19, 401 (2004)

... changes with POUNDerS

T_{lab} bin (MeV)	POUNDerS-NNLO(500)
0-35	0.85
35-125	1.17
125-183	1.87
183-290	6.09
0-290	**2.95**

χ^2/datum, *np* scattering data (1999 database)

The previous picture...

T_{lab} bin (MeV)	N3LO	NNLO[1]	NLO[1]	AV18
0-100	1.06	1.71	5.20	0.95
100-190	1.08	12.9	49.3	1.10
190-290	1.15	19.2	68.3	1.11
0-290	**1.10**	**10.1**	**36.2**	**1.04**

[1] E. Epelbaum et al., Eur. Phys. J. A19, 401 (2004)

... changes with POUNDerS

T_{lab} bin (MeV)	POUNDerS-NNLO(500)
0-35	0.85
35-125	1.17
125-183	1.87
183-290	6.09
0-290	**2.95**

χ^2/datum, *pp* scattering data (1999 database)

The previous picture...

T_{lab} bin (MeV)	N3LO	NNLO[1]	NLO[1]	AV18
0-100	1.05	6.66	57.8	0.96
100-190	1.50	28.3	62.0	1.31
190-290	1.93	66.8	111.6	1.82
0-290	**1.50**	**35.4**	**80.1**	**1.38**

[1] E. Epelbaum et al., Eur. Phys. J. A19, 401 (2004)

... changes with POUNDerS

T_{lab} bin (MeV)	POUNDerS-NNLO(500)
0-35	1.11
35-125	1.56
125-183	23.95 (4.35[a])
183-290	29.26
0-290	**17.10 (14.03)**[2]

χ^2/datum, *pp* scattering data (1999 database)

The previous picture...

T_{lab} bin (MeV)	N3LO	NNLO[1]	NLO[1]	AV18
0-100	1.05	6.66	57.8	0.96
100-190	1.50	28.3	62.0	1.31
190-290	1.93	66.8	111.6	1.82
0-290	**1.50**	**35.4**	**80.1**	**1.38**

[1] E. Epelbaum et al., Eur. Phys. J. A19, 401 (2004)

... changes with POUNDerS

T_{lab} bin (MeV)	POUNDerS-NNLO(500)
0-35	1.11
35-125	1.56
125-183	23.95 (4.35^a)
183-290	29.26
0-290	**17.10 (14.03)**[2]

POUNDerS-NNLO: NN+3NF

$A = 3, 4$-systems

$$c_D = 0.50$$
$$c_E = -0.210$$

	^{3}H	^{3}He	^{4}He
NNLO	-8.249	-7.501	-27.759
NNLO+NNN	-8.470	-7.723	-28.290
Experiment	-8.482	-7.717	-28.296

Parameters re-fitted to $A = 3, 4$ binding energies only.

The data

V. G. J. Stoks *et al.* Phys. Rev. **C** 48, 792 (1993)

Phase shifts

They are not observables. Obtained from a partial wave analysis (PWA) of various scattering cross sections (Nijmegen). Thus, phase shifts parametrize the actual scattering data.

- Given phase shifts, it is trivial to compute observables
- The reverse procedure is *not* trivial, since the equations are transcendental.

TABLE IV. *pp* isovector phase shifts and their multienergy error in degrees as obtained in the multienergy *pp* analysis. Errors smaller than 0.0005° are not shown. The lower part lists the phase shifts as obtained in the combined $pp+np$ analysis.

T_{lab}	$^1S_0$	$^1D_2$	$^1G_4$	$^3P_0$	$^3P_1$	$^3F_3$	$^3P_2$	ε_2	$^3F_2$	$^3F_4$	ε_4	$^3H_4$
1	32.684	0.001	0.000	0.134	−0.081	−0.000	0.014	−0.001	0.000	0.000	−0.000	0.000
	±0.005											
5	54.832	0.043	0.000	1.582	−0.902	−0.005	0.214	−0.052	0.002	0.000	−0.000	0.000
	±0.017			±0.006	±0.001		±0.001					
10	55.219	0.165	0.003	3.729	−2.060	−0.032	0.651	−0.200	0.013	0.001	−0.004	0.000
	±0.025			±0.017	±0.002		±0.002					
25	48.672	0.696	0.040	8.575	−4.932	−0.231	2.491	−0.810	0.105	0.020	−0.049	0.004
	±0.039	±0.001		±0.053	±0.008		±0.008	±0.001				
50	38.899	1.711	0.152	11.47	−8.317	−0.690	5.855	−1.712	0.338	0.108	−0.195	0.026
	±0.049	±0.004		±0.09	±0.017		±0.016	±0.004		±0.001		
100	24.97	3.790	0.418	9.45	−13.258	−1.517	11.013	−2.659	0.817	0.478	−0.539	0.108
	±0.08	±0.018	±0.001	±0.11	±0.032	±0.003	±0.025	±0.017	±0.004	±0.007		
150	14.75	5.606	0.700	4.74	−17.434	−2.100	13.982	−2.873	1.197	1.032	−0.849	0.211
	±0.13	±0.033	±0.003	±0.14	±0.045	±0.010	±0.039	±0.029	±0.014	±0.022		
200	6.55	7.058	0.993	−0.37	−21.25	−2.487	15.63	−2.759	1.424	1.678	−1.108	0.321
	±0.16	±0.045	±0.010	±0.17	±0.07	±0.025	±0.052	±0.037	±0.034	±0.039		
250	−0.31	8.27	1.272	−5.43	−24.77	−2.724	16.59	−2.542	1.47	2.325	−1.314	0.428
	±0.18	±0.06	±0.024	±0.21	±0.12	±0.049	±0.07	±0.046	±0.06	±0.051		
300	−6.15	9.42	1.503	−10.39	−27.99	−2.84	17.17	−2.34	1.34	2.89	−1.47	0.526
	±0.25	±0.08	±0.048	±0.33	±0.19	±0.11	±0.10	±0.09	±0.11	±0.06		
350	−11.13	10.69	1.64	−15.30	−30.89	−2.87	17.54	−2.21	1.04	3.30	−1.588	0.608
	±0.46	±0.14	±0.08	±0.57	±0.27	±0.13	±0.15	±0.11	±0.16	±0.11	±0.001	
100	24.97	3.782	0.418	9.55	−13.245	−1.518	11.013	−2.654	0.816	0.471	−0.539	0.108
	±0.08	±0.017		±0.09	±0.030	±0.002	±0.021	±0.016	±0.003	±0.006		
200	6.55	7.039	0.993	−0.27	−21.18	−2.499	15.65	−2.731	1.414	1.656	−1.107	0.321
	±0.16	±0.043	±0.008	±0.17	±0.06	±0.021	±0.05	±0.035	±0.029	±0.034		
300	−6.22	9.42	1.501	−10.44	−27.80	−2.89	17.15	−2.27	1.30	2.95	−1.473	0.526

$^1S_0$ proton-proton phase shifts

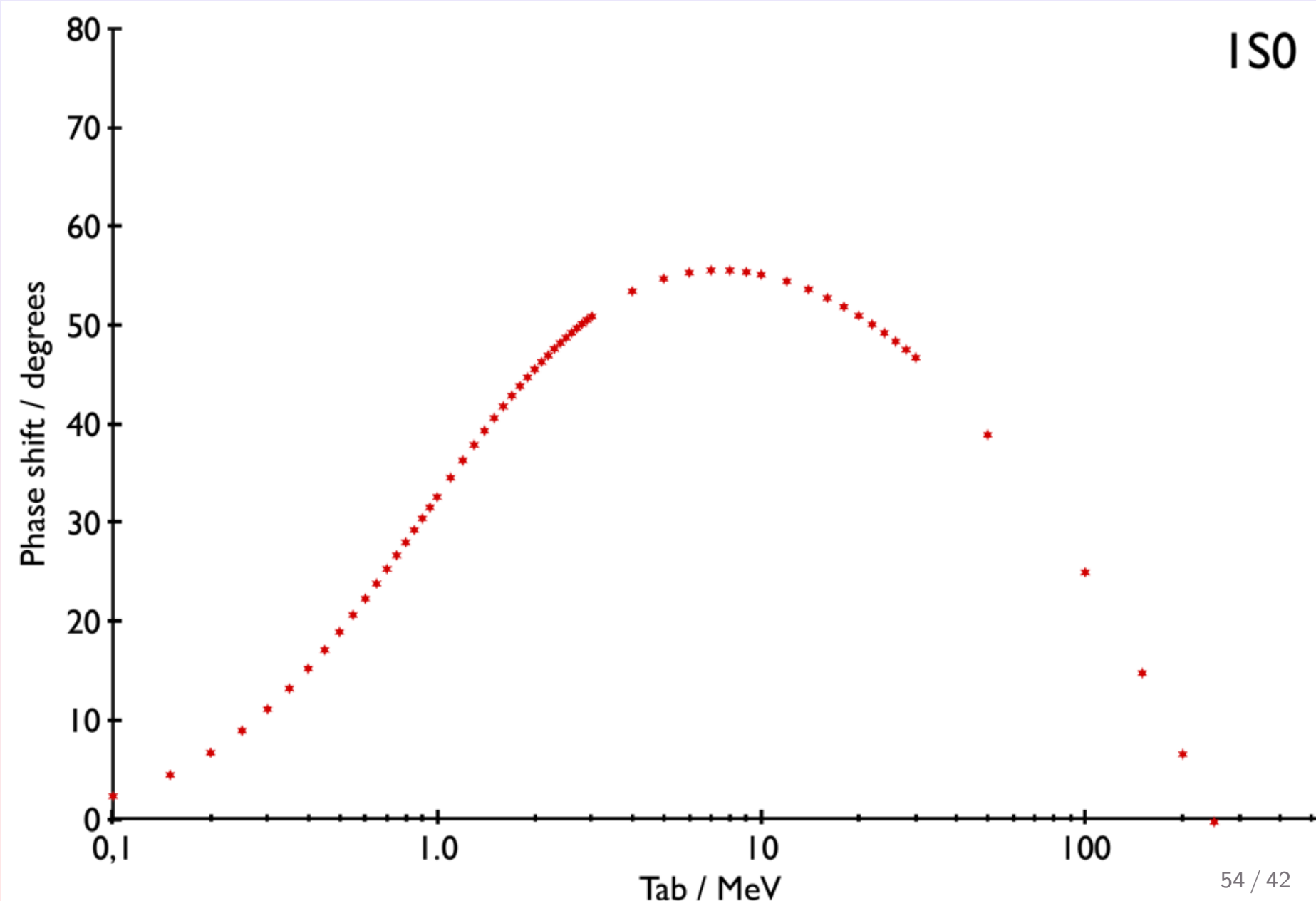

$^1S_0$ proton-proton Nuclear interaction

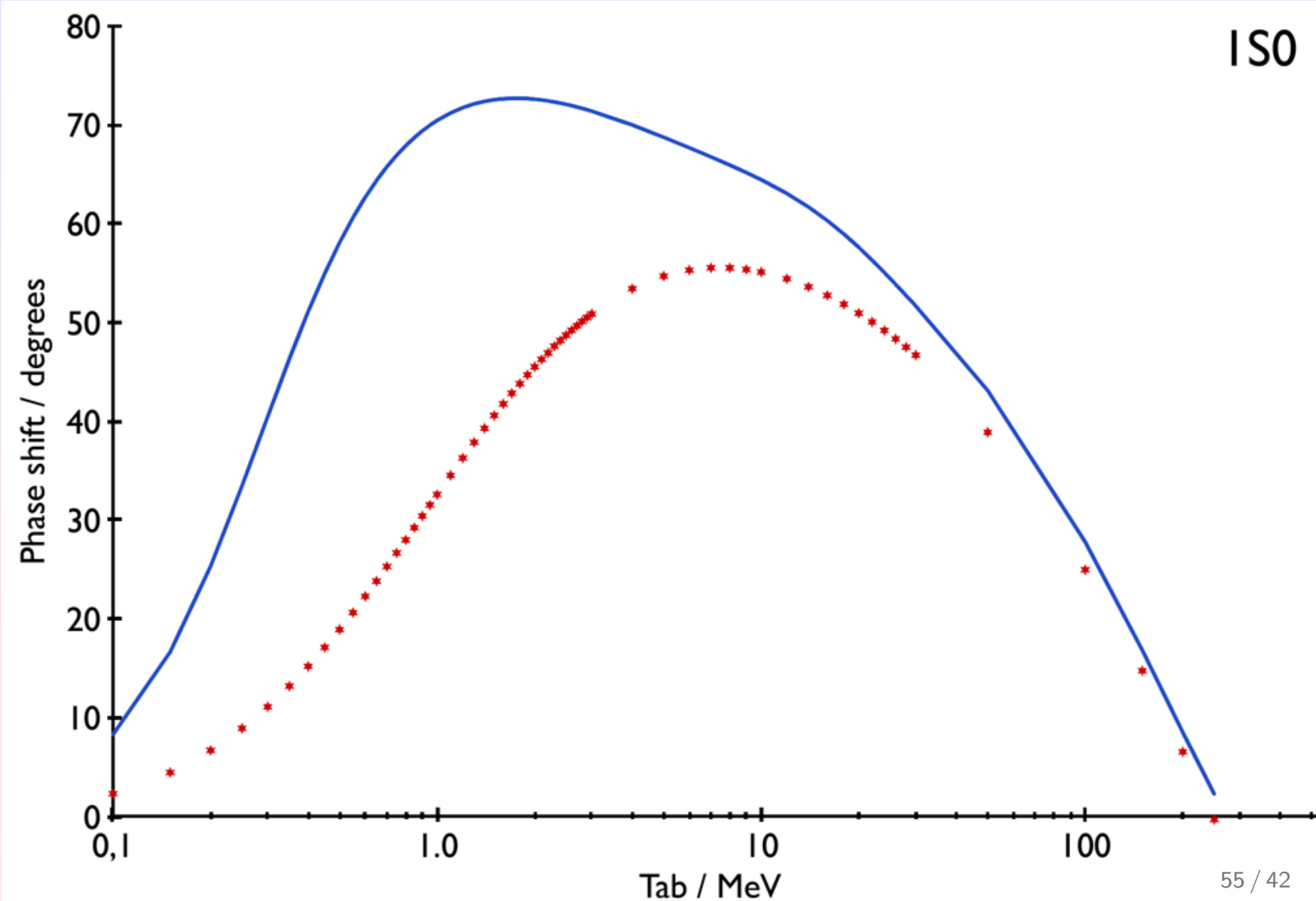

$^1S_0$ proton-proton Nuclear + Coulomb interaction

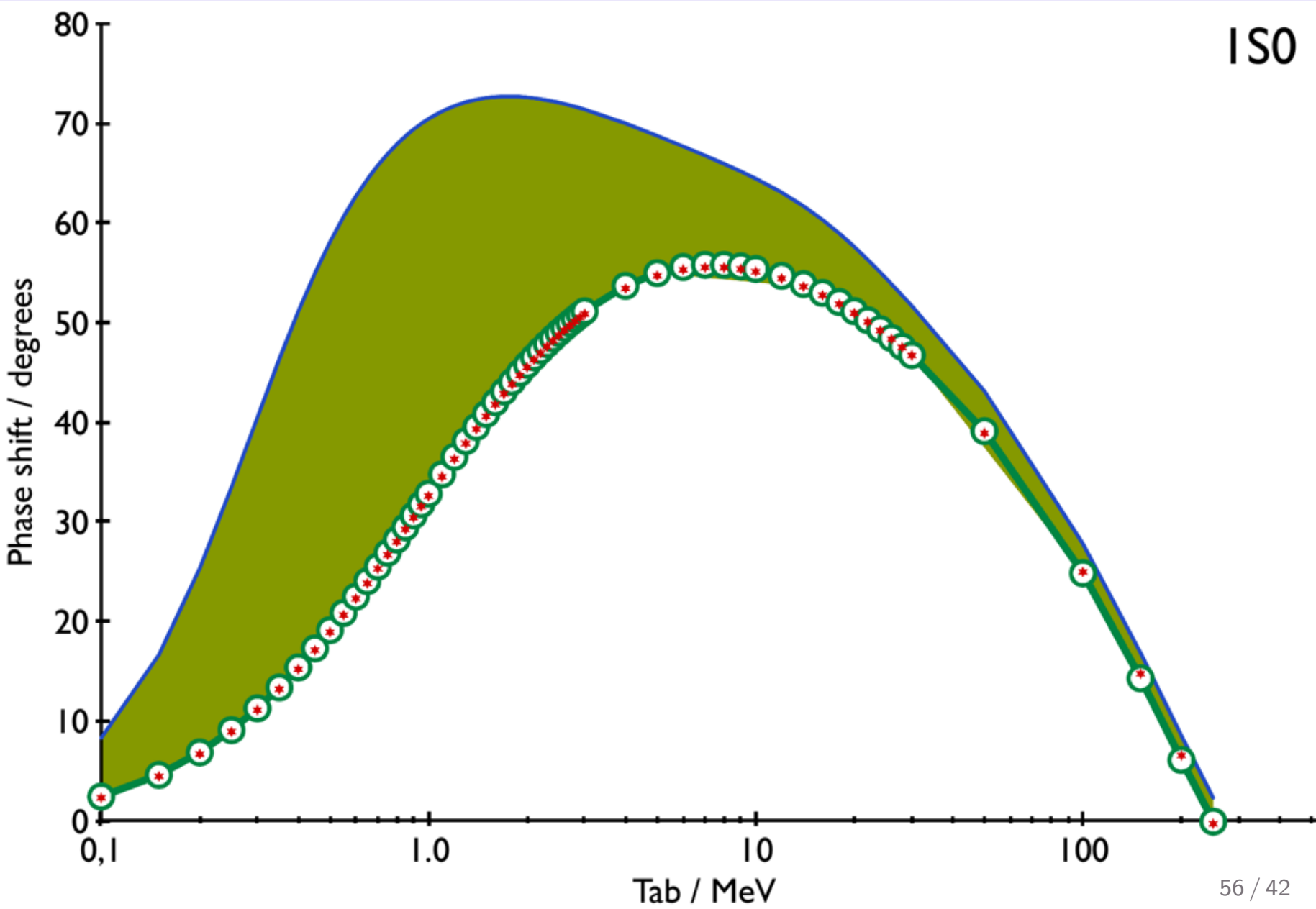

Defining the objective function

Practical Optimization Using No Derivatives (Square/Structure)

Objective function

$$f(\vec{x}) = \sum_{q=1}^{N_q} \left(\frac{\delta_q^{\mathrm{NNLO}}(\vec{x}) - \delta_q^{\mathrm{Nijm93}}}{w_q} \right)^2$$

Two choices for the w_q weight:

q^3-weighting [NN LECs]

For nuclear structure the low-energy phase shifts are more important.

uncertainty-weighting [πN LECs]

Simply use the uncertainties from the Nijmegen PWA

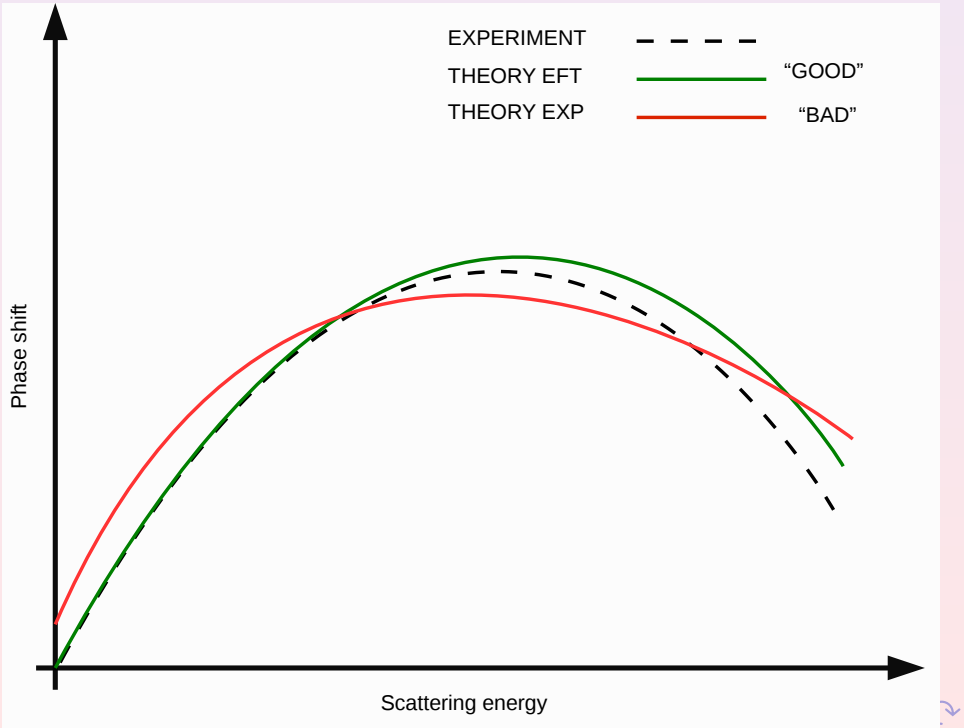

Optimization strategy

πN

The πN contacts c_1, c_3, c_4 were optimized simultaneously using the peripheral ($L \geq 2$) waves ${}^1D_2, {}^3D_2, {}^3F_2, E_2, {}^3F_3, {}^1G_4$, and ${}^3F_4$

NN-contacts

The NN contacts $\tilde{C}^{pp}_{{}^1S_0}$ $\tilde{C}^{nn}_{{}^1S_0}$ $\tilde{C}^{np}_{{}^1S_0}$ $C_{{}^3P_0}$ $C_{{}^1P_1}$ $C_{{}^1S_0}$ $\tilde{C}_{{}^3S_1}$ $C_{{}^3S_1}$ $C_{{}^3S_1-{}^3D_1}$ $C_{{}^3P_2}$ were optimized in the respective partial wave.

Two remarks

- When computing the χ^2/datum, it turns out that this is lowered when the ${}^1P_1$-wave is weighted with experimental uncertainties
- The ${}^3S_1 - {}^3D_1$ coupled-channel is optimized with the additional constraint of reproducing the deuteron binding energy.

Everything else is a prediction

Optimization strategy

πN

The πN contacts c_1, c_3, c_4 were optimized simultaneously using the peripheral ($L \geq 2$) waves ${}^1D_2, {}^3D_2, {}^3F_2, E_2, {}^3F_3, {}^1G_4$, and ${}^3F_4$

NN-contacts

The NN contacts $\tilde{C}^{pp}_{{}^1S_0}$ $\tilde{C}^{nn}_{{}^1S_0}$ $\tilde{C}^{np}_{{}^1S_0}$ $C_{{}^3P_0}$ $C_{{}^1P_1}$ $C_{{}^1S_0}$ $\tilde{C}_{{}^3S_1}$ $C_{{}^3S_1}$ $C_{{}^3S_1-{}^3D_1}$ $C_{{}^3P_2}$ were optimized in the respective partial wave.

Two remarks

- When computing the χ^2/datum, it turns out that this is lowered when the ${}^1P_1$-wave is weighted with experimental uncertainties
- The ${}^3S_1 - {}^3D_1$ coupled-channel is optimized with the additional constraint of reproducing the deuteron binding energy.

Everything else is a prediction

Optimization strategy

πN

The πN contacts c_1, c_3, c_4 were optimized simultaneously using the peripheral ($L \geq 2$) waves ${}^1D_2, {}^3D_2, {}^3F_2, E_2, {}^3F_3, {}^1G_4$, and ${}^3F_4$

NN-contacts

The NN contacts $\tilde{C}^{pp}_{{}^1S_0}$ $\tilde{C}^{nn}_{{}^1S_0}$ $\tilde{C}^{np}_{{}^1S_0}$ $C_{{}^3P_0}$ $C_{{}^1P_1}$ $C_{{}^1S_0}$ $\tilde{C}_{{}^3S_1}$ $C_{{}^3S_1}$ $C_{{}^3S_1-{}^3D_1}$ $C_{{}^3P_2}$ were optimized in the respective partial wave.

Two remarks

- When computing the χ^2/datum, it turns out that this is lowered when the ${}^1P_1$-wave is weighted with experimental uncertainties
- The ${}^3S_1 - {}^3D_1$ coupled-channel is optimized with the additional constraint of reproducing the deuteron binding energy.

Everything else is a prediction

Optimization strategy

πN

The πN contacts c_1, c_3, c_4 were optimized simultaneously using the peripheral ($L \geq 2$) waves ${}^1D_2, {}^3D_2, {}^3F_2, E_2, {}^3F_3, {}^1G_4$, and ${}^3F_4$

NN-contacts

The NN contacts $\tilde{C}^{pp}_{{}^1S_0}$ $\tilde{C}^{nn}_{{}^1S_0}$ $\tilde{C}^{np}_{{}^1S_0}$ $C_{{}^3P_0}$ $C_{{}^1P_1}$ $C_{{}^1S_0}$ $\tilde{C}_{{}^3S_1}$ $C_{{}^3S_1}$ $C_{{}^3S_1-{}^3D_1}$ $C_{{}^3P_2}$ were optimized in the respective partial wave.

Two remarks

- When computing the χ^2/datum, it turns out that this is lowered when the ${}^1P_1$-wave is weighted with experimental uncertainties
- The ${}^3S_1 - {}^3D_1$ coupled-channel is optimized with the additional constraint of reproducing the deuteron binding energy.

Everything else is a prediction

χ^2/datum, *np* scattering data (1999 database)

The previous picture...

T_{lab} bin (MeV)	N3LO	NNLO[1]	NLO[1]	AV18
0-100	1.06	1.71	5.20	0.95
100-190	1.08	12.9	49.3	1.10
190-290	1.15	19.2	68.3	1.11
0-290	**1.10**	**10.1**	**36.2**	**1.04**

[1] E. Epelbaum et al., Eur. Phys. J. A19, 401 (2004)

... changes with POUNDerS

T_{lab} bin (MeV)	POUNDerS-NNLO(500)
0-35	0.85
35-125	1.17
125-183	1.87
183-290	6.09
0-290	**2.95**

χ^2/datum, *np* scattering data (1999 database)

The previous picture...

T_{lab} bin (MeV)	N3LO	NNLO[1]	NLO[1]	AV18
0-100	1.06	1.71	5.20	0.95
100-190	1.08	12.9	49.3	1.10
190-290	1.15	19.2	68.3	1.11
0-290	**1.10**	**10.1**	**36.2**	**1.04**

[1] E. Epelbaum et al., Eur. Phys. J. A19, 401 (2004)

... changes with POUNDerS

T_{lab} bin (MeV)	POUNDerS-NNLO(500)
0-35	0.85
35-125	1.17
125-183	1.87
183-290	6.09
0-290	**2.95**

χ^2/datum, *pp* scattering data (1999 database)

The previous picture...

T_{lab} bin (MeV)	N3LO	NNLO[1]	NLO[1]	AV18
0-100	1.05	6.66	57.8	0.96
100-190	1.50	28.3	62.0	1.31
190-290	1.93	66.8	111.6	1.82
0-290	**1.50**	**35.4**	**80.1**	**1.38**

[1] E. Epelbaum et al., Eur. Phys. J. A19, 401 (2004)

... changes with POUNDerS

T_{lab} bin (MeV)	POUNDerS-NNLO(500)
0-35	1.11
35-125	1.56
125-183	23.95 (4.35[a])
183-290	29.26
0-290	**17.10 (14.03)**[2]

χ^2/datum, *pp* scattering data (1999 database)

The previous picture...

T_{lab} bin (MeV)	N3LO	NNLO[1]	NLO[1]	AV18
0-100	1.05	6.66	57.8	0.96
100-190	1.50	28.3	62.0	1.31
190-290	1.93	66.8	111.6	1.82
0-290	**1.50**	**35.4**	**80.1**	**1.38**

[1] E. Epelbaum et al., Eur. Phys. J. A19, 401 (2004)

... changes with POUNDerS

T_{lab} bin (MeV)	POUNDerS-NNLO(500)
0-35	1.11
35-125	1.56
125-183	23.95 (4.35^a)
183-290	29.26
0-290	**17.10 (14.03)**[2]

POUNDerS-NNLO optimized parameter values

'empirical' values

πN LEC	πN-scattering[1]	NN-PWA[2]	NNLO[3]	N3LO
c_1 [GeV^{-1}]	-0.81±0.15	-0.76±0.07	-0.81	-0.81
c_3 [GeV^{-1}]	-4.69±1.34	-4.78±0.10	-3.40	-3.20
c_4 [GeV^{-1}]	+3.40±0.04	+3.96 ±0.22	+3.40	+5.40

[1] πN Fit 1, in P. Büttiker, U-G. Meißner Nucl. Phys. A **668**, 97 (2000)
[2] *NN* PWA, in M. C. M. Rentmeester *et al.* Phys. Rev C **67** 044001 (2003)

[3] E. Epelbaum et al., Eur. Phys. J. A19, 401 (2004)

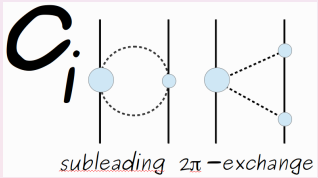

POUNDerS

πN LEC	POUNDerS
c_1 [GeV^{-1}]	-0.9186
c_3 [GeV^{-1}]	-3.8887
c_4 [GeV^{-1}]	+4.3103

POUNDerS-NNLO optimized parameter values

'empirical' values

πN LEC	πN-scattering[1]	NN-PWA[2]	NNLO[3]	N3LO
c_1 [GeV^{-1}]	-0.81±0.15	-0.76±0.07	-0.81	-0.81
c_3 [GeV^{-1}]	-4.69±1.34	-4.78±0.10	-3.40	-3.20
c_4 [GeV^{-1}]	+3.40±0.04	+3.96 ±0.22	+3.40	+5.40

[1] πN Fit 1, in P. Büttiker, U-G. Meißner Nucl. Phys. A **668**, 97 (2000)
[2] *NN* PWA, in M. C. M. Rentmeester *et al.* Phys. Rev C **67** 044001 (2003)

[3] E. Epelbaum et al., Eur. Phys. J. A19, 401 (2004)

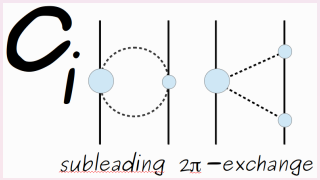

POUNDerS

πN LEC	POUNDerS
c_1 [GeV^{-1}]	-0.9186
c_3 [GeV^{-1}]	-3.8887
c_4 [GeV^{-1}]	+4.3103

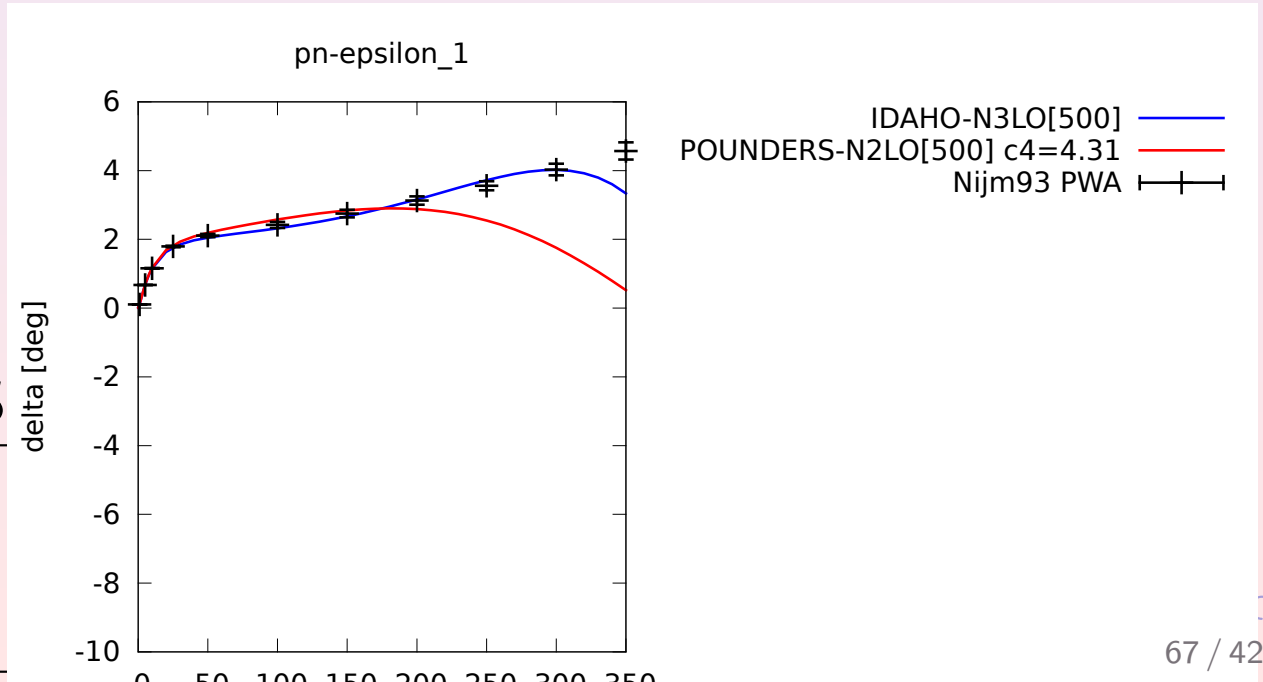

POUNDerS-NNLO optimized parameter values

'empirical' values

πN LEC	πN-scattering[1]	NN-PWA[2]	NNLO[3]	N3LO
c_1 [GeV^{-1}]	-0.81±0.15	-0.76±0.07	-0.81	-0.81
c_3 [GeV^{-1}]	-4.69±1.34	-4.78±0.10	-3.40	-3.20
c_4 [GeV^{-1}]	+3.40±0.04	+3.96 ±0.22	+3.40	+5.40

[1] πN Fit 1, in P. Büttiker, U-G. Meißner Nucl. Phys. A **668**, 97 (2000)
[2] *NN* PWA, in M. C. M. Rentmeester *et al.* Phys. Rev C **67** 044001 (2003)

[3] E. Epelbaum et al., Eur. Phys. J. A19, 401 (2004)

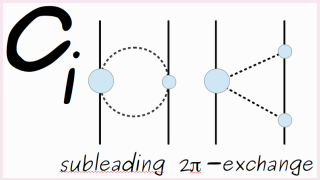

POUNDerS

πN LEC	POUNDerS
c_1 [GeV^{-1}]	-0.9186
c_3 [GeV^{-1}]	-3.8887
c_4 [GeV^{-1}]	+4.3103

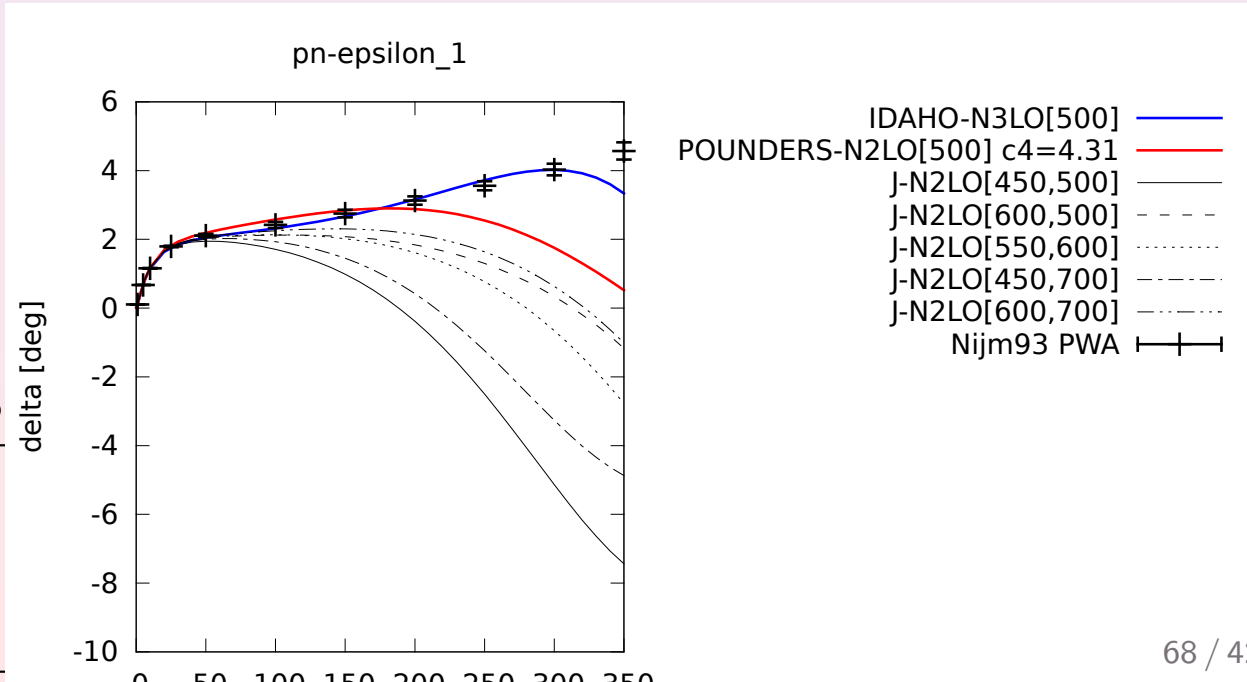

POUNDerS-NNLO optimized parameter values

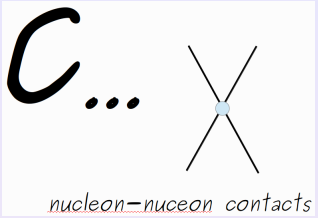

NN LEC	POUNDerS
$\tilde{C}_{^1S_0}^{pp}$ [10^4 GeV^{-2}]	-0.151366037
$\tilde{C}_{^1S_0}^{nn}$ [10^4 GeV^{-2}]	-0.152141088
$\tilde{C}_{^1S_0}^{np}$ [10^4 GeV^{-2}]	-0.151764746
$C_{^1S_0}$ [10^4 GeV^{-4}]	2.404021944
$C_{^3P_0}$ [10^4 GeV^{-4}]	1.263390763
$C_{^1P_1}$ [10^4 GeV^{-4}]	0.417045542
$C_{^3P_1}$ [10^4 GeV^{-4}]	-0.782658500
$\tilde{C}_{^3S_1}$ [10^4 GeV^{-2}]	-0.158434177
$C_{^3S_1}$ [10^4 GeV^{-4}]	0.928384663
$C_{^3S_1-^3D_1}$ [10^4 GeV^{-4}]	0.61814141
$C_{^3P_2}$ [10^4 GeV^{-4}]	-0.677808511

POUNDerS-NNLO optimized parameter values

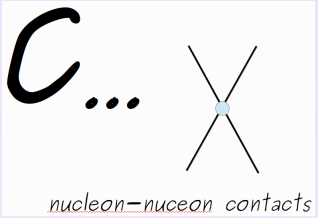

NN LEC	POUNDerS	JUELICH[450,700][3]
$\tilde{C}^{pp}_{^1S_0}$ [10^4 GeV^{-2}]	-0.151366037	-0.1525954
$\tilde{C}^{nn}_{^1S_0}$ [10^4 GeV^{-2}]	-0.152141088	-0.1529976
$\tilde{C}^{np}_{^1S_0}$ [10^4 GeV^{-2}]	-0.151764746	-0.1533360
$C_{^1S_0}$ [10^4 GeV^{-4}]	2.404021944	2.4121537
$C_{^3P_0}$ [10^4 GeV^{-4}]	1.263390763	1.2507864
$C_{^1P_1}$ [10^4 GeV^{-4}]	0.417045542	0.2812238
$C_{^3P_1}$ [10^4 GeV^{-4}]	-0.782658500	-0.7668429
$\tilde{C}_{^3S_1}$ [10^4 GeV^{-2}]	-0.158434177	-0.1733403
$C_{^3S_1}$ [10^4 GeV^{-4}]	0.928384663	0.5568150
$C_{^3S_1-^3D_1}$ [10^4 GeV^{-4}]	0.61814141	-0.4997024
$C_{^3P_2}$ [10^4 GeV^{-4}]	-0.677808511	-0.6259670

POUNDerS-NNLO Phase shifts

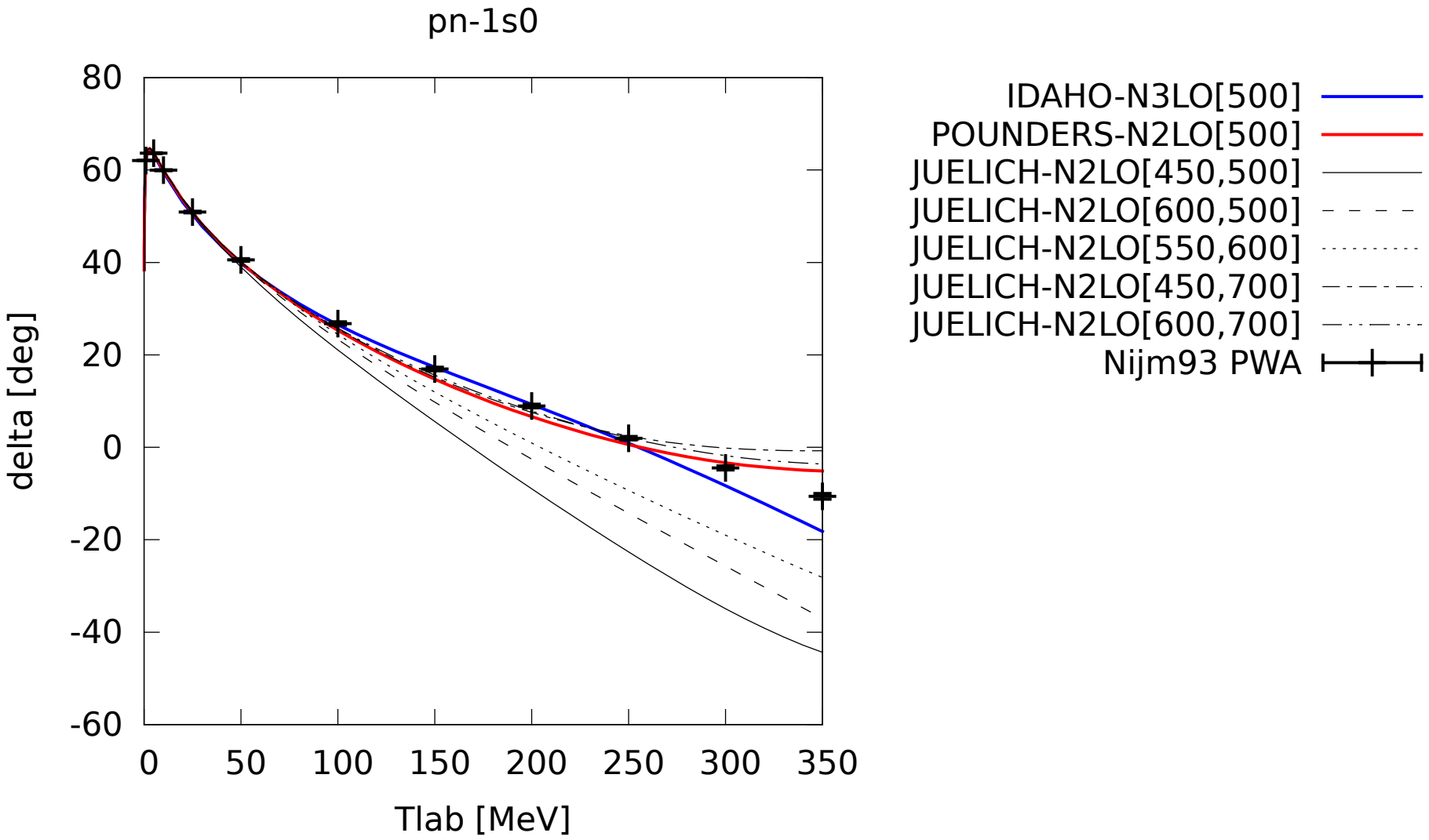

POUNDerS-NNLO Phase shifts

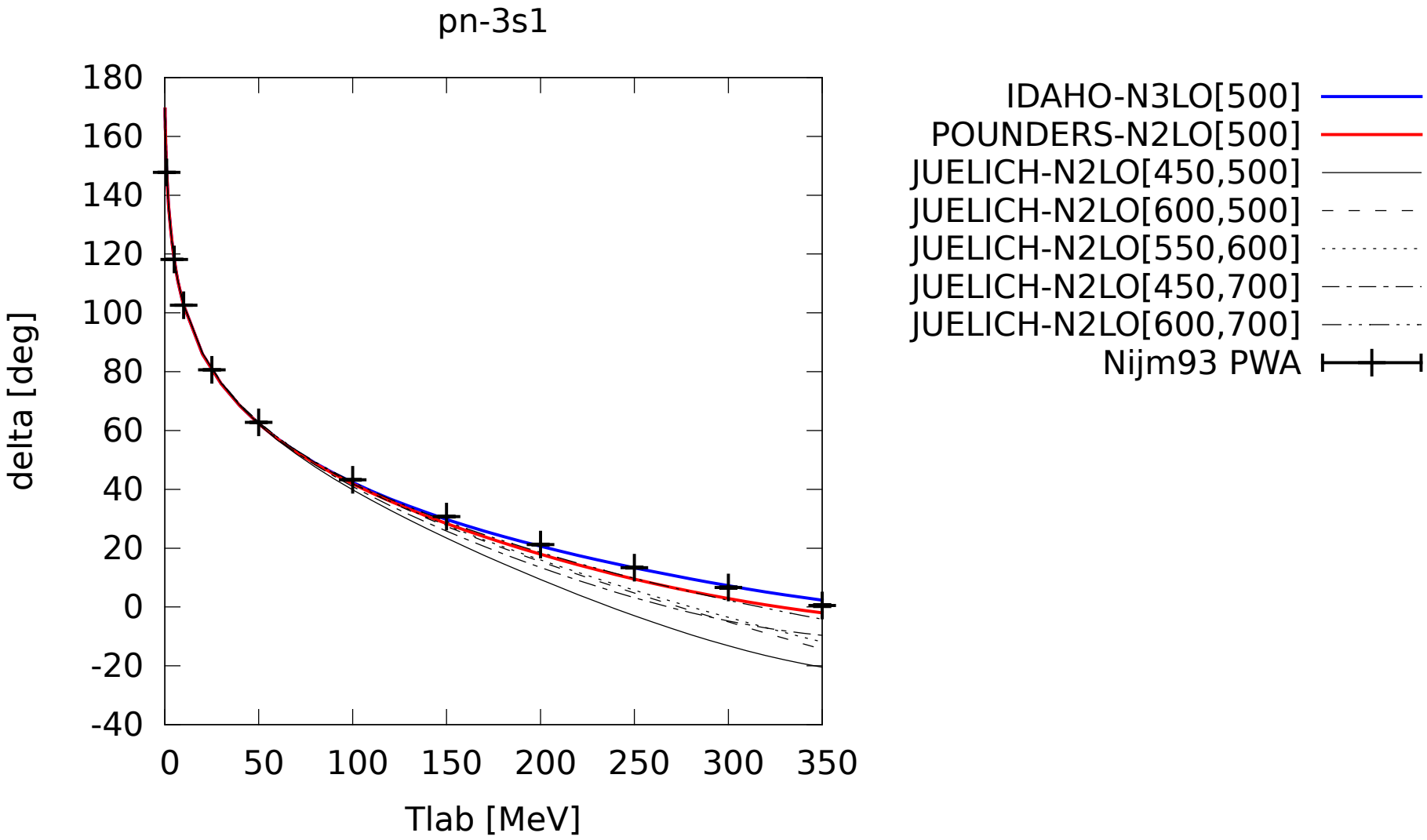

POUNDerS-NNLO Phase shifts

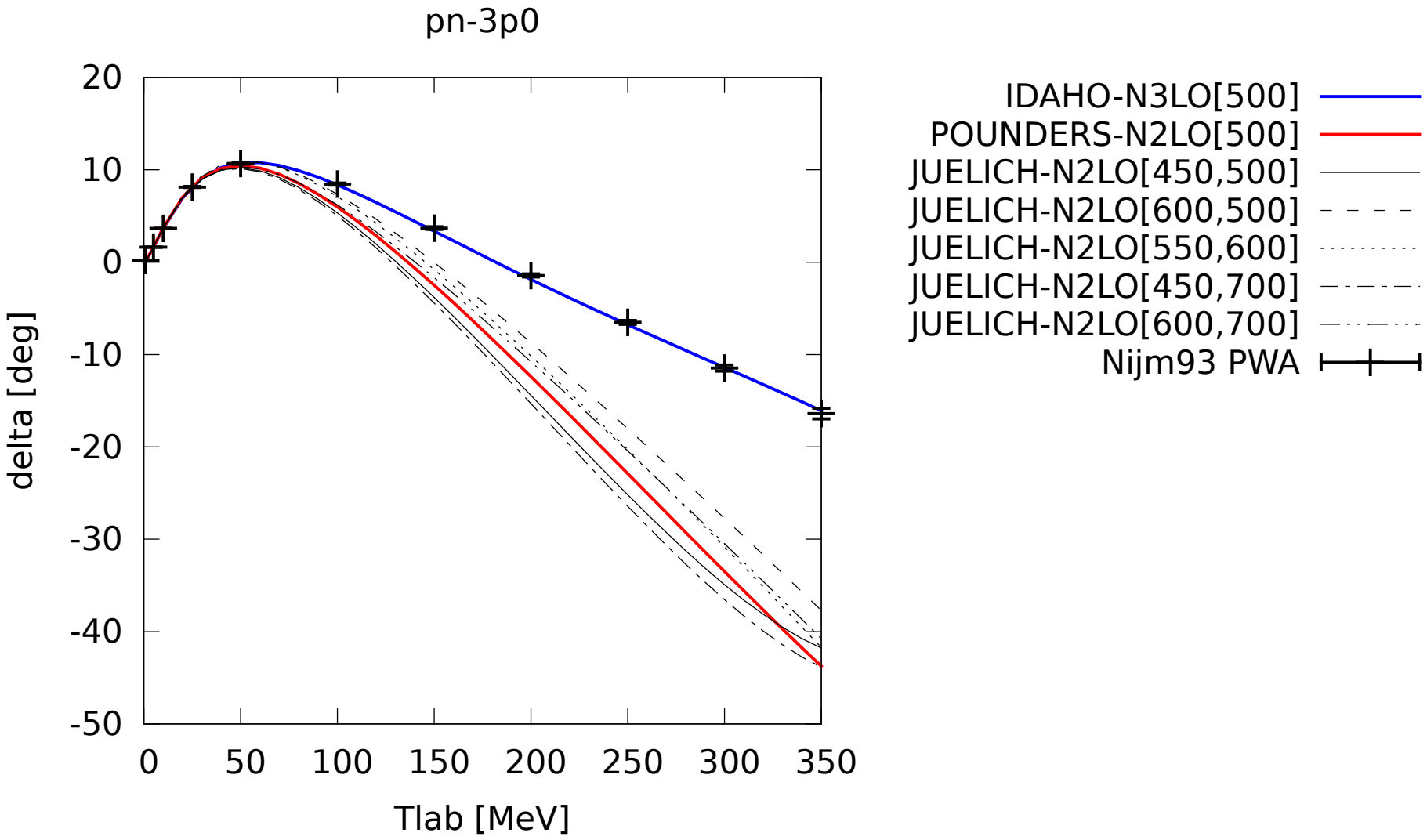

Constructing NN observables

Setup a spin-scattering scattering matrix **M**, related to the usual scattering matrix

$$M(\vec{p}_i, \vec{p}_f) = \frac{2\pi}{ik} \langle \theta_f \varphi_f | S - 1 | \theta_i \varphi_i \rangle$$

$$\mathbf{M} = \begin{vmatrix} M_{11} & M_{10} & M_{1-1} & 0 \\ M_{01} & M_{00} & M_{0-1} & 0 \\ M_{-11} & M_{-10} & M_{M_{-1-1}} & 0 \\ 0 & 0 & 0 & M_{ss} \end{vmatrix}$$

$$M_{ss}^{np} = \frac{1}{2ik} \sum_L (2L+1)(\exp(2i\delta_L) - 1) P_L \quad , M_{11}^{np} = \ldots \quad M_{10} = \ldots$$

e.g. differential cross section:

$$I_0 = \tfrac{1}{2}|M_{11}|^2 + \tfrac{1}{4}|M_{00}|^2 + \tfrac{1}{4}|M_{ss}|^2 + \tfrac{1}{2}|M_{10}|^2 + \tfrac{1}{2}|M_{01}|^2 + \tfrac{1}{2}|M_{1-1}|^2$$

Constructing NN observables

Setup a spin-scattering scattering matrix **M**, related to the usual scattering matrix

$$M(\vec{p}_i, \vec{p}_f) = \frac{2\pi}{ik}\langle\theta_f\varphi_f|S-1|\theta_i\varphi_i\rangle$$

$$\mathbf{M} = \begin{vmatrix} M_{11} & M_{10} & M_{1-1} & 0 \\ M_{01} & M_{00} & M_{0-1} & 0 \\ M_{-11} & M_{-10} & M_{M_{-1-1}} & 0 \\ 0 & 0 & 0 & M_{ss} \end{vmatrix}$$

$$M_{ss}^{np} = \frac{1}{2ik}\sum_L (2L+1)(\exp(2i\delta_L)-1)P_L \quad , M_{11}^{np} = \ldots \quad M_{10} = \ldots$$

e.g. differential cross section:

$$I_0 = \tfrac{1}{2}|M_{11}|^2 + \tfrac{1}{4}|M_{00}|^2 + \tfrac{1}{4}|M_{ss}|^2 + \tfrac{1}{2}|M_{10}|^2 + \tfrac{1}{2}|M_{01}|^2 + \tfrac{1}{2}|M_{1-1}|^2$$

Constructing NN observables

Setup a spin-scattering scattering matrix **M**, related to the usual scattering matrix

$$M(\vec{p}_i, \vec{p}_f) = \frac{2\pi}{ik}\langle\theta_f\varphi_f|S-1|\theta_i\varphi_i\rangle$$

$$\mathbf{M} = \begin{vmatrix} M_{11} & M_{10} & M_{1-1} & 0 \\ M_{01} & M_{00} & M_{0-1} & 0 \\ M_{-11} & M_{-10} & M_{M_{-1-1}} & 0 \\ 0 & 0 & 0 & M_{ss} \end{vmatrix}$$

$$M_{ss}^{np} = \frac{1}{2ik}\sum_L (2L+1)(\exp(2i\delta_L)-1)P_L \quad , M_{11}^{np} = \ldots \quad M_{10} = \ldots$$

e.g. differential cross section:

$$I_0 = \tfrac{1}{2}|M_{11}|^2 + \tfrac{1}{4}|M_{00}|^2 + \tfrac{1}{4}|M_{ss}|^2 + \tfrac{1}{2}|M_{10}|^2 + \tfrac{1}{2}|M_{01}|^2 + \tfrac{1}{2}|M_{1-1}|^2$$

Constructing NN observables

Setup a spin-scattering scattering matrix **M**, related to the usual scattering matrix

$$M(\vec{p}_i, \vec{p}_f) = \frac{2\pi}{ik}\langle\theta_f\varphi_f|S-1|\theta_i\varphi_i\rangle$$

$$\mathbf{M} = \begin{vmatrix} M_{11} & M_{10} & M_{1-1} & 0 \\ M_{01} & M_{00} & M_{0-1} & 0 \\ M_{-11} & M_{-10} & M_{M_{-1-1}} & 0 \\ 0 & 0 & 0 & M_{ss} \end{vmatrix}$$

$$M_{ss}^{np} = \frac{1}{2ik}\sum_L (2L+1)(\exp(2i\delta_L)-1)P_L \quad , M_{11}^{np} = \ldots \quad M_{10} = \ldots$$

e.g. differential cross section:

$$I_0 = \tfrac{1}{2}|M_{11}|^2 + \tfrac{1}{4}|M_{00}|^2 + \tfrac{1}{4}|M_{ss}|^2 + \tfrac{1}{2}|M_{10}|^2 + \tfrac{1}{2}|M_{01}|^2 + \tfrac{1}{2}|M_{1-1}|^2$$

NN Observables

Differential cross section

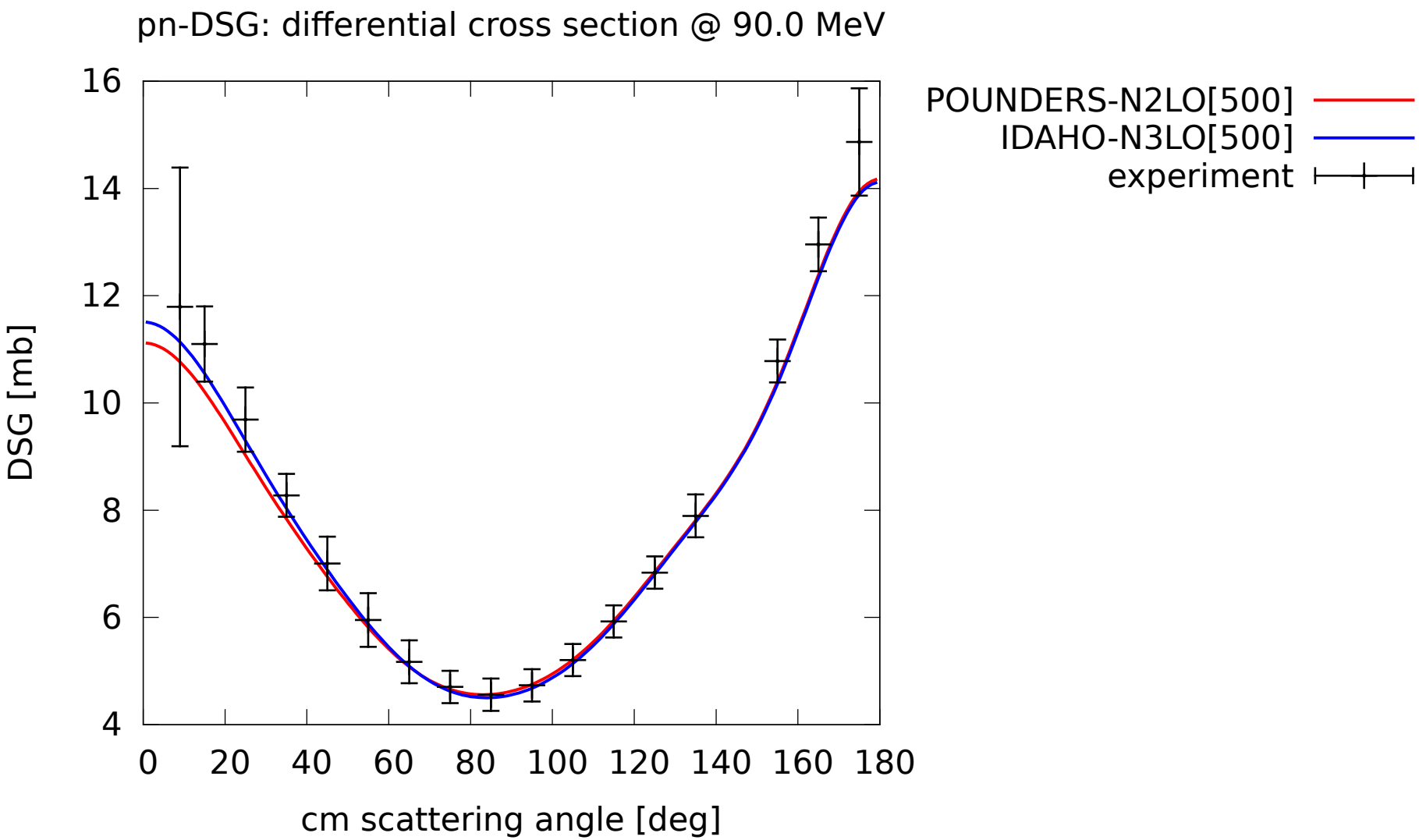

NN Observables

Differential cross section

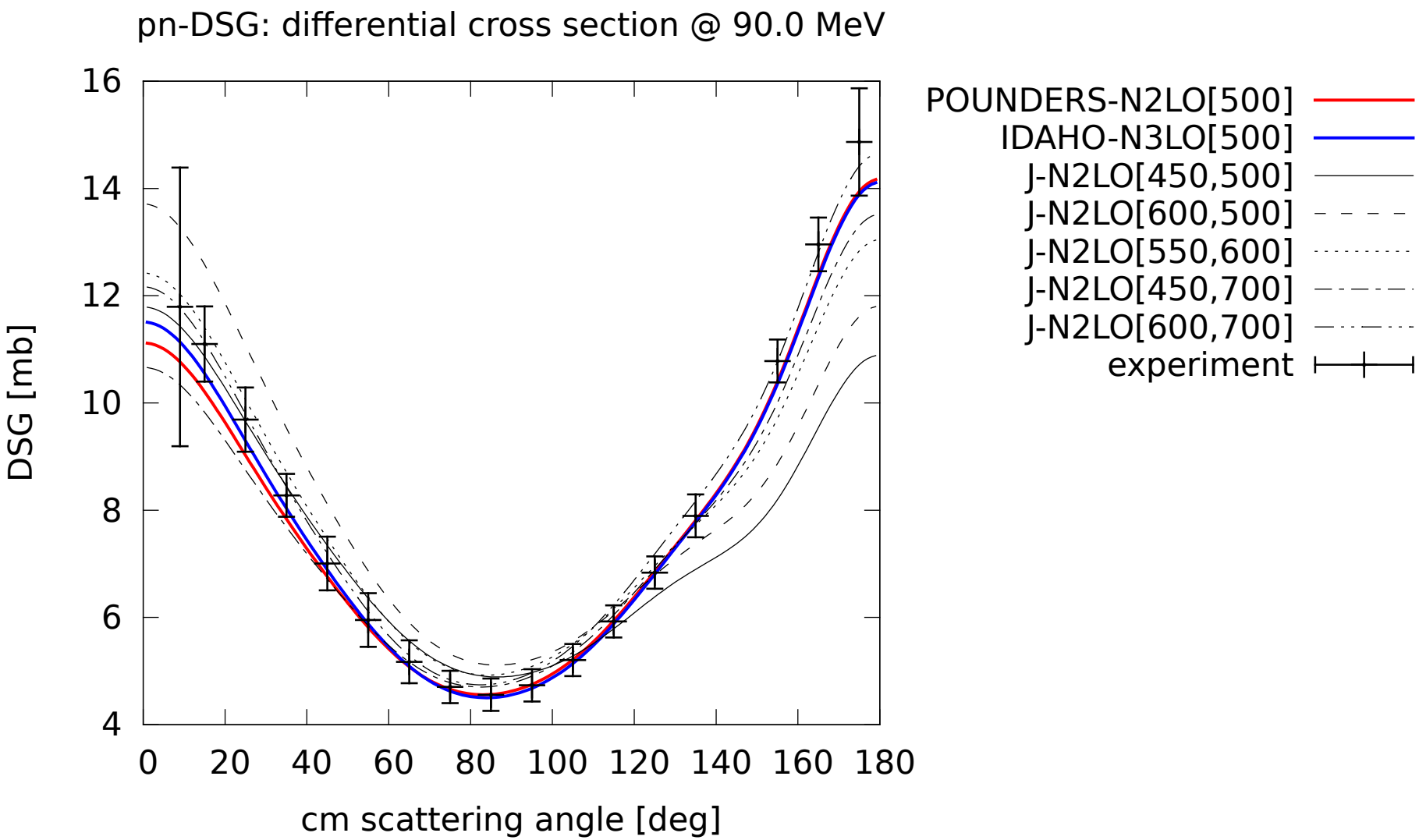

NN Observables

Differential cross section - c_4 variation

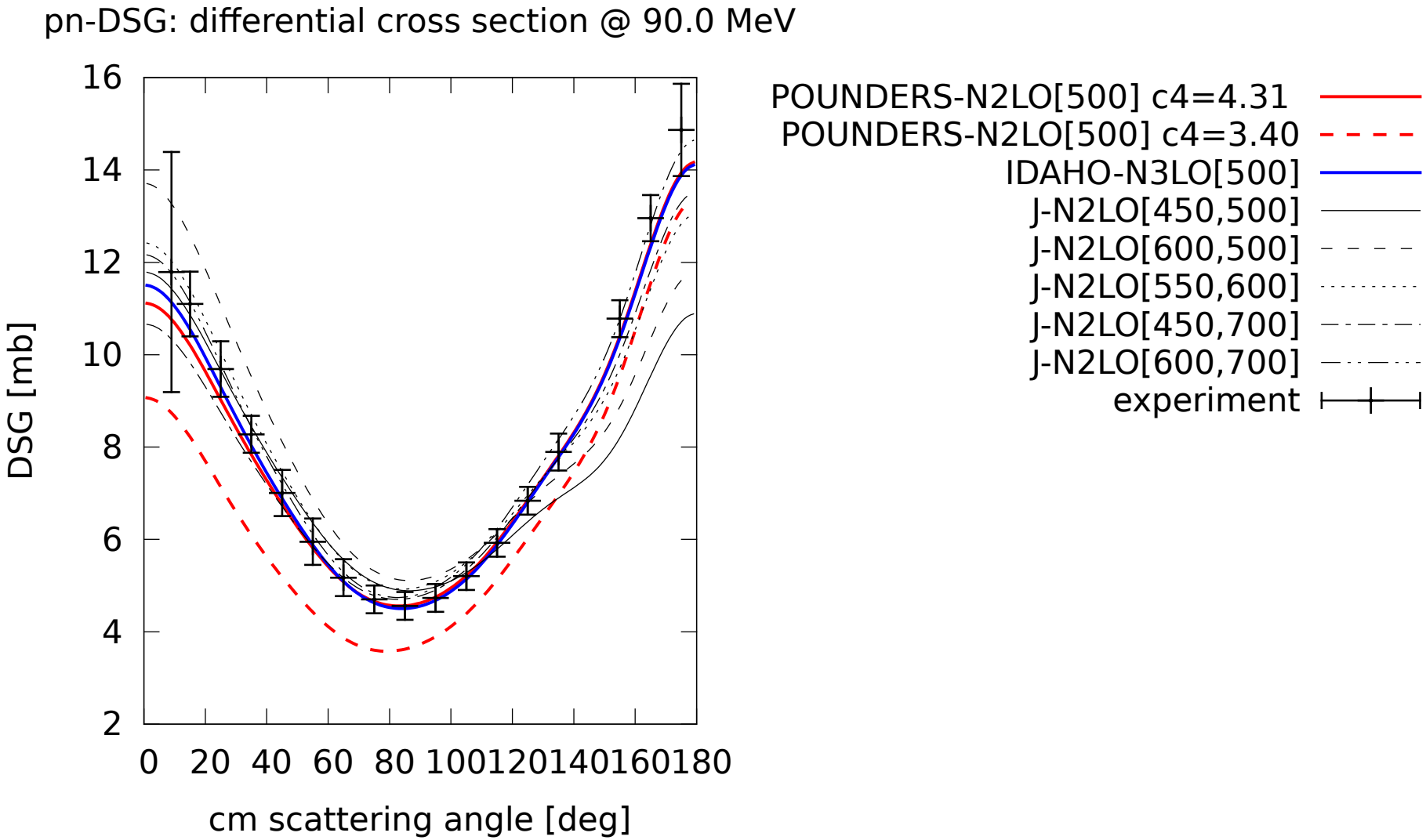

NN Observables

Differential cross section

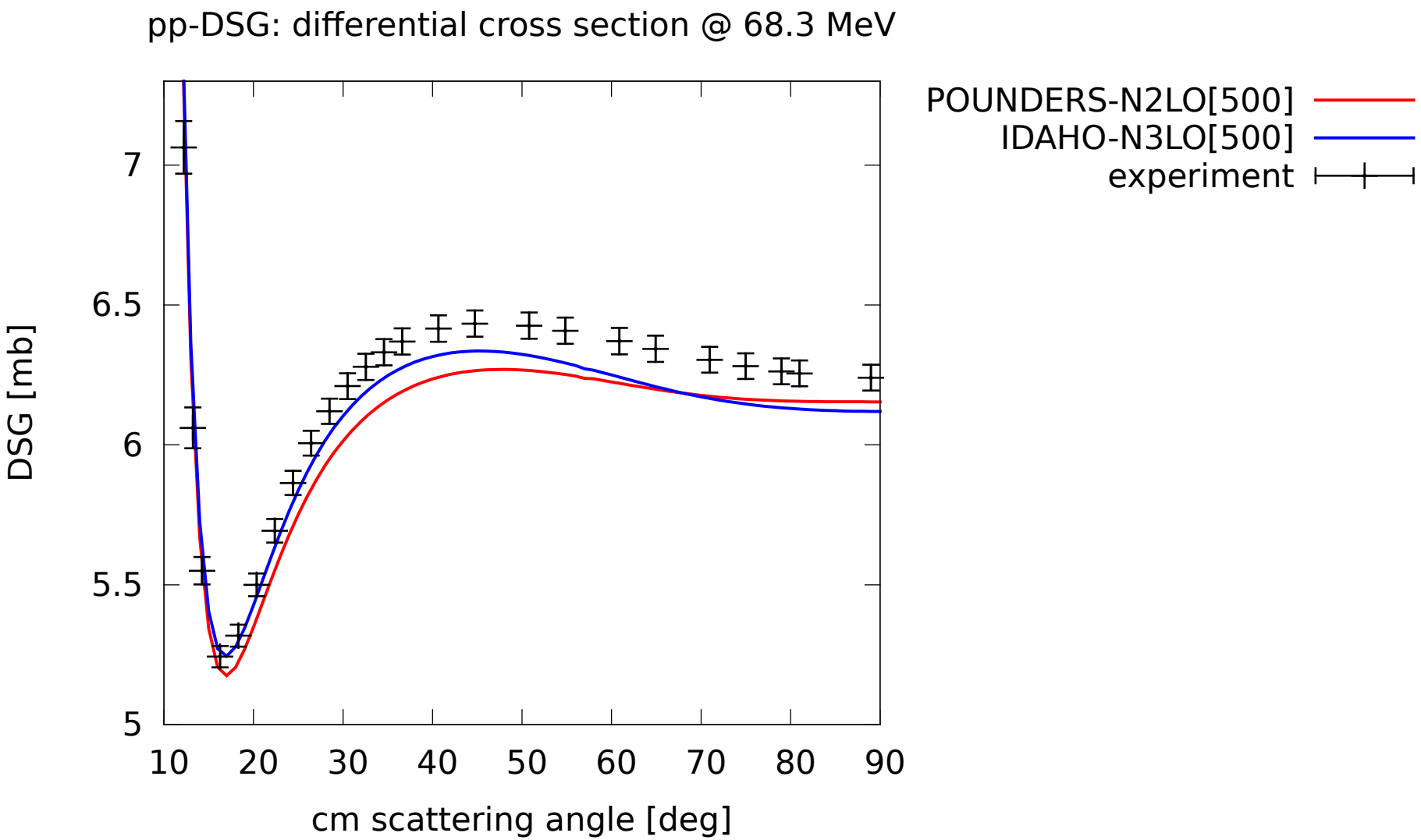

NN Observables

Differential cross section

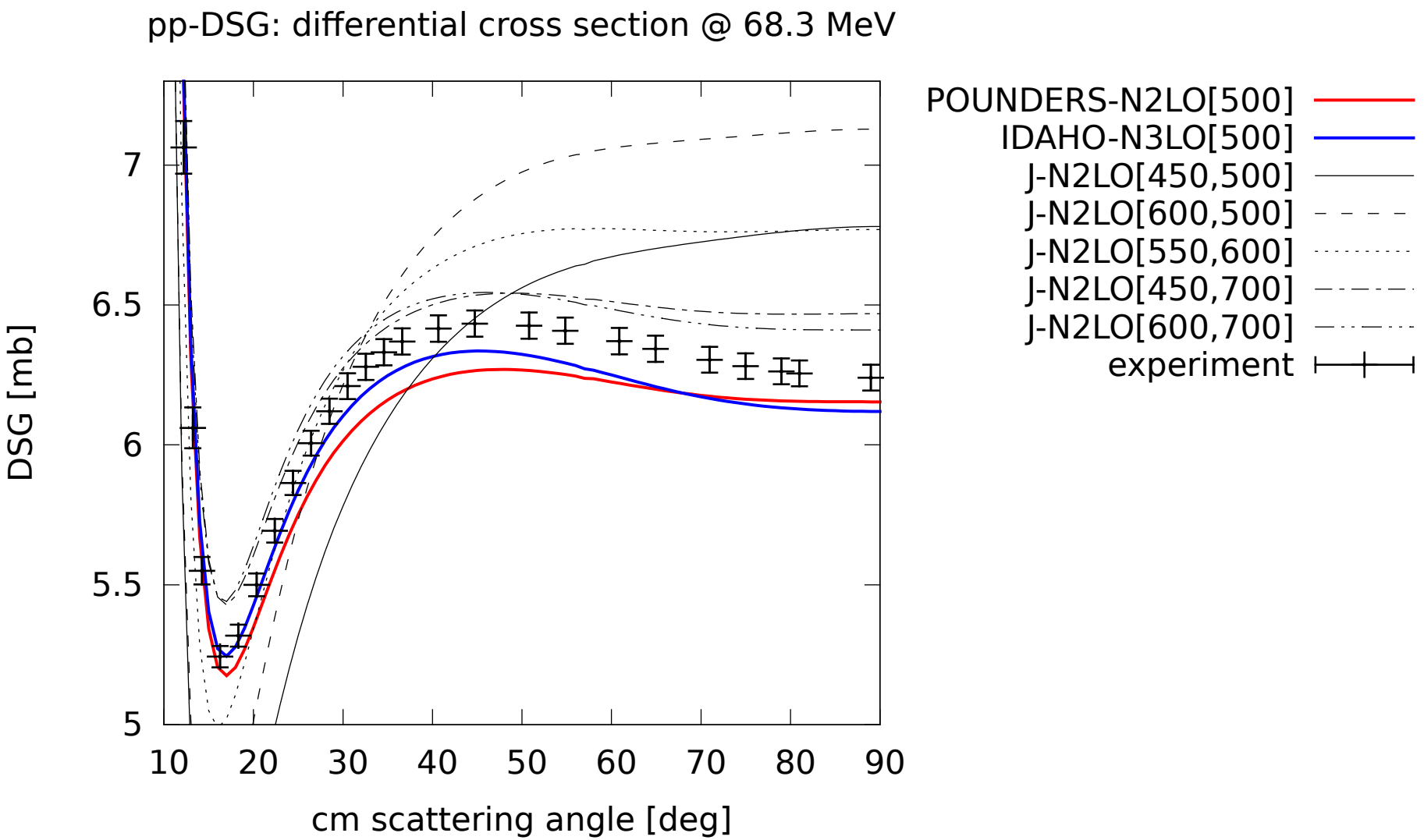

NN Observables

Differential cross section

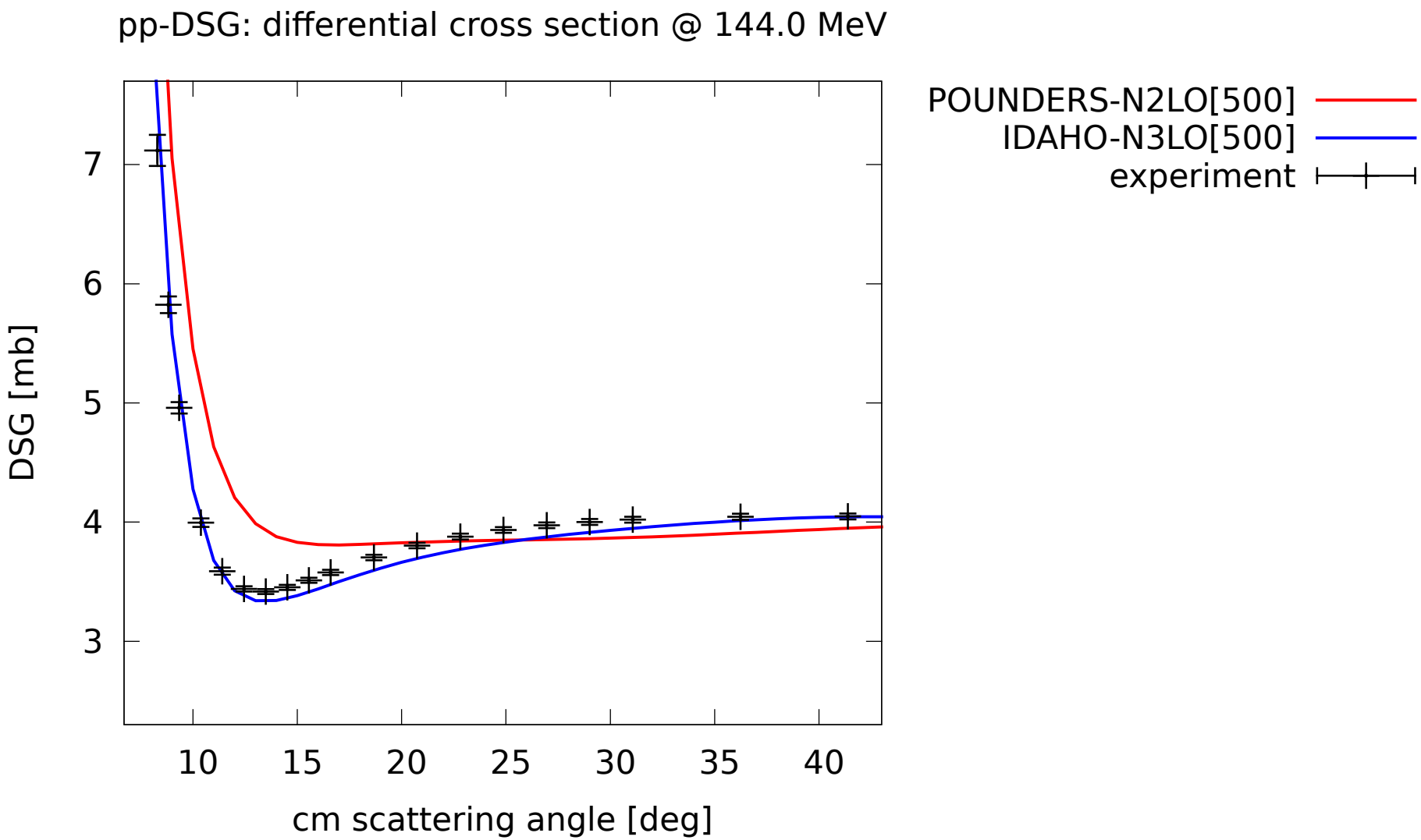

NN Observables

Differential cross section

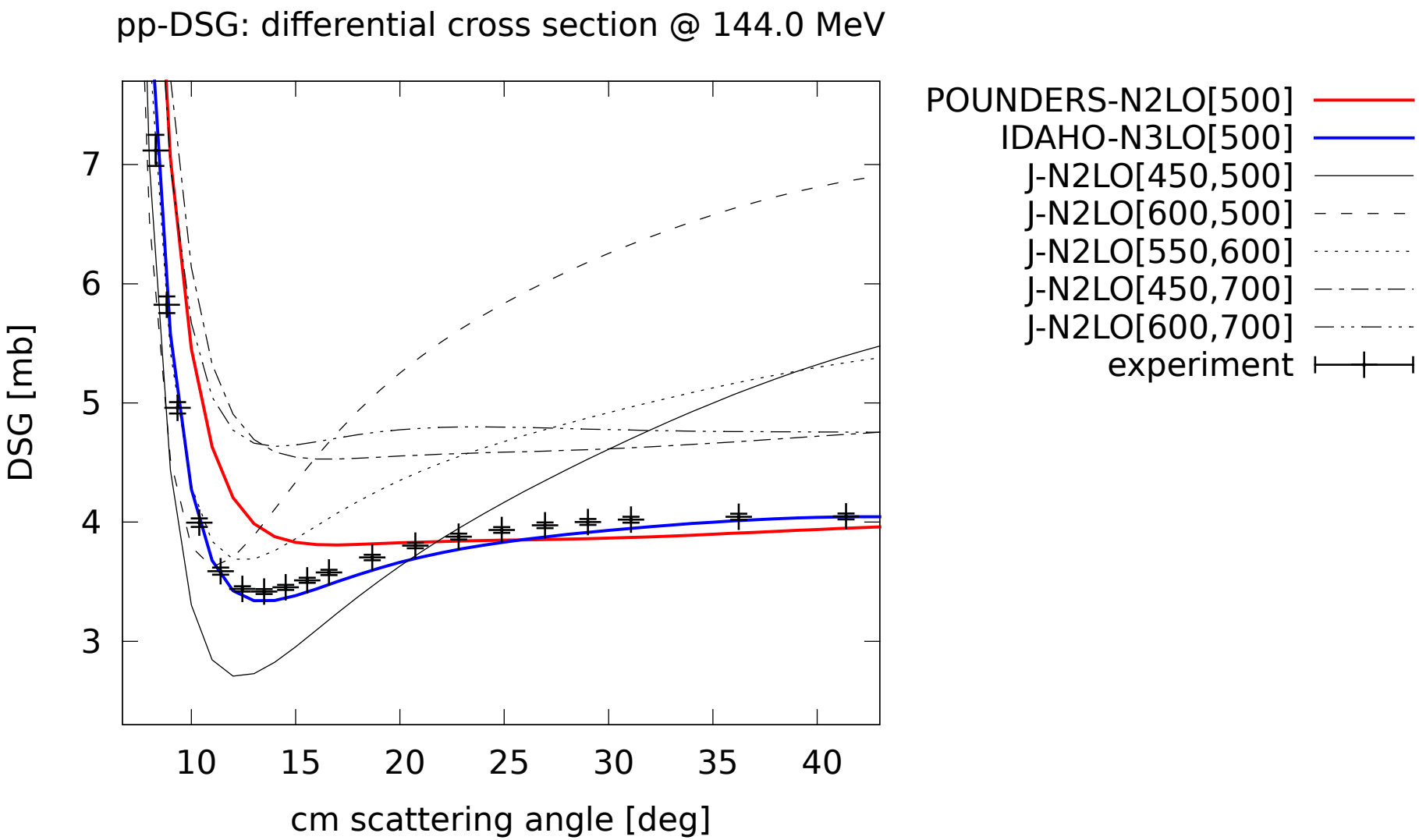

NN Observables

Differential cross section

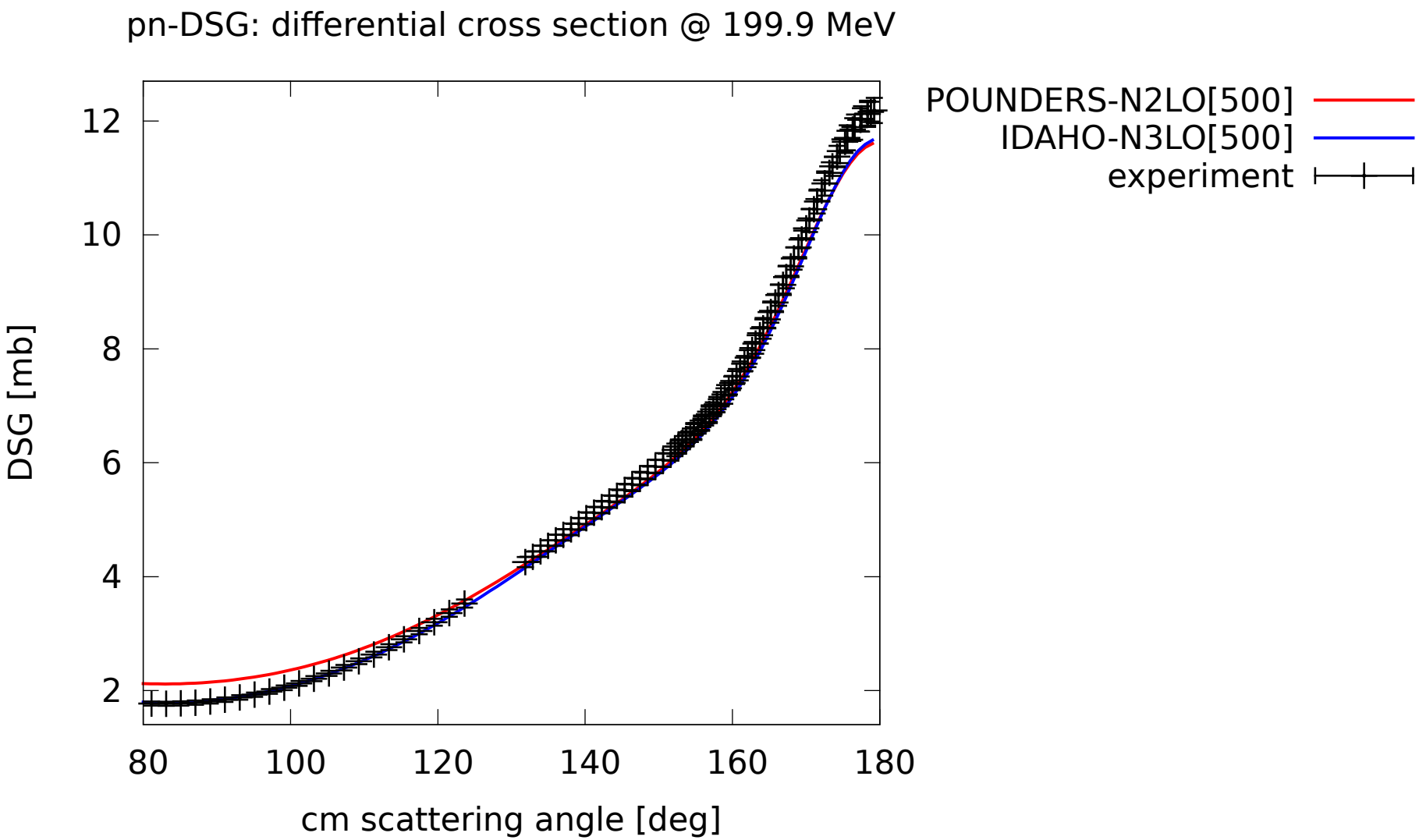

NN Observables

Differential cross section

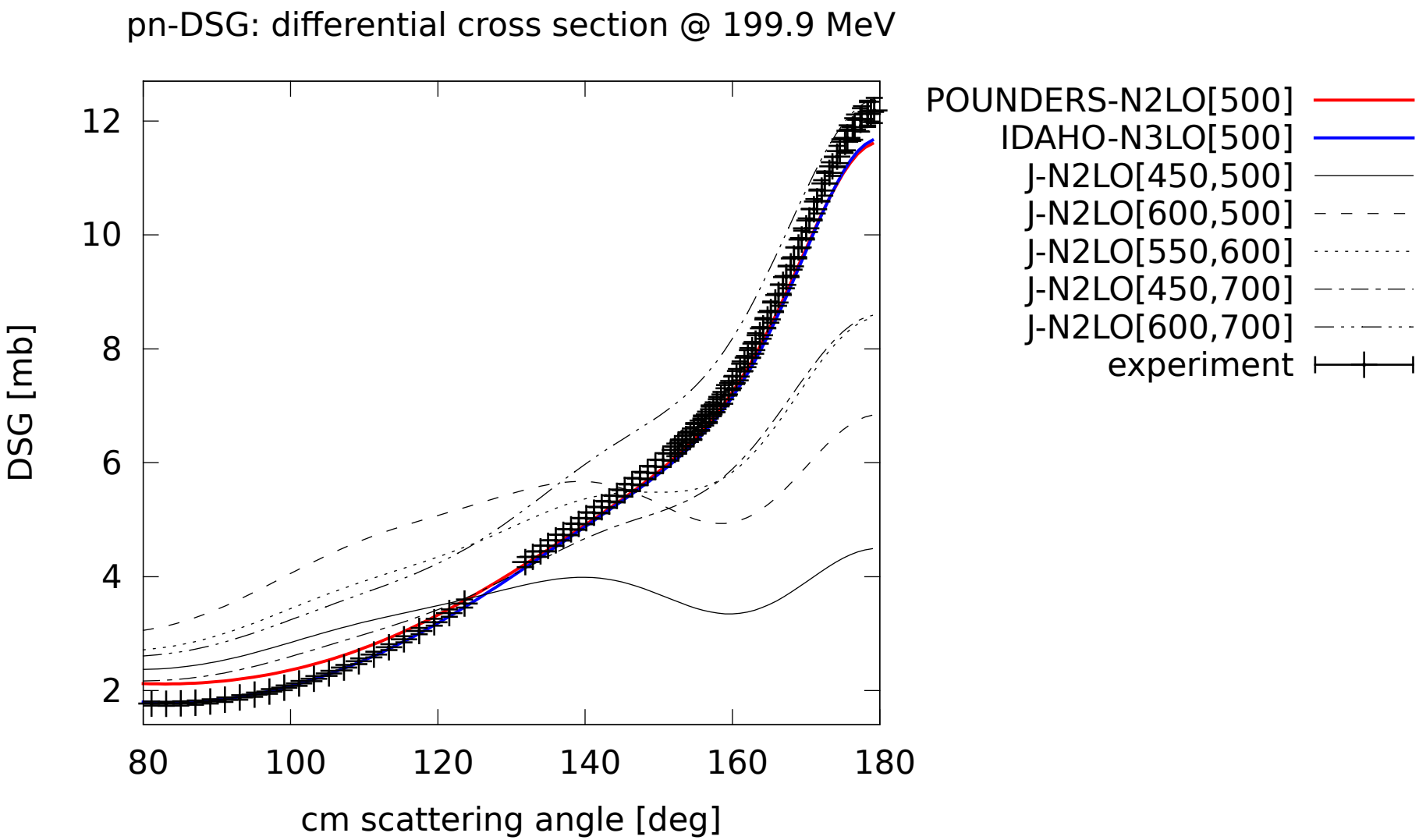

$^1S_0$ scattering observables

	N^{3}LO	POUNDerS-NNLO	Empirical
a_{pp}^C	-7.8188	-7.8174	-7.8196(26)
			-7.8149(29)
r_{pp}^C	2.795	2.755	2.790(14)
			2.769(14)
a_{pp}^N	-17.083	-17.825	
r_{pp}^N	2.876	2.817	
a_{nn}^N	-18.900	-18.889	-18.95(40)
r_{nn}^N	2.838	2.797	2.75(11)
a_{np}	-23.732	-23.749	-23.740(20)
r_{np}	2.725	2.684	2.77(5)

The deuteron

	N^{3}LO	POUNDerS-NNLO	Empirical
B_D (MeV)	2.224575	2.224582	2.224575(9)
r_D (fm)	1.975	1.967	1.97535(85)
Q_D (fm^2)	0.275	0.272	0.2859(3)
P_D	**4.51**	**4.05**	

Titanium isotopes with three-body forces, Hagen *et al*, Hagen *et al*, arXiv:1204.3612

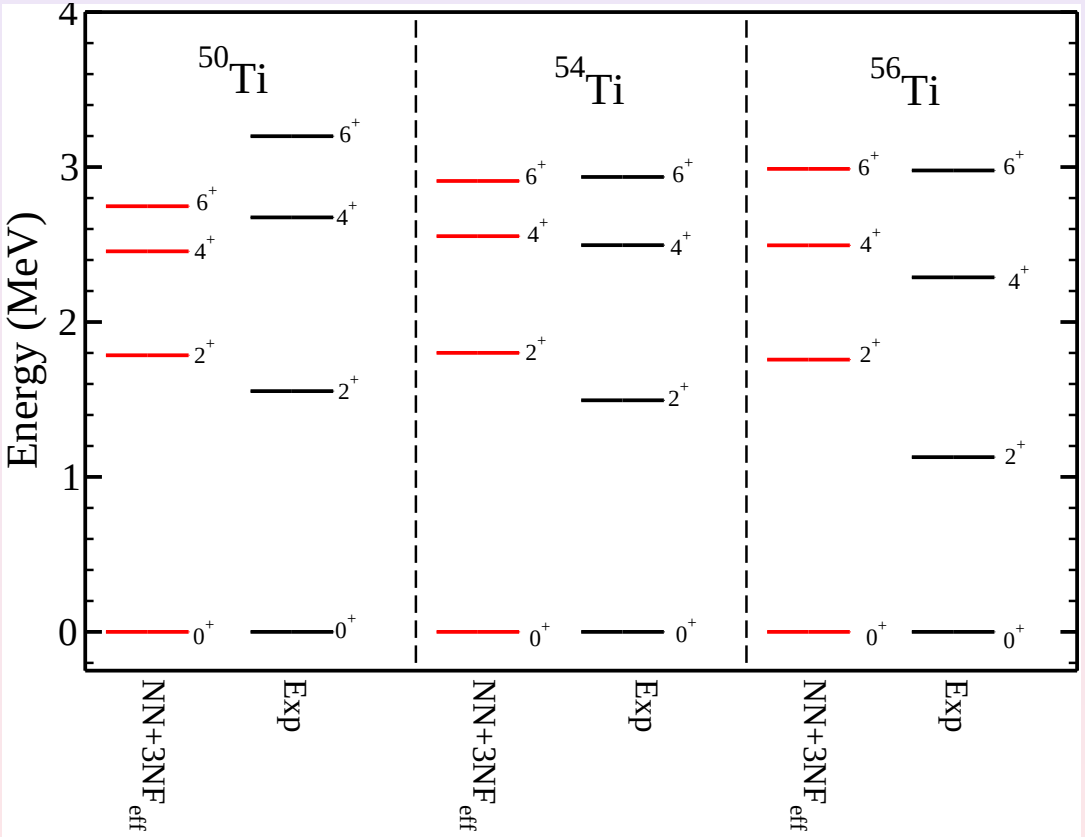

Missing correlations!

- ^{50}Ti essentially two-particle structure
- Calculations not yet converged, performed in $N = 16$ major shells.
- Two-particle attached coupled-cluster theory, the 2^+ states in ^{54}Ti and ^{56}Ti not yet converged as function of oscillator parameter $\hbar\omega$.
- Indication of missing correlations.

Coupled cluster wavefunction

Manybody basis - All possible Slater determinants that can be constructed out of a given set of single particle wavefunctions.

$$|\Psi\rangle = \widehat{\mathbf{C}}\,|\Phi_0\rangle \qquad \widehat{\mathbf{C}} = \widehat{\mathbf{1}} + \widehat{\mathbf{C}}_1 + \widehat{\mathbf{C}}_2 + \ldots + \widehat{\mathbf{C}}_A$$

$$\widehat{\mathbf{C}}_n = \left(\frac{1}{n!}\right)^2 \sum_{\substack{i_1,i_2,\ldots i_n \leq F \\ a_1,a_2,\ldots a_n}} c_{i_1 i_2 \ldots i_n}^{a_1 a_2 \ldots a_n}\, a_{a_1}^\dagger a_{a_2}^\dagger \ldots a_{a_n}^\dagger a_{i_n} \ldots a_{i_2} a_{i_1}.$$

Reparametrization of $\widehat{\mathbf{C}}_n$, not a change of basis.

$$\widehat{\mathbf{C}}_1 = \widehat{\mathbf{T}}_1 \qquad \widehat{\mathbf{C}}_2 = \frac{1}{2}\widehat{\mathbf{T}}_1^2 + \widehat{\mathbf{T}}_2$$

$$\widehat{\mathbf{C}}_3 = \frac{1}{6}\widehat{\mathbf{T}}_1^3 + \widehat{\mathbf{T}}_1\widehat{\mathbf{T}}_2 + \widehat{\mathbf{T}}_3 \qquad \widehat{\mathbf{C}}_4 = \frac{1}{24}\widehat{\mathbf{T}}_1^4 + \frac{1}{2}\widehat{\mathbf{T}}_1^2\widehat{\mathbf{T}}_2 + \frac{1}{2}\widehat{\mathbf{T}}_2^2 + \widehat{\mathbf{T}}_1\widehat{\mathbf{T}}_3 + \widehat{\mathbf{T}}_4$$

$$\vdots \qquad \vdots$$

Coupled Cluster in Pictures

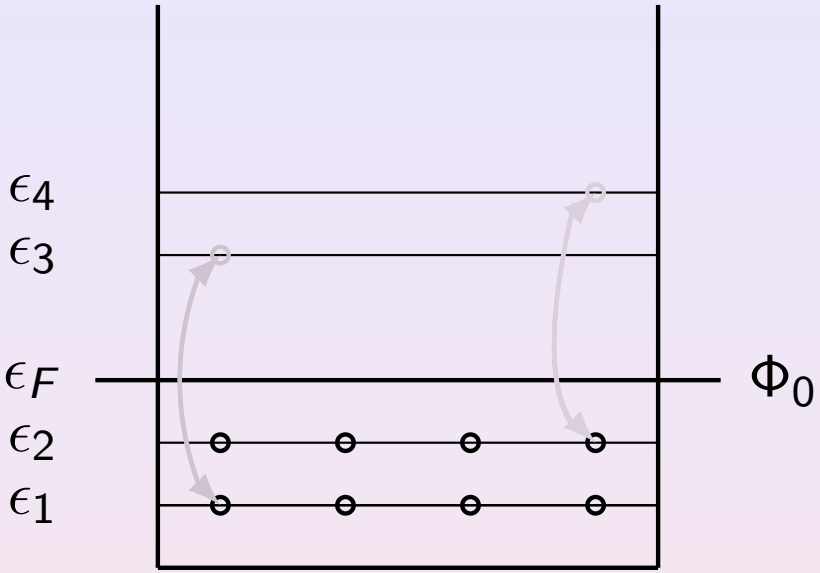

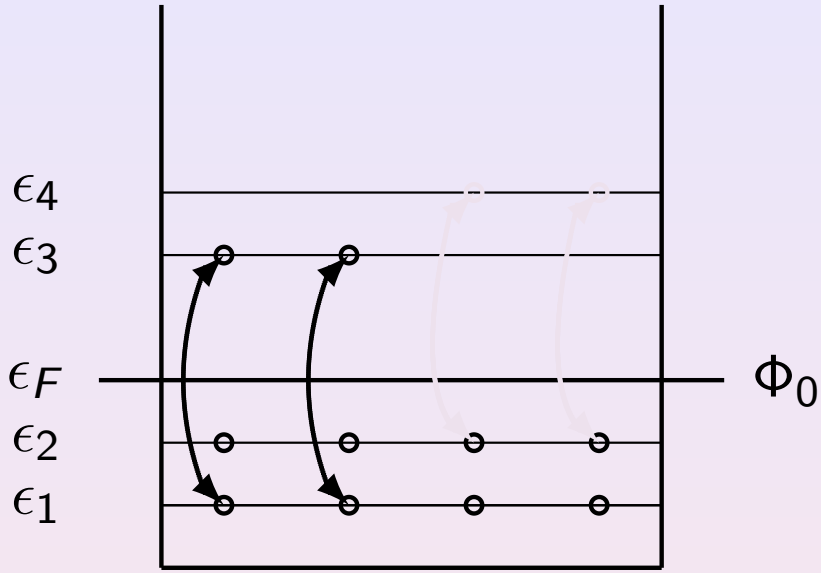

From T_1 to T_1^2

$T_1 = \sum_{i<\varepsilon_f, a>\varepsilon_f} t_i^a a_a^+ a_i$

From T_2 to T_2^2

$T_2 = \sum_{i,j<\varepsilon_f; ab>\varepsilon_f} t_{ij}^{ab} a_a^+ a_b^+ a_j a_i$

Coupled Cluster in Pictures

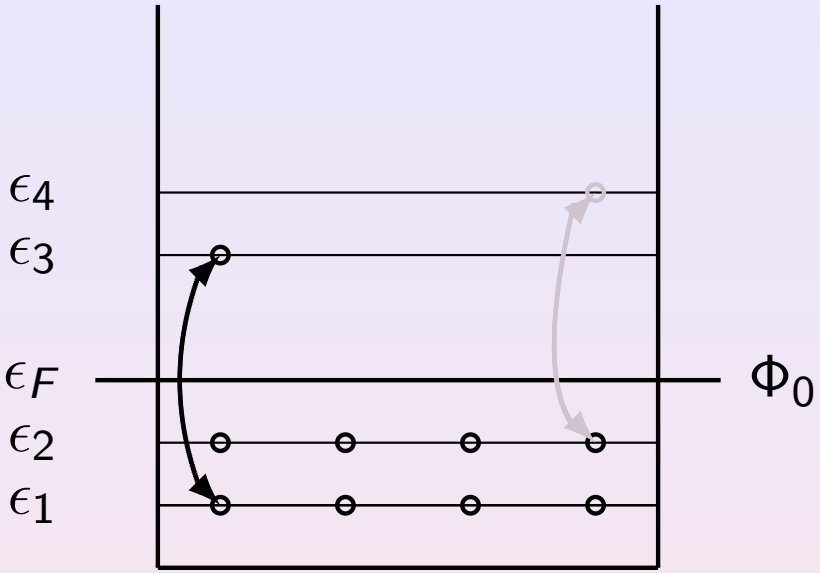

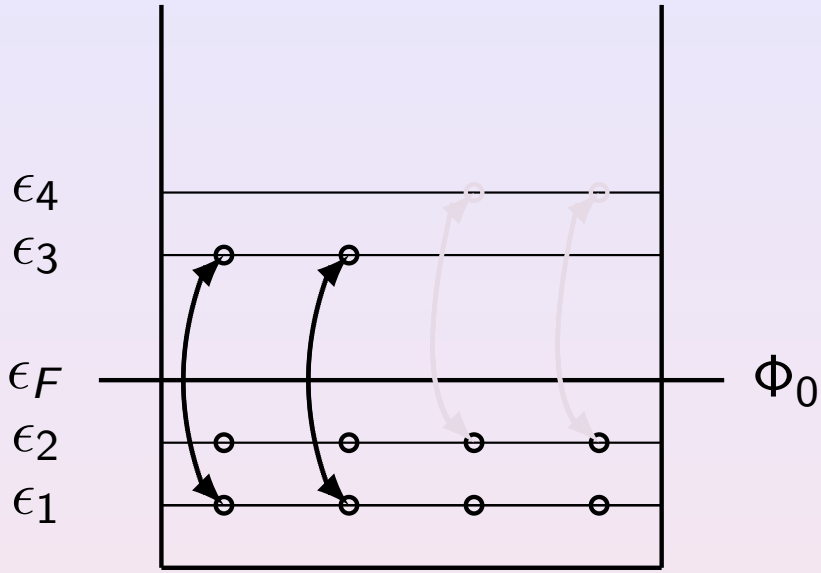

From T_1 to T_1^2

$$T_1 = \sum_{i<\varepsilon_f, a>\varepsilon_f} t_i^a a_a^+ a_i$$

From T_2 to T_2^2

$$T_2 = \sum_{i,j<\varepsilon_f; ab>\varepsilon_f} t_{ij}^{ab} a_a^+ a_b^+ a_j a_i$$

Coupled Cluster in Pictures

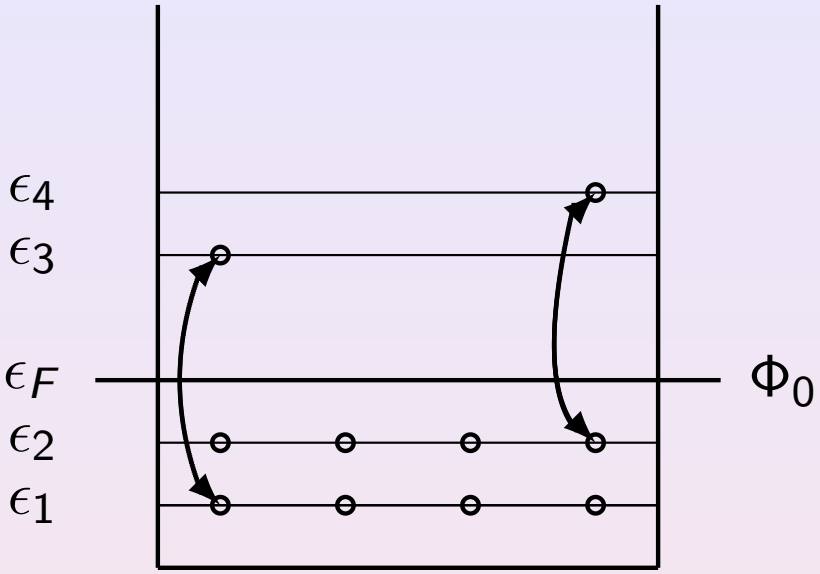

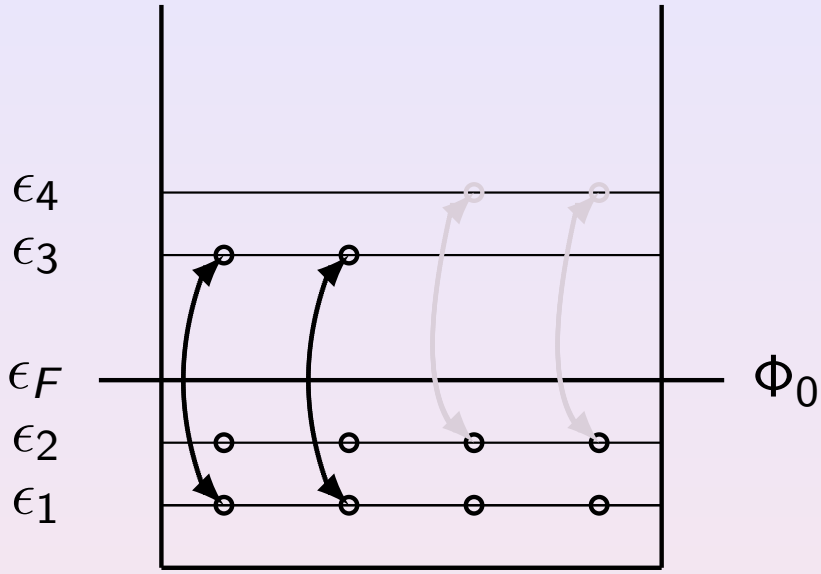

From T_1 to T_1^2

$$T_1 = \sum_{i<\varepsilon_f, a>\varepsilon_f} t_i^a a_a^+ a_i$$

From T_2 to T_2^2

$$T_2 = \sum_{i,j<\varepsilon_f; ab>\varepsilon_f} t_{ij}^{ab} a_a^+ a_b^+ a_j a_i$$

Coupled Cluster in Pictures

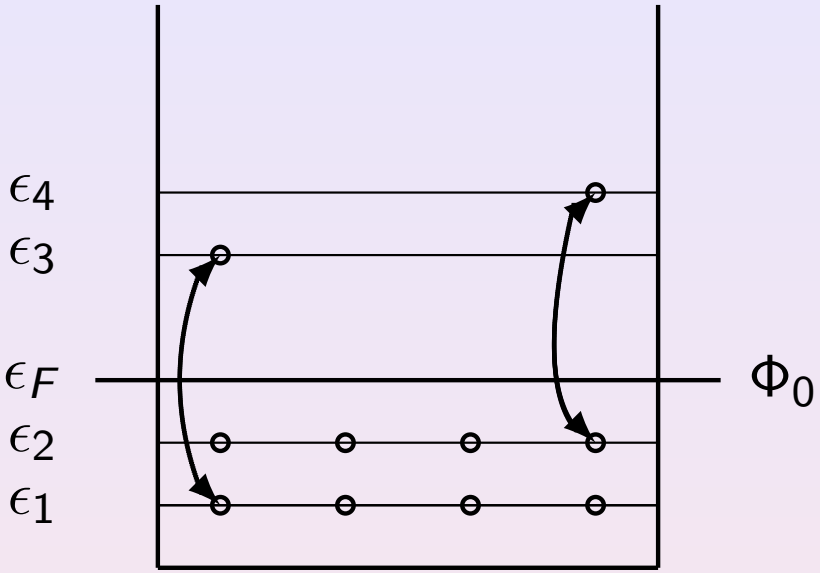

From T_1 to T_1^2

$T_1 = \sum_{i<\varepsilon_f, a>\varepsilon_f} t_i^a a_a^+ a_i$

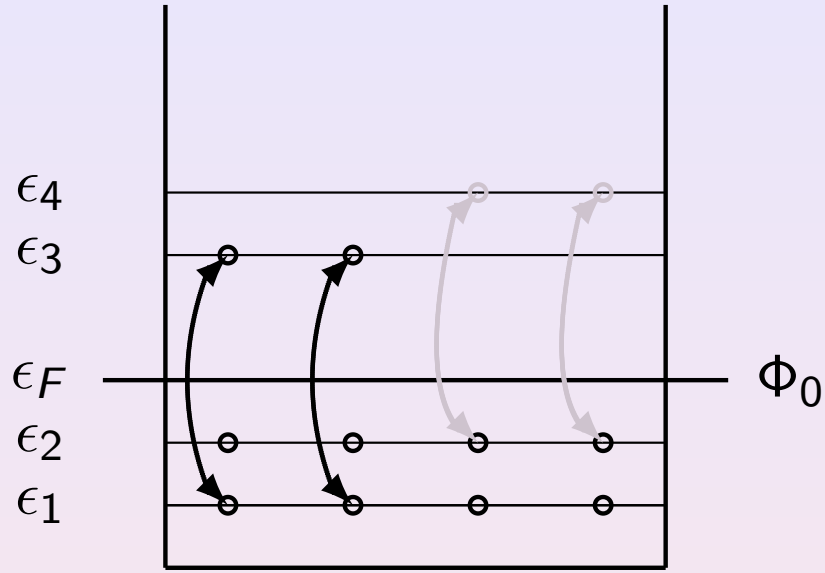

From T_2 to T_2^2

$T_2 = \sum_{i,j<\varepsilon_f; ab>\varepsilon_f} t_{ij}^{ab} a_a^+ a_b^+ a_j a_i$

Coupled Cluster in Pictures

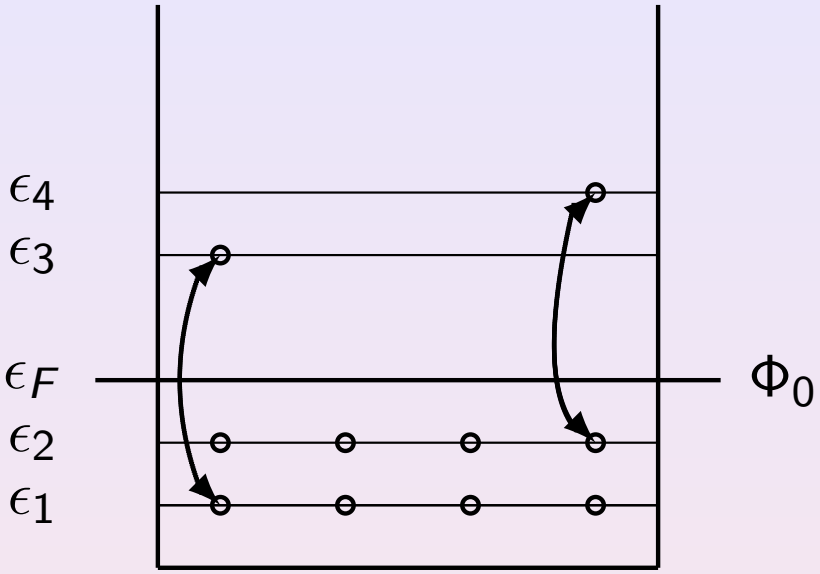

From T_1 to T_1^2

$T_1 = \sum_{i<\varepsilon_f, a>\varepsilon_f} t_i^a a_a^+ a_i$

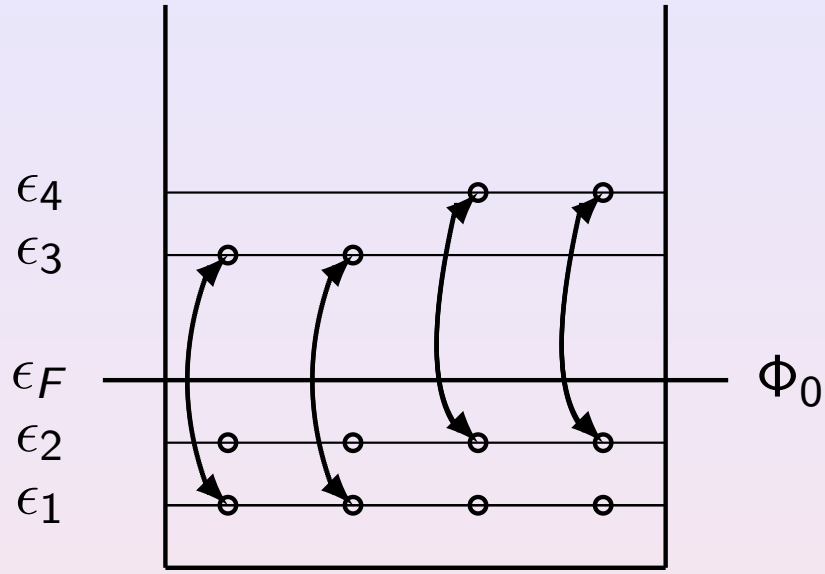

From T_2 to T_2^2

$T_2 = \sum_{i,j<\varepsilon_f; ab>\varepsilon_f} t_{ij}^{ab} a_a^+ a_b^+ a_j a_i$

More Coupled Cluster in Pictures

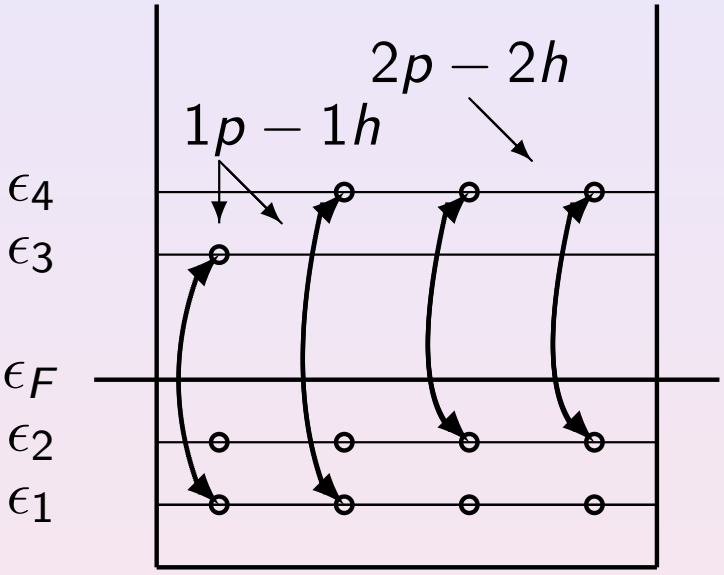

$T_1^2 T_2$

CCSD and Shell-Model Truncations

- Truncated shell model with $2p-2h$ has $\Psi_{2p-2h} = (1 + T_1 + T_2)\Phi_0$
- Energy contains then

$$E_{2p-2h} =$$

$$\langle \Phi_0(1+T_1^\dagger+T_2^\dagger)|H|(1+T_1+T_2)\Phi_0\rangle$$

- But CCSD has also $T_1^2 T_2$. Not in truncated shell model.

Oxygen isotopes with three-body forces, Hagen *et al*, arXiv:1202.2839 and Phys. Rev. Lett., **108**, in press.

Excited states in ^{24}O

Experiment

[Hoffman et al. PRC 83, 031303 (2011)] Unbound states in ^{24}O populated by knockout from ^{26}F. Observation of ^{22}O and two-neutron cascade. Speculation: single resonance or superposition of states with $J^\pi = 1^+$ to 4^+.

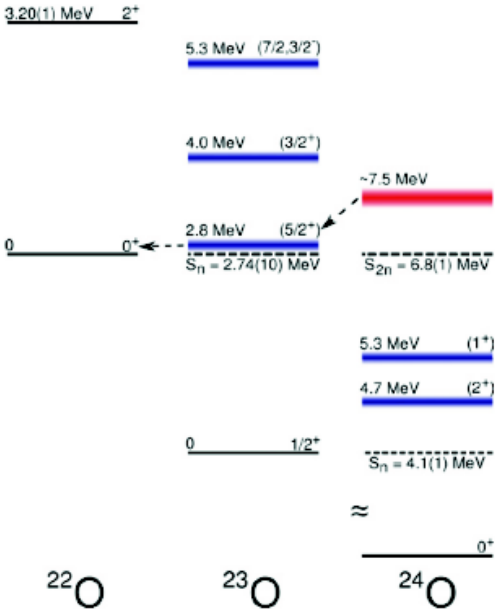

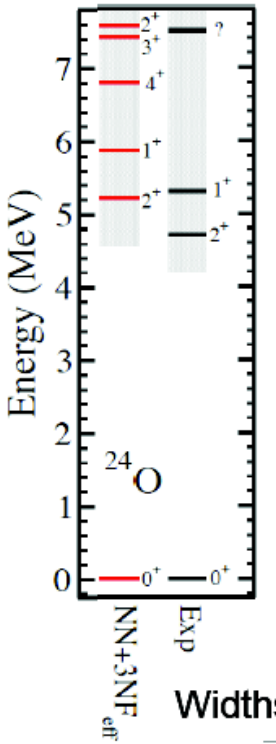

Theory

Experiment has seen superposition of states with $J^\pi = 2^+$ to 4^+.

Widths agree well with available data

J^π	2_1^+	1_1^+	4_1^+	3_1^+	2_2^+	1_2^+
E_{CC}	5.2	5.9	6.8	7.4	7.6	8.9
E_{Exp}	4.7(1)	5.33(10)				
Γ_{CC}	0.03	0.05	0.006	0.02	0.04	0.57
Γ_{Exp}	$0.05^{+0.21}_{-0.05}$	$0.03^{+0.12}_{-0.03}$				

How large a model space do we need?

Estimate for model spaces and Hamiltonian matrix dimension

1. Assume we want to compute the binding energy of $A = 16$ in a wave function based approach. Assume that the interaction has a momentum cutoff $\Lambda = 600$ MeV.
2. What are the minimum requirements for the model space?

We assume that our favourite single-particle basis is the harmonic oscillator, with single-particle energies $\varepsilon_{nl} = \hbar\omega(2n + l + 3/2)$, with ω the oscillator frequency, $n = 0, 1, 2, \ldots$ being the number of nodes and l the single-particle orbital momentum. The oscillator length b is defined as

$$b = \sqrt{\frac{\hbar}{m\omega}}.$$

How large a model space do we need?

Answer

We define $p = 0, 1, 2, \ldots, P$ with $P = 2n + l$ as the quantum number p of the highest-filled level. The level labelled p can accommodate $(p+1)(p+2)$ fermions, with a spin degeneracy of two for every single-particle state taken into account. For a given maximum value of $P = 2n_{\max} + l_{\max}$, we have a total of

$$N = \sum_{p=0}^{P} (p+1)(p+2) = \frac{(P+1)(P+2)(P+3)}{3},$$

single-particle states.

How large a model space do we need?

Example: ^{16}O

The largest single-particle excitation energy (corresponding to possible one-particle-one-hole correlations) is then

$$\Lambda = \hbar\omega P = \hbar\omega(2n_{\max} + l_{\max}).$$

The value of $\hbar\omega$ can be extracted from the mean-squared radius of a given nucleus. One can show that this results in (see Kirson NPA**781**, 350 (2007))

$$\hbar\omega \approx \left(\frac{3}{2}\right)^{4/3} \frac{\hbar^2}{2m_N r_0^2} A^{-1/3},$$

with $r_0 \approx 1$ fm. Setting $A = 16$ and $\Lambda = 600$ MeV results in $P \approx 42$. The largest possible value for n is then $n_{\max} \approx 21$, or 22 major shells. With $P = 42$, the total number of single-particle states in this model space is 28380!

How large a model space do we need?

Example: ^{16}O

For ^{16}O, this means that we have to distribute eight protons and eight neutrons in 28380 single-particle states, respectively. The total number of Slater determinants, with no restrictions on energy excitations, is

$$\left(\begin{array}{c} 28380 \\ 8 \end{array} \right) \times \left(\begin{array}{c} 28380 \\ 8 \end{array} \right) \approx 10^{62}.$$

Any direct diagonalization method in such a huge basis is simply impossible. One possible approach is to introduce a smaller model space with a pertinent effective interaction.
Need effective interactions or smarter methods for doing ab initio calculations. See JPG **37**, 064035, for examples and further discussion.

A curiosity: Error from CCSD calculations

Nucleus	$\Delta E/A$ (MeV)	Nucleus	$\Delta E/A$ (MeV)
^{16}O	1.25	^{18}O	1.35
^{18}F	1.24	^{22}O	1.60
^{23}O	1.50	^{24}O	1.42
^{25}O	1.25	^{26}O	1.09
^{26}F	1.36	^{27}O	1.25
^{28}O	1.06	^{40}Ca	0.84
^{48}Ca	1.27		

Missing contributions

- Additionl correlations in the CC operators.
- Three-body and higher-body forces.
- Here also continuum coupling.

Coupled-cluster results for $A = 17$, Hagen *et al*, PRL104, 2010

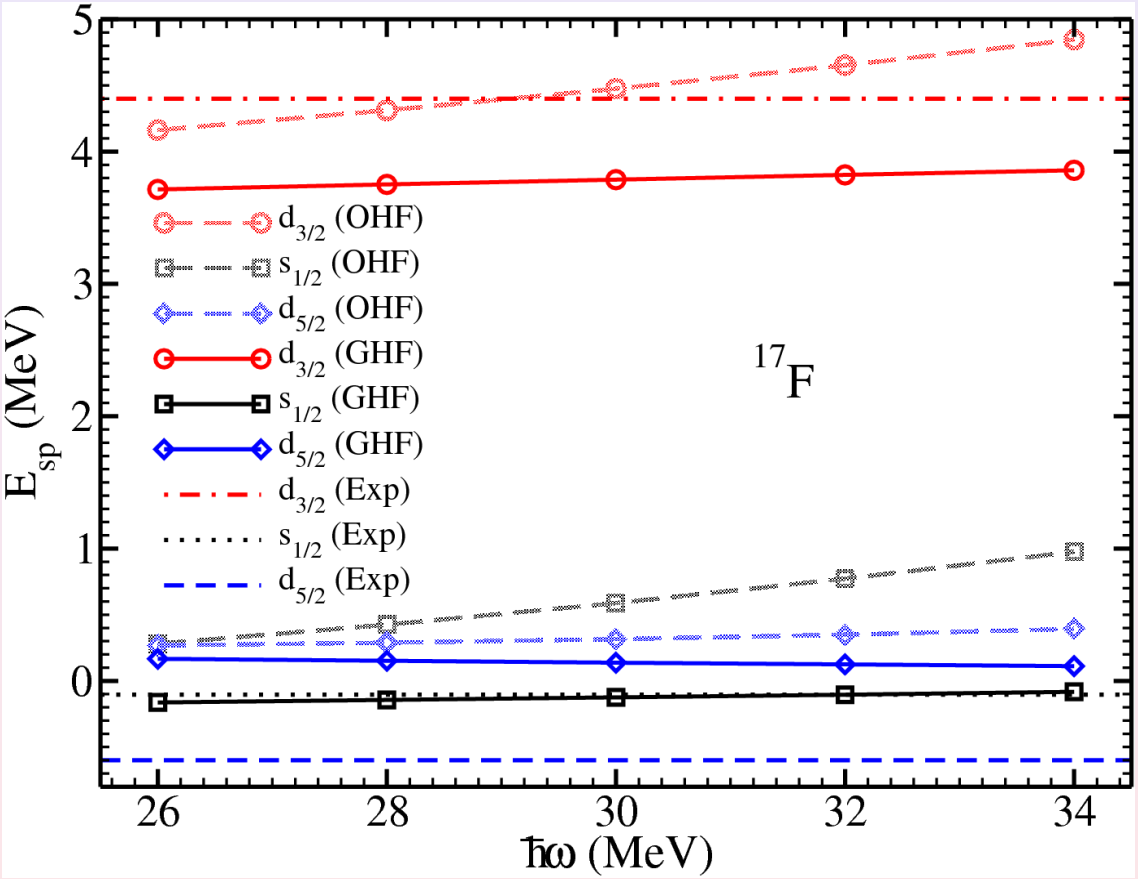

- N^3LO with $\Lambda = 500$ MeV interaction
- Berggren basis and realistic nucleon-nucleon interactions (GHF)
- Standard harmonic oscillator basis with Hartree-Fock calculation (OHF)
- 17 oscillator shells plus 30 Woods-Saxon Berggren states for each of the $s_{1/2}$, $d_{5/2}$, and $d_{3/2}$ states

Role of possible missing many-body physics

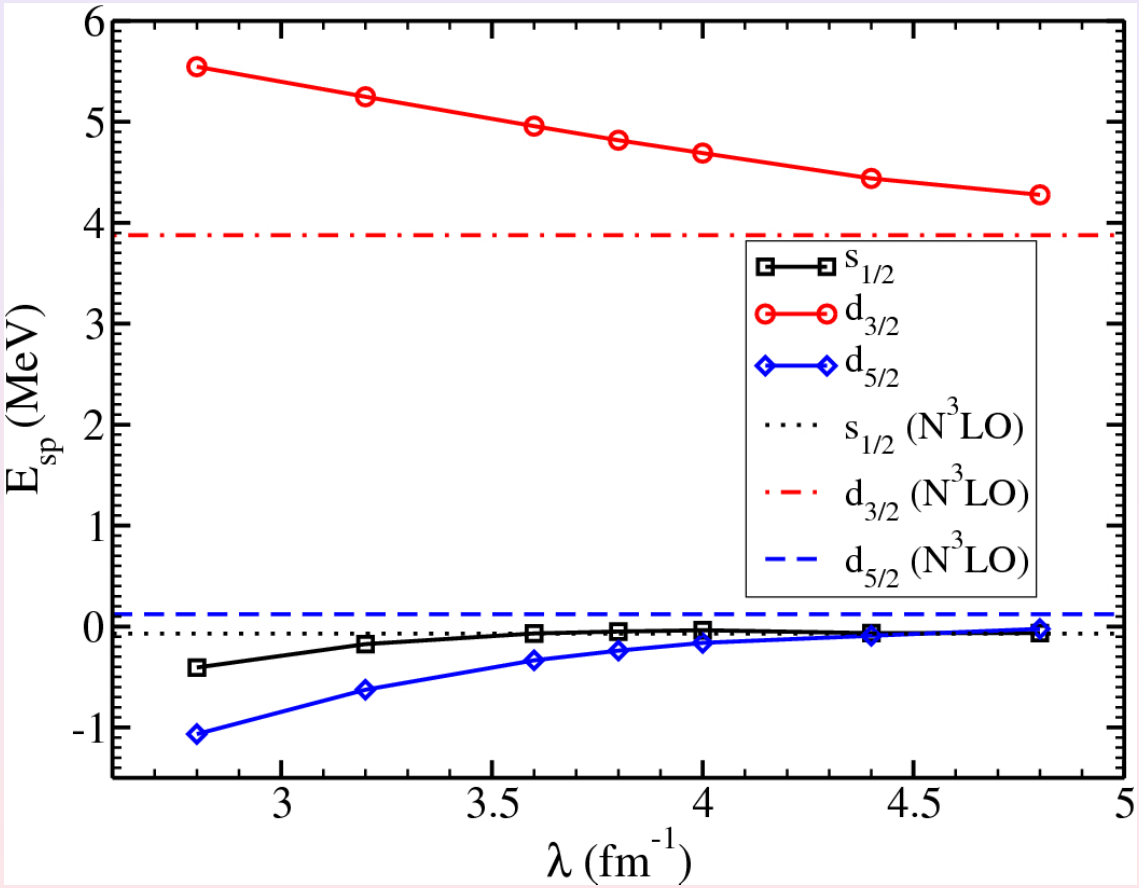

- $s_{1/2}$ state is a halo state ($r_{\rm rms} = 5.333$ fm), no influence from short-range effects
- $1/2^+$ halo state is dominated by long-ranged forces.
- Spin-orbit splitting between the $3/2^+$ and $5/2^+$ states increases with decreasing cutoff. Evidence of missing many-body physics.

Spectroscopic factors for ^{24}O, Ø. Jensen *et al*, PRC **83**, 021305(R) (2011)

$$S^A_{A-1}(lj) = \left| O^A_{A-1}(lj; r) \right|^2 , \tag{1}$$

$$O^A_{A-1}(lj; r) = \sum_n \int \langle A-1 || \tilde{a}_{nlj} || A \rangle \phi_{nlj}(r). \tag{2}$$

Here, $O^A_{A-1}(lj; r)$ is the radial overlap function of the many-body wavefunctions for the two independent systems with A and $A-1$ particles respectively. The double bar denotes a reduced matrix element, and the integral-sum over n represents both the sum over the discrete spectrum and an integral over the corresponding continuum part of the spectrum.

Spectroscopic factors for ^{24}O, Ø. Jensen *et al*, PRC **83**, 021305(R) (2011)

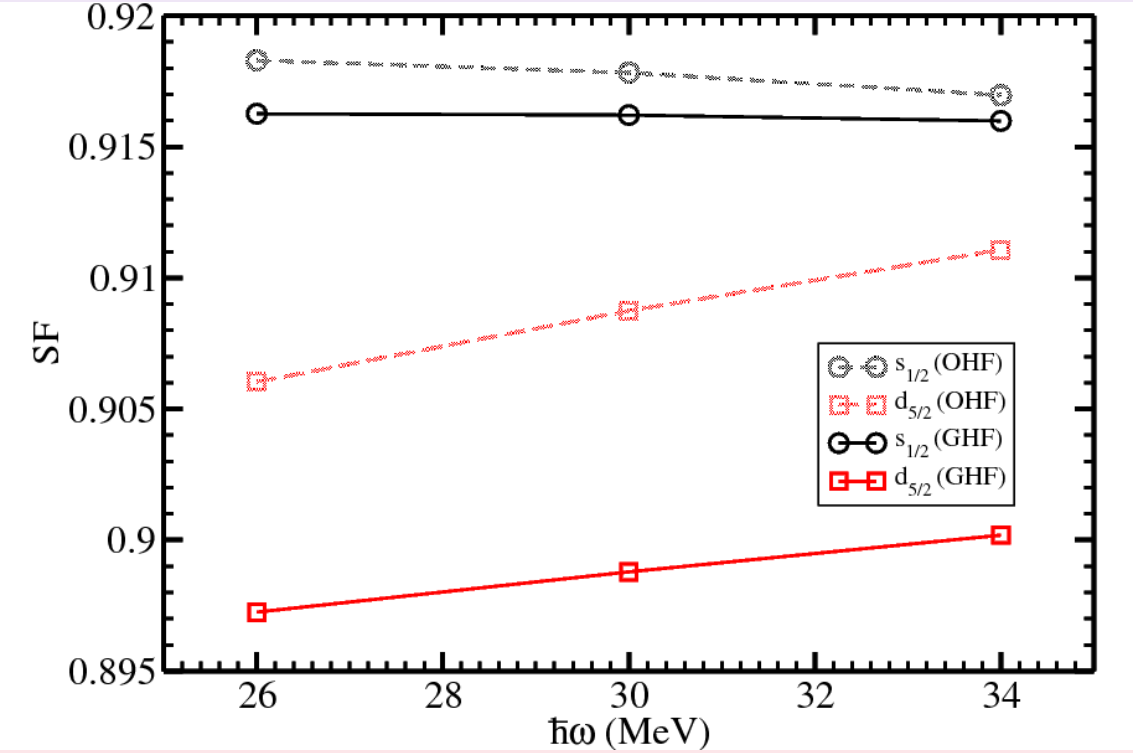

- N^{3}LO with $\Lambda = 500$ MeV interaction, CCSD calculation
- Bergren basis (GHF) and Harmonic oscillator basis (OHF)
- **Spectroscopic factors for neutron $d_{5/2}$ and $s_{1/2}$**
- 17 oscillator shells plus 30 Woods-Saxon Berggren states for each of the $s_{1/2}$, $d_{5/2}$, and $d_{3/2}$ states
- ^{24}O seemingly good closed shell nucleus.

Spectroscopic factors from Gade *et al*, PRC **77**, 044306 (2008). Can we understand these quenchings?

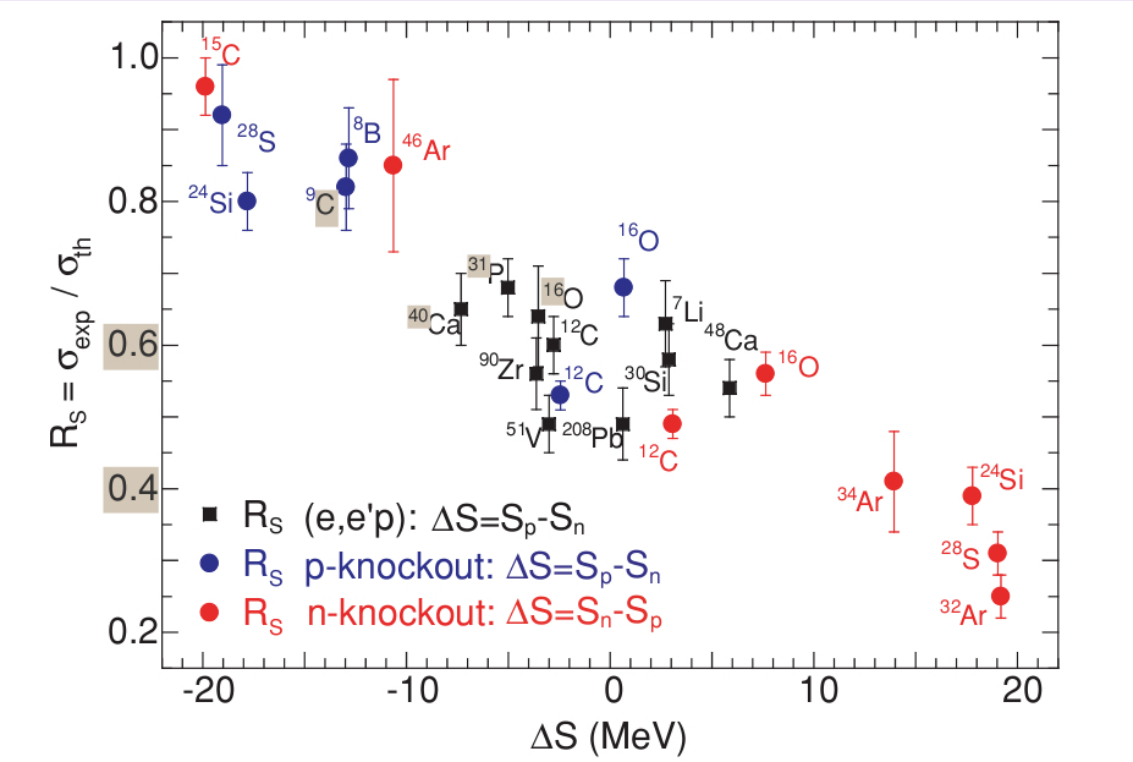

- Reduction of measured nucleon knock-out cross sections relative to theoretical
- Plotted as function of separation energies of the two nucleon species
- Results from heavy-ion induced one-π and one-ν knockout reactions and electron-induced proton removal from stable nuclei.
- Only expt uncertainties included

Wigner cusp due to continuum coupling, Michel, Nazarewicz, and Płoszajczak, Nucl. Phys. A **794**, 29 (2007).

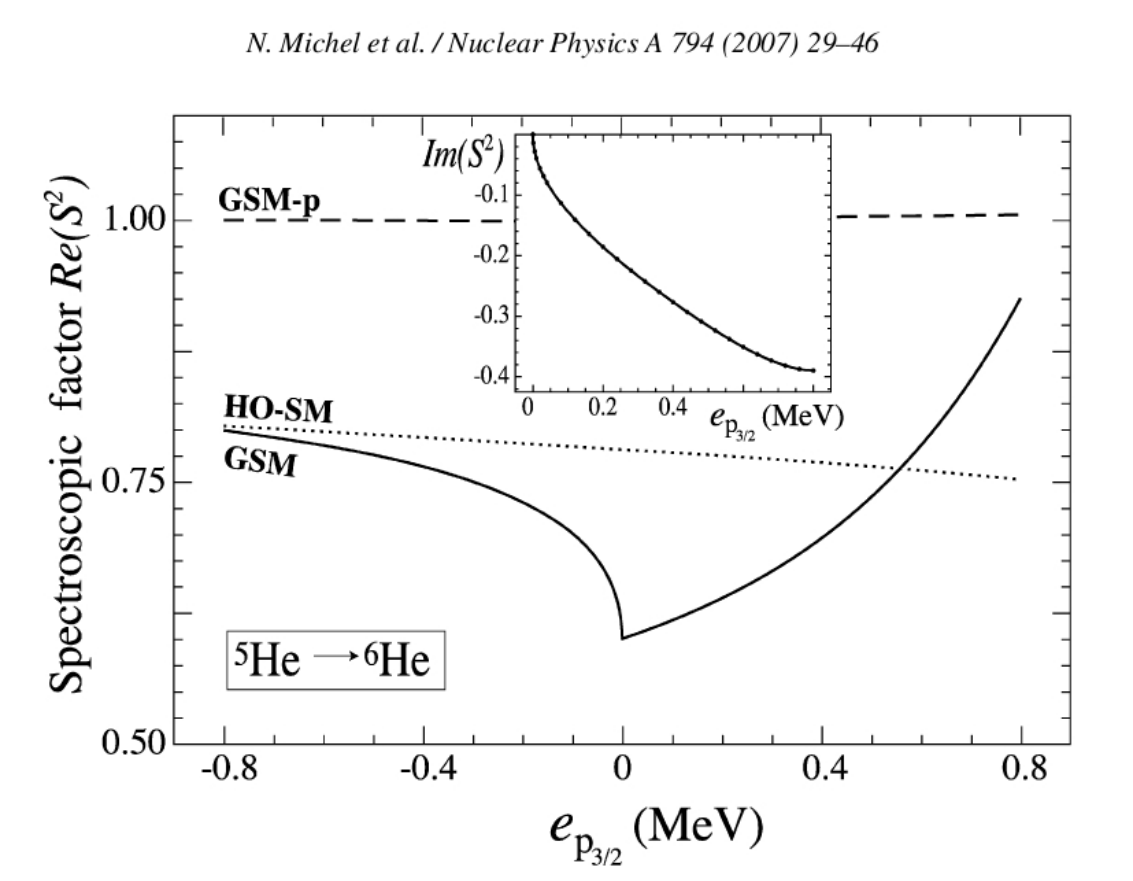

- Simple model for $^5\mathrm{He}+n \rightarrow {}^6\mathrm{He}$
- Single-particle energies obtained using complex basis
- Vary the binding energy (and thereby separation energy) of $p_{3/2}$ state
- Cusp in SF due to coupling to scattering states

Spectroscopic factors for ^{14}O, ^{16}O, ^{22}O, ^{24}O and ^{28}O, Ø. Jensen *et al*, PRL **107**, 032501 (2011)

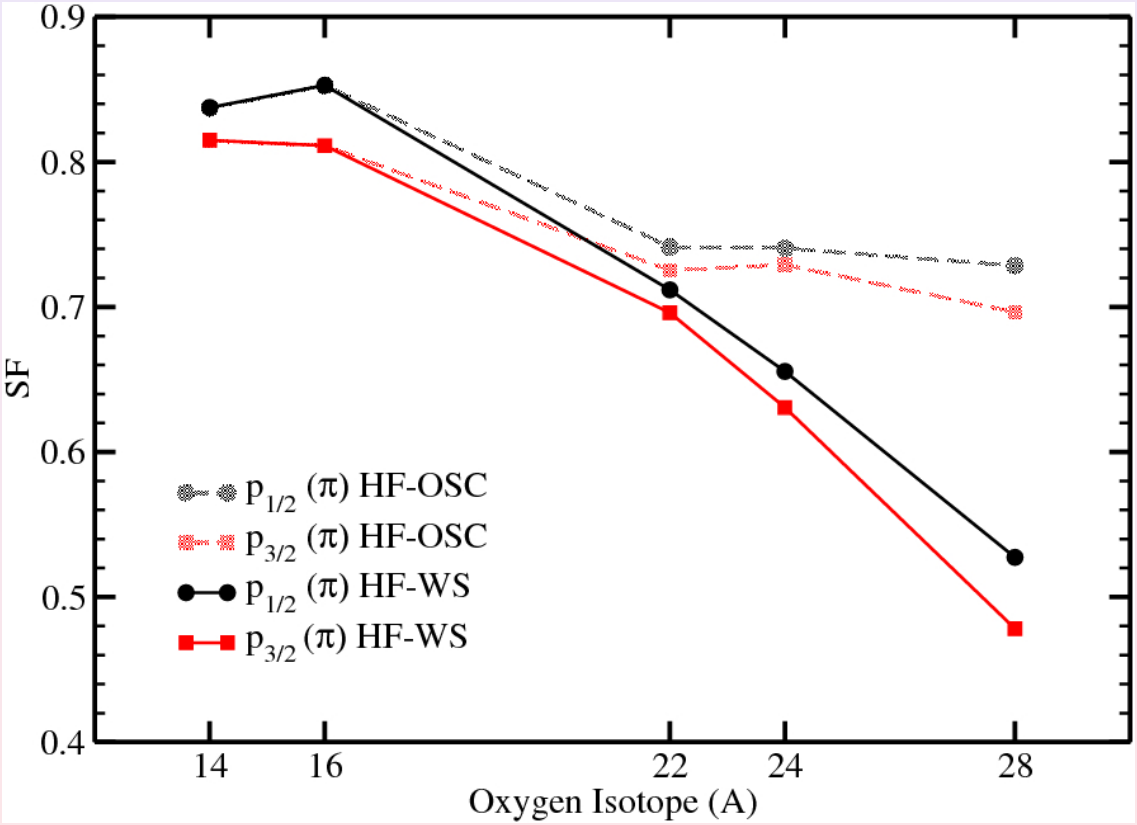

- N^3LO with $\Lambda = 500$ MeV interaction, CCSD calculation
- Spectroscopic factors for proton $p_{3/2}$ and $p_{1/2}$
- Quenching due to coupling to scattering states
- Different from standard scenario (long-range, short-range+tensor correlations)

SFs and separation energies ^{14}O, ^{16}O, ^{22}O, ^{24}O and ^{28}O, Ø. Jensen *et al*, in PRL **107**, 032501 (2011)

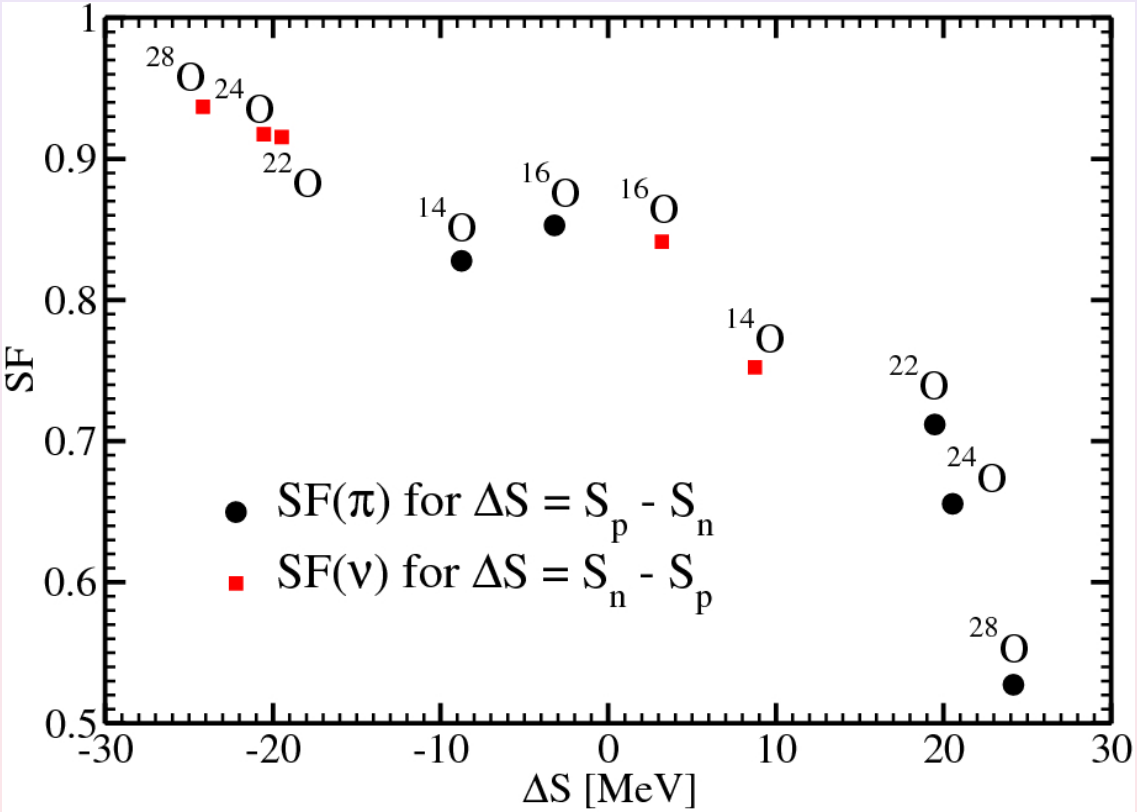

- SFs for $p_{1/2}$ as function of separation energies
- When large differences in separation energies, large quenchings for protons
- Neutrons are weakly bound and less quenched.

Many-body correlations Ø. Jensen *et al*, PRL **107**, 032501 (2011). SF for $p_{1/2}$ as function of various cutoffs for ^{24}O

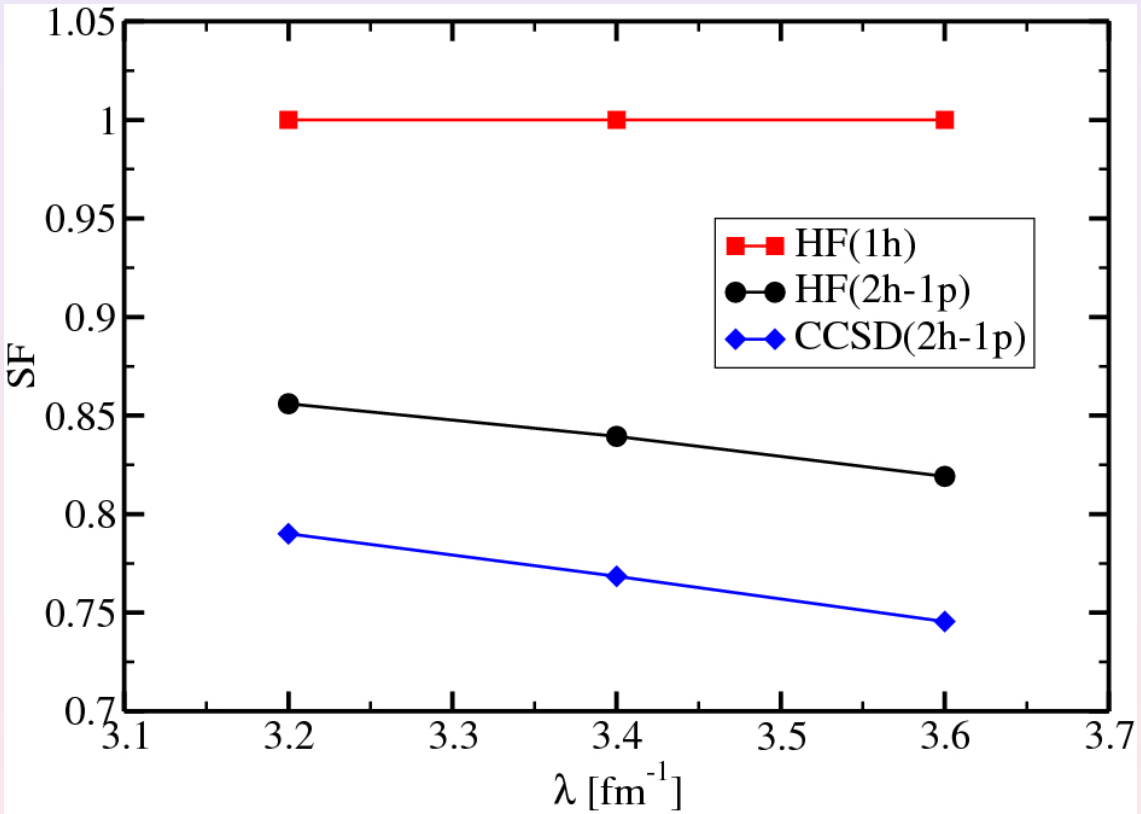

- N^{3}LO interaction evolved to a lower momentum cutoff λ
- Case 1: SFs using a mean-field HF solution for the A and $A-1$ nuclei
- Case 2: HF for A nucleus and 2p1h for $A-1$ nucleus
- Case 3: full calculation

SF summary

- Quenching of spectroscopic factors for deficient nucleon species due to coupling to scattering states.
- Need experimental data.
- New interesting cases with large proton/neutron asymmetries where we can run calculations: ^{24}S (last bound), ^{30}S, ^{32}S (data) and ^{36}S; and ^{22}Si, ^{28}Si, ^{30}Si and ^{34}Si (data).
- **Preliminary:** last bound protons ($d_{3/2}$) in calcium isotopes up to ^{60}Ca show small quenching.
- Speculations: do we see these quenchings due to the continuum only for light systems (low l-values)?

Calcium cross section (courtesy of Oleg Tarasov, NSCL)